SIMULATION OF STREAM FLOW AND SOIL EROSION IN KRISHNA LOWER SUB BASIN

N. BIDYARANI CHANU

B. Tech. (Agril. Engg.)

MASTER OF TECHNOLOGY

IN

AGRICULTURAL ENGINEERING

(SOIL AND WATER ENGINEERING)

2017

SIMULATION OF STREAM FLOW AND SOIL EROSION IN KRISHNA LOWER SUB BASIN

BY

N. BIDYARANI CHANU

B. Tech (Agril. Engg.)

THESIS SUBMITTED TO THE ACHARYA N. G. RANGA AGRICULTURAL UNIVERSITY IN PARTIAL FULFILMENT OF THE REQUIREMENTS FOR THE AWARD OF THE DEGREE OF

MASTER OF TECHNOLOGY
IN
AGRICULTURAL ENGINEERING

(SOIL AND WATER ENGINEERING)

CHAIRPERSON: Dr. A. MANI

DEPARTMENT OF SOIL AND WATER ENGINEERING
ACHARYA N. G. RANGA AGRICULTURAL UNIVERSITY
COLLEGE OF AGRICULTURAL ENGINEERING
BAPATLA – 522 101

2017

DECLARATION

I, **Ms. N. BIDYARANI CHANU,** hereby declare that the thesis entitled "**SIMULATION OF STREAM FLOW AND SOIL EROSION IN KRISHNA LOWER SUB BASIN**" submitted to the **Acharya N. G. Ranga Agricultural University** for the degree of **Master of Technology in Agricultural Engineering** in the major field of **Soil and Water Engineering** is the result of original research work done by me. I also declare that no material contained in the thesis has been published earlier in any manner.

Date : **(N. BIDYARANI CHANU)**

Place: **I.D. No: BEM-15-16**

CERTIFICATE

Ms. N. BIDYARANI CHANU has satisfactorily prosecuted the course of research and that thesis entitled "**SIMULATION OF STREAM FLOW AND SOIL EROSION IN KRISHNA LOWER SUB BASIN**" submitted is the result of original research work and is of sufficiently high standard to warrant its presentation to the examination. I also certify that neither the thesis nor its part thereof has been previously submitted by her for a degree of any University.

Date: **(Dr. A. MANI)**

Place: **Chairperson**

CERTIFICATE

This is to certify that the thesis entitled "**SIMULATION OF STREAM FLOW AND SOIL EROSION IN KRISHNA LOWER SUB BASIN**" submitted in partial fulfillment of the requirements for the degree of "Master of Technology in Agricultural Engineering" in the major field of "**Soil and Water Engineering"** of the Acharya N.G. Ranga Agricultural University, Guntur is a record of the bonafide original research work carried out by **Ms. N. Bidyarani Chanu** under our guidance and supervision.

No part of the thesis has been submitted by the student for any other degree or diploma. The published part and all the assistance received during the course of the investigations have been duly acknowledged by the author of the thesis.

Thesis is approved by Student Advisory Committee

CHAIRPERSON: **Dr. A. Mani**
Associate Dean
College of Agricultural Engineering
Bapatla

MEMBER: **Dr. M. Raghu Babu**
Professor (Academic) and
University Head of SWE,
O/o of the Dean of Agril. Engineering
& Technology, ANGRAU,
Guntur

MEMBER: **Ms. M. Venkata Suneela**
Assistant Professor
Dept. of Mathematics
College of Agricultural Engineering
Bapatla

ACKNOWLEDGEMENT

Accomplishment of this thesis is the result of benevolence of ***Almighty,*** *benedictions of my* ***teachers****, love of my* ***parents****, and impetus of my* ***friends*** *and well* ***wishers****.*

First and foremost, I wish to express my deep sense of gratitude and indebtedness to my guide and supervisor ***Dr. A. Mani****, Associate Dean, College of Agricultural Engineering, Bapatla for giving me an opportunity to work under her guidance and providing the necessary resources to complete my work. Her valuable critiques, assistance and encouragement, which enable me to carry on the project successfully. I am highly obliged for her support throughout the program.*

I express my sincere thanks to ***Dr. M. Raghu Babu****, Professor (Academic) & University Head(SWE), ANGRAU, Guntur and* ***Ms. M. Venkata Suneela,*** *Assistant Professor, Dept. of Mathematics, College of Agricultural Engineering, Bapatla and member of my advisory committee for support and help.*

I own respectable regards to ***Dr. G. Ravi Babu****, Assoc. Prof. and Head, Dept. of Soil and Water Engineering, College of Agricultural Engineering, Bapatla, for providing valuable research facilities to do my project. I am so grateful to* ***Dr. Hema Kumar, Er. Krupavathi and Er. R. Ganesh Babu*** *for their co-operation and encouragement extended to me during my course work as well as research work.*

I own respectable regards to ***Dr. B. V. S Prasad****, Prof. and Head, Dept. of Agril. Processing and Food Engineering and Dept. of Farm Machinery and Power, College of Agricultural Engineering, Bapatla for their co-operation and encouragement extended to me during my course work as well as research work.*

I am deeply thankful to ***Mr. Ch Kranthi Kumar,*** *SRF for helping, supporting and his encouragement throughout the project.*

It's my great pleasure to thank **all the faculty members**, **Ph.D scholars** *and* **P.G. students** *of all the departments for creating a very friendly and wonderful environment in the department during whole course work. They are an important part of my successful completion of the course and my project work*

I am sincerely thankful to my ***lovely juniors****,* ***M. Lakshmi Durga, K. Sai Manogna, Sachin Shivhare, K. Vamsi, L. Madhuri, B. Joshna, D. Vashnavi*** *for their help and support in my project work***.**

I am in dearth of words to express my unboundful gratitude and love my beloved parents for their unbounding love and dedicated efforts to educate me to this level without whose encouragement brings out the best in every one of my endeavours.

In final, I thank all my well-wishers and others who helped me directly or indirectly not placed here, for their kind cooperation and support rendered to me.

Place: **(N. BIDYARANI CHANU)**

Date:

CONTENTS

LIST OF TABLES

LIST OF FIGURES

LIST OF SYMBOLS AND ABBREVIATIONS

A. P.	:	Andhra Pradesh
ANSWERS	:	Areal Nonpoint Source Watershed Environmental Resources Simulation
ARS	:	Agricultural Research Station
C	:	Crop management factor
^{0}C	:	Degree centigrade
CN	:	Curve number
Cusec	:	Cubic feet per second
DC	:	Determination coefficient
DEM	:	Digital Elevation Model
DHSVM	:	Distributed Hydrology Soil Vegetation Model
ERDAS	:	Earth Resources Data Analysis System
e.g	:	For example
et al	:	And others
FAO	:	Food and Agricultural Organization
Fig.	:	Figure
GAMES	:	Guelph Model for Agriculture Management Systems on Erosion and Sedimentation
GIS	:	Geographic Information System
h	:	Hour
ha	:	Hectare
HEC-HMS	:	Hydrological Engineering Centers Hydrologic Modeling System
HEC-GeoHMS	:	Hydrologic Engineering Center’s Geospatial Hydrologic Modeling System
i.e.	:	That is
K	:	Erodibility factor

km	:	Kilometer
km^2	:	Square Kilometer
LS	:	Topographic factor
LULC	:	Land Use and Land Cover
m	:	Meter
m/s	:	Meter per second
m^3/s	:	Meter cube per second
mm	:	Millimeter
Mha	:	Million hectares
MJ ha^{-1} yr^{-1}	:	Mega Joule per hectare per year
MUSLE	:	Modified Universal Soil Loss Equation
NBSSLUP	:	National Bearua of Soil Survey and Land Use Planning
NOAA	:	National Oceanic and Atmospheric Administrations
P	:	Conservation practice factor
USPED	:	Unit Stream Power-based Erosion Deposition
R	:	Erosivity factor
RMSE	:	Root mean square error
RS	:	Remote Sensing
RUSLE	:	Revised Universal Soil Loss Equation
SCS	:	Soil Conservation Service
SRTM	:	Shuttle Rader Topography Mission
t ha^{-1} yr^{-1}	:	Tons per hectare per year
USLE	:	Universal Soil Loss Equation
Viz.,	:	Namely
%	:	Per cent

ABSTRACT

Name of the Author	**:**	**Ms. N. BIDYARANI CHANU**
Title of the thesis	**:**	**SIMULATION OF STREAM FLOW AND SOIL EROSION IN KRISHNA LOWER SUB BASIN**
Submitted for the award of	**:**	**MASTER OF TECHNOLOGY**
Faculty	**:**	**AGRICULTURAL ENGINEERING & TECHNOLOGY**
Discipline	**:**	**SOIL AND WATER ENGINEERING**
Major Advisor	**:**	**Dr. A. MANI**
University	**:**	**ACHARYA N.G. RANGA AGRICULTURAL UNIVERSITY**
Year of submission	**:**	**2017**

Quantification of water resources in a catchment, particularly stream flow is necessary for a systematic analysis of water availability for long-term planning of water utilization. Stream flow is the spatial integration of runoff which is a major component of the catchment water balance. The lower Krishna basin is a deficit basin and it depends mainly on inflow from the upper basin and on upstream water uses. There is a declining trend of surface water inflow due to prevention of flow in the upper basin and lead to shrinkage of surface irrigation. Therefore, the project entitled 'Simulation of stream flow and soil erosion in Krishna lower sub basin' was proposed for systematic analysis of water availability.

The different DEMs were downloaded from different sources to generate basin characteristics namely drainage area, elevation, slope steepness, slope length, and streams relief ratio. Among these DEMs, SRTM 90 m produced correct stream network. The IRS P_6, LISS III images for 2014 and 2015 were downloaded from Bhuvan. The LULC maps were prepared for the study. Soil map developed by National Bureau of Soil Survey and Land Use Planning (NBSSLUP) was taken as reference map and clipped to the study area to identify the type of soils.

The study area consisted of mainly four types of soils. Majority of the area is under silt soils (46%) and clay soils (43%). Remaining 7 percent and 4 percent are under loam and water bodies. The average annual rainfall of study area for 23 years during 1990 to 2015 was 931.31 mm. The highest amount of rainfall was recorded in 2010 as 1620.71 mm and the lowest amount of rainfall was recorded in 2009 as 566.54

mm. About 91% of the area is nearly level and remaining 8% of the area occupied moderate slope to steep slope.

ArcGIS, ERDAS and HEC-HMS softwares were used and the SRTM DEM was used to derive parameters for the hydrological modelling. The results acquired using Geo-HMS were the catchment area of each sub-basin, slope of each sub-basin, flow length and time of concentration. After preparation of various input parameters, stream flow for a period of 23 years was simulated using SCS-CN technique. The time to peak and peak discharges for different storm events was also estimated.

Simulated runoff was more for the years with high rainfall. The annual runoff is highly correlated with annual rainfall with coefficient of 0.9. The simulated runoff depth was 1383.5 mm in the year 2010. It was only 261.97 mm in the year 2002. The average annual runoff depth during the period of 1993 to 2015 was 668.59 mm. Build up areas have produced more runoff followed by scrub land, current fallow, rabi crop, kharif crop, forest, plantation and double crop/triple crop areas. The simulated peak runoff rates were matched well with the inflow discharges that are available at Pulichintala project for different storm events and were in good agreement with R2=0.89. Hence, the model HEC- HMS can be used to predict runoff rate to plan flood mitigation measures.

RUSLE model integrated with GIS and RS techniques was used for estimation of annual average soil loss rate (t ha^{-1} yr^{-1}). The potential soil erosion in Krishna lower sub basin of Andhra Pradesh were mapped and quantified using RUSLE model from 1993-2015. The maximum annual average soil loss occurred in the Krishna lower sub basin for the year 1993 to 2015 was 28.69 t $ha^{-1}yr^{-1}$. Around 43.02% of catchment was prone to slight erosion. About 42.41% of area showed moderate soil erosion. Strong to severe erosion occurred in around 12.45% are in 1.3% area. Very severe erosion occurred in 0.8% which was very less compared to other classes. The study revealed that the average annual soil loss was sensitive to rainfall factor, R and the type of land use.

The very severe erosion was occured in 13.45% (262.66 km^2) of build up and 9.28% (21.65 km^2) of wasteland. Severe erosion occurred in 38.77% (768.561 km^2) percent of scrubland, in 18.62% (233.26 km^2) and 4.73% (43.93 km^2) of rabi crop area and waste land. Moderate erosion occurred in double/triple cropping area and slight erosion occurred in forest and Kharif crop. Percolation tank and check dams were suggested as conservation measures in severely eroded area.

Hence, the hydrological model HEC-HMS can be used for event based simulation of rainfall events in lower Krishna sub basin of Andhra Pradesh. RUSLE erosion model integrated with GIS and remote sensing can be used to map the soil loss in lower Krishna sub basin of Andhra Pradesh.

Chapter I

INTRODUCTION

Water is an abundant, yet a scarce natural resource. Water is one of the most basic necessities of life. All the activities we perform require water in one form or the other, directly or indirectly, in its primary form or in its virtual form. Hence, it is very important to ensure judicious use and equitable distribution of this precious natural resource. Also its per capita availability is decreasing, water is becoming a contentious issue worldwide. India is blessed with good rainfall well distributed over 5-6 months in the year. The average annual rainfall in the country is 1170 mm with a wide range between 100 mm in desert areas of Rajasthan to 10000 mm in Cherapunji. The total available water in the country is 4000 billion m^3 per annum. Out of this, over 1047 billion m^3 water is lost due to evaporation, transpiration and runoff, reducing the available water to 1953 billion m^3 and the usable water to 1123 billion m^3. It is disturbing to note that only 18% of the rainwater is used effectively while 48% enters the river and most of which reaches the ocean. Out of the total usable water, 728 billion m^3 is contributed from surface water and 395 billion m^3 is contributed by replenishable ground water. Against the above supply, the water consumed during the year 2006 in India was 829 billion m^3 which is likely to increase to 1093 billion m^3 in 2025 and 1047 billion m^3 in 2050, as estimated by the Government of India (Narayan, 2010). As the potential for increasing the volume of utilization of water is hardly 5-10%, India is bound to face severe scarcity of water in the near future.

Quantification of water resources in a catchment, particularly stream flow is necessary for a systematic analysis of water availability for long-term planning of water utilization. Stream flow is the spatial integration of runoff which is a major component of the catchment water balance. Stream flow is composed of base flow and storm flow. The relative importance of each of the flow mechanisms is mainly controlled by catchment attributes related to geology, soils, topography, climate, land cover, the level of antecedent soil water content, and rainfall intensity (Price, 2011). Stream flow serves a number of essential purposes, such as irrigation, recreation, drinking water, industrial uses, and transport (Quintero *et al.,* 2009). However, stream flow also carries some negative implications for society and environment. In fact, flooding is considered to be one of the prime catastrophic events threatening society in many countries. The flooding risk may increase under global environmental changes as a consequence of land use modifications (Betts *et al.*, 2007). The land use controls the water yield of surface streams and ground water aquifers and thus the amount of water available in a watershed.

Urbanization affects the hydrological characteristics of a catchment by reducing infiltration of rain water into the ground and increasing the volume and speed of surface runoff. The replacement of forest cover with paved surfaces or other land use types increases water yield due to reduction in water losses as a result of compaction of soil. This increases stream discharge, an important element in fluvial processes of erosion and sediment transportation. The processes of soil erosion result from an interrelated set of natural, human and hydrologic factors within a river basin. The natural factors responsible for erosion are topography, geology and soils. The hydrologic factors are climate, the amount and distribution of surface water runoff and ground water discharge; while land use is the main human factor. The effect of land use on river flow, and the consequent land degradation, is one of the most important environmental problems of our time.

Changes in land cover and vegetation have an effect on surface and groundwater hydrology and stream flow in sub-basins, and can alter the hydrological cycle. It is necessary to understand stream flow responses to changes in land use land cover in the basin. Information on stream flow and erosion is vital at this stage to facilitate decision making on sustainable water utilization and soil and water conservation measures for the rivers under rehabilitation so as to protect the ecosystem. Information on stream flow can be used to predict surface runoff. Reliable prediction of surface runoff from rainfall in a catchment is essential for several purposes in catchment treatment. Prediction of both volume and rate of runoff from a catchment is vital in the design of hydraulic structures including soil and water conservation, rainwater harvesting, flood control, and hydroelectric power generation structures. A major challenge still remaining is the accurate prediction of catchment runoff responses to rainfall events (McColl and Aggett, 2006).

Hydrological modeling is a commonly used tool to estimate the catchment hydrological response due to rainfall. Hydrologic models are symbolic or mathematical representation of known or assumed functions expressing the various components of hydrological cycle. A number of models were developed to simulate runoff. Simulation models that predict runoff are useful in examining the effects of land use and management practices on water flow behavior for natural resources management in catchment. Various simple models and procedures are available which can quantify the stream flow. The Hydrologic Engineering Centers Hydrologic Modeling System (HEC-HMS) is a reliable model and popularly used to simulate rainfall-runoff process even in ungauged catchments. Land use change, in particular clearing forests for agriculture, settlement and other infrastructural developments that increase paved surfaces, increases surface runoff and stream flow.

The prominent effect of land use change on soil erosion and soil loss monitoring is an urgent need. In this sense, the use of remote sensing is very important because one of the main application of the satellite data is change detection, due to the repetitive coverage and consistent quality of the satellite images. Remote sensing makes it possible to apply techniques and technologies to detect changes. A recent and emerging technology represented by Geographic Information System (GIS) is used as the tool to generate, manipulate and spatially organize geographic data. GIS when integrated with hydrological process models provide the basis for generating spatial information needs. Revised Universal Soil Loss Equation (RUSLE) (Renard *et al.,* 1997), is used for predicting spatial distribution of soil loss especially in watershed areas due to their ease of application.

Integrated hydrological models with GIS can be used for identifying suitable sites for soil and water conservation structures, prioritizing watersheds and for developing alternate watershed plans. The information on catchment degradation, resulting from erosion of the catchment and will facilitate planning for soil and water conservation programs. These conservation measures will be necessary to reduce the rates of soil loss caused by streamflow. Stream flow information will provide a scientific foundation for flood planning and management.

The river Krishna is one of the longest rivers in the Peninsular India (about 1,300 km in length). The Krishna basin is split into 7 sub-basins and Krishna lower sub-basin occupies 15.5% of the total Krishna basin. The lower Krishna sub basin drains in Andhra Pradesh an area of 11317.36 km^2. It covers two districts of Andhra Pradesh i.e. Guntur and Krishna. Annual rainfall of sub basin varies between 800-1200 mm. The lower sub basin of Krishna contains three major projects. Nagarjuna Sagar Dam with discharge capacity of 20,000 cusecs is providing irrigation for 8.5 lakh ha. Prakasam Barrage has the irrigation facility for 4.85 lakh ha. Pulichintala Project is about 85 km upstream of Prakasam barrage, Vijayawada and stabilizing an ayacut under Krishna Delta to an extent of 5.06 lakh ha. However, the lower Krishna basin is a deficit basin and it depends mainly on inflow from the upper basin and on upstream water uses. There is a declining trend of surface water inflow due to prevention of flow in the upper basin and lead to shrinkage of surface irrigation. It is also the region where most of the water is depleted by over consumptive uses. Hence, knowledge of water resources availability, particularly stream flow is very much needed for water resources management in lower Krishna basin.

Therefore, the present project entitled 'Simulation of stream flow and soil erosion in Krishna lower sub basin' is proposed for a systematic analysis of water availability using HEC-HMS model for its long-term planning of the water allocation and to avoid negative impact of flood with the following objectives.

Objectives

1. To simulate the runoff and soil erosion in Krishna lower sub basin using hydrological model
2. To assess the effect of land use land cover on stream flow and soil erosion
3. To identify technological measures for efficient utilisation of stream flow

Chapter II

REVIEW OF LITERATURE

Stream flow is the main factor which influences the hydrological characteristics in many ways. It is related to soil characteristics also in many ways. There is a need to develop and use quantitative methods for predicting the impact of land use changes on hydrology and soil erosion in simulating hydrological processes and technological interventions in planning land management strategies for a watershed. The review has been used for formulating the objectives and development of methodology. Keeping the above points in view, the extensive review of literature pertaining to different aspects related to streamflow, land use land cover, soil erosion are presented under the following sub headings.

2.1 Simulation of stream flow

2.2 Soil erosion

2.3 Technological measures for efficient utilization of streamflow

2.1 Simulation of streamflow

Hydrology is concerned with study of the motion of the earth's waters through the hydrologic cycle, and the transport of constituents such as sediment and pollutants in the water as it flows. Hydrological phenomena are extremely complex, highly non-linear and highly variable in space and time. A hydrological model is a simplified simulation of the complex hydrological system.

Modeling is one field of scientific activity which has developed the capability of delivering customized solutions through identifying a variety of arrangements or changes within a system to comply with both external and internal highly developed mathematical capabilities and versatile software tools.

The hydrological models can be classified according to whether the hydrological processes are described as conceptual, empirical, or fully physically based as shown in Fig 1 (Dwarakish and Ganasri, 2015).

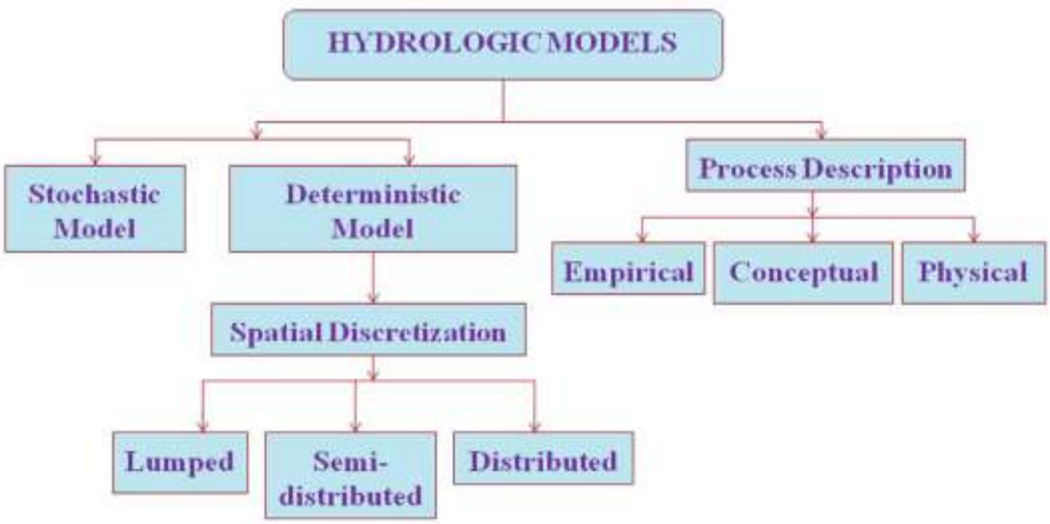

Fig. 2.1 Classification of hydrologic models

Catchment models simulate the hydrologic processes by which rainfall is converted into stream flow. The catchment is the system being modeled; with rainfall corresponding to the input parameter and runoff characteristics being computed. Hydrological models vary greatly in their computational capabilities and enormous range in levels of sophistication including the input data requirements of the model based on the recent advances in computer technology (Devries and Hromadka, 1993). Hydrological models have high importance to quantify the processes of the hydrological cycle in an entire catchment or parts of it and allow assessing the potential impacts of land use and land cover and climate change on the hydrological cycle.

2.1.1 Methods of estimating streamflow

Choosing a model of appropriate complexity is equally important to consider the ability of the model to perform the desired land use or climate change scenarios. Among the models, distributed models rely on a physically based description of the runoff generation and the effects of different land covers play an important role in exploring hydrologic effects of land-use changes in the catchment. The Mike SHE, Soil and Water Assessment Tool (SWAT), Hydrologic Engineering Centers Hydrologic Modeling System (HEC-HMS), Distributed Hydrology Soil Vegetation Model (DHSVM), L-THIA and CELTHYM, Rainfall–runoff Modelling System (PRMS) have been extensively used to assess the effects of land use changes on hydrologic processes.

Distributed models generally require large amount of data. However, the governing physical processes are modelled in detail, and if properly applied, they can provide the highest degree of accuracy. In semi- distributed models, parameters are partially allowed to vary in space by dividing the basin into number of smaller sub-basins. The main advantage of these models is that their structure is more physically-based than the structure of lumped models, and they are less demanding on input data than fully distributed models. HEC-HMS, SWAT, HBV are some examples of semi-distributed models (Sintayehu, 2015)

2.1.2 HEC-HMS overview

The HEC-HMS simulates the precipitation-runoff process particularly for dendritic watershed systems. The HEC-HMS is a semi-distributed physically based hydrologic model. It uses deterministic mathematical modelling to compute various components of the hydrologic cycle. These are evapotranspiration, precipitation, infiltration, and runoff. HMS is applicable in a wide range of geographic areas for solving the widest possible range of problems including large river basin water supply and flood hydrology, and small urban or natural watershed runoff. Hydrographs produced by HMS are used directly or in conjunction with other software for studies of water availability, urban drainage, flow forecasting, future urbanization impact, reservoir spillway design, flood damage reduction, floodplain regulation, and systems operation.

HEC-GeoHMS is a geospatial hydrology toolkit designed to prepare data for HEC-HMS simulations. The program allows users to visualize spatial information, document watershed characteristics, perform spatial analysis, delineate sub-basins and streams, construct inputs to hydrologic models and assist with report preparations. HEC-GeoHMS creates input files which can be used for HEC-HMS simulations.

2.1.3 Application of HEC-HMS

The HEC-HMS is in use for more than 30 years in hydrologic simulation. It is freely available for download from the HEC website and is supported by the US Army Corps of Engineers. It provides a graphical user interface making it easier to use the software and the program is widely used and accepted for many official purposes. The model can be applied as well to small scale urban drainage basins as to large scale river basins to simulate water supply and flood hydrographs (Feldman, 2000).

Azam *et al.,* (2017) assessed and forecasted an early flood warning system for Mushim stream watershed using HEC-HMS. Sensitivity analysis performed on the basis of three statistical evaluation criteria showed that the HEC-HMS hydrologic model is more sensitive to the CN value over the study area. During the calibration process, it was noted that Clark unit hydrograph was better able to simulate the flows with lesser value of objective function than the Snyder unit hydrograph method.

Devakota and Dhiraj (2015) assessed the hydrological regime of the Koshi River in Nepal using HEC-HMS. The results concluded that the average water availability was not much affected by the climate change. However, temporal flow variations will increase in the future.

Kishor *et al*., (2014) simulated the rainfall-runoff process in Balijore Nala Watershed of Odisha, India using HEC-HMS model. Runoff and discharges were simulated using 24 random rainstorm events covering four year (2010 – 2013) data. For calibration of model, the statistical tests of error functions like mean absolute relative error (MARE) and root mean square error (RMSE) between the observed and simulated data were used. The results indicated values of RMSE as 0.09 $m^3 s^{-1}$ and MARE as 0.06 for peak discharge and RMSE as 0.70 mm and MARE as 0.05 for runoff depth. The model could help to save time and money in obtaining the runoff data in un-gauged watershed where there was no gauging station to measure runoff.

Jiang *et al.*, (2014) carried out streamflow simulations using HEC-HMS at monthly and annual scales and found that the relationship between streamflow and precipitation was positive, whereas the same between streamflow and temperature is negative in the Luanhe basin of North China.

Mangolika *et al*., (2014) evaluated the runoff of Damodar river basin in eastern India using HEC-HMS model. Sensitivity analysis of the model was carried out for the input parameters. The study revealed that both the peak discharge and runoff volumes to be sensitive to rate of infiltration and percentage of impervious area. The Nash-Sutcliffe model efficiency criterion, percentage error in volume, the percentage error in peak and net difference of observed and simulated time to peak, were used for performance evaluation. The model demonstrated good performance, with aforementioned performance indices values ranging from 75-81%, -10.5-19.4%, -18.0-29.6% and 0-1 day for simulation of stream flow. Thus the model might be successfully applied to watersheds in the Damodar river basin.

Majidi and Shahedi (2012) used the HEC-HMS hydrological model to simulate rainfall-runoff process in Abnama watershed located in south of Iran. To compute infiltration, rainfall excess and flow routing, Green-Ampt, SCS Unit hydrograph and Muskingum routing were chosen, respectively.

Asgari and Hosseinzade (2008) carried out hydrological modeling of Shirvan dam using HEC-HMS model. The results showed that there is a little difference between simulated and observed peak flow.

Markus *et al.,* (2007) estimated the design precipitation in Northeastern Illinois using HEC-HMS. The results were compared with those published in TP-40, Bulletin 70, and NOAA-14. The average design precipitation for 12 watersheds in the study, based on the current study was 24.32% larger than that of TP-40, which resulted in 46.92% larger design discharges. For the 12 watershed locations, the differences in average design precipitation and average design discharges between the current study and more recent sources (Bulletin 70 and NOAA-14) did not exceed 5%.

Yener *et al*., (2007) simulated the rainfall runoff process by dividing the basin into three subbasins: Kirazdere, Kazandere, and Serindere and each sub basin is modeled with its own parameters. Modeling consisted of two things: event-based hourly simulations and runoff scenarios using intensity-duration-frequency curves. Infiltration loss and baseflow parameters of each sub basin are calibrated with hourly simulations. This study concluded that the simulated runoff values can be used for flood control and flood damage estimation studies.

Radmanesh *et al.,* (2006) calibrated and validated the HEC-HMS model in Yellow River watershed in southwestern Iran. The results showed that the SCS method resulted in better agreement between peak discharge of observed and simulated hydrographs than other HEC runoff computation methods.

Kathol *et al.,* (2003) applied HEC-HMS model to determine the peak discharge and volume of runoff in two agricultural areas in South East of South Dakota state. The study used SCS method and SCS unit hydrograph to determine rainfall losses and watershed hydrograph respectively. Model parameters showed that the amount of curve numbers is highly sensitive, while the initial absorption was less sensitive to changes in the objective function in HEC-HMS model.

2.1.4 Effect of land use land cover on streamflow

Land use and land cover is two separate terminologies which are often used interchangeably. Land cover corresponds to the physical condition of the ground surface, for example, forest, grassland, concrete pavement etc., while land use reflects human activities such as the use of the land, for example, industrial zones, residential zones, agricultural fields etc. Land-use refers to the way in which land has been used by humans and their habitat, usually with accent on the functional role of land for economic activities.

Land use affects land cover and changes in land cover affect land use. Changes in land cover by land use do not necessarily imply degradation of the land. However, many shifting land use patterns driven by a variety of social causes, result in land cover changes that affects biodiversity, water and radiation budgets, trace gas emissions and other processes that come together to affect climate and biosphere.

Amin *et al.,* (2012) carried out a study on land use land cover mapping of Srinagar city in Kashmir Valley. They observed that the Srinagar city has experienced significant changes during 1990 to 2007. The analysis also showed that changes in land use pattern have resulted in the loss of forest area, open spaces, etc. Mehta *et al.* (2012) presented an integrated approach of remote sensing and GIS for land use and land cover study of arid environment of Kutch region in Gujarat in between year 1999 and 2009. Kumar *et al.,* (2013) carried out study on biomass estimation of Sariska Wildlife Reserve using forest inventory and geospatial approach to develop a model based on the statistical correlation between biomass measured at plot level and the associated spectral characteristics.

Land use changes have significant impact on the quantity and quality of runoff from the catchment areas. In parallel with the development of cities, impermeable surfaces such as roofs, streets, sidewalks, parking lots and runways, replacing the natural and permeable land and precipitations which have been influential in the soil and cause vegetation growth, because of the expansion of impermeable surfaces, changed into urban floods, causing damage to buildings and facilities and water logging in city pathways.

Amin *et al.,* (2015) monitored the land use change at Ardabil using HEC-HMS model and Remote Sensing and GIS technique. The study investigated the changes in land use and determined its impact on the flooding area using satellite images, maps of land use pertaining the years 1984, 1994, 2004, 2014 as well as changes in population between the years 1984 to 2014. The curve number (CN) for the years 1984, 1994, 2004, 2014 was 84, 87, 92 and 96 respectively in increasing trend. During the 30 years of the study, the built up area has been increased from 1,796.22 ha (1984) to 5225.04 ha (2014) which represents an increase of 2.9 times in the 30 years.

Chen *et al*., (2015) analysed the effect of land use change on flood characteristics at Xiaoqinhe catchment and its sub-catchments, a part of lower Yellow river basin in Northern China where intensive urban expansion had taken place during 1995–2008. The peak discharge was occurred (130 $m^3 s^{-1}$) on 5th August at 13:00LT for the 2008 scenario, while the peak discharge decreased to 117 $m^3 s^{-1}$ and the time of the peak was 5 h ahead in 1995 scenario. Land cover change between 1995 and 2008 had produced 11.1% of peak discharge increment and 15.3% of excessive flood volume. The peak discharges increased 16.7% and 23.1%, while the peak time delayed 5 h and 6 h respectively under 1995 and 2008 land cover.

Alexakis *et al*., (2014) assessed the impact of land use change on flood hydrology of Yialias basin in Cyprus. The study described the hydrological processes and internal basin dynamics of the three major sub-basins in order to study the diachronic effects of land use changes. The results indicated the increase of runoff response under the changed land use conditions of 2010. The change was estimated to be 10.2%, 7% and 11.1% for the sub basins Kotsiatis, Nisou and Potamia respectively in comparison to 2000.

Joy *et al*., (2014) evaluated the varying degrees of land-use/cover (LULC) changes across sub-catchments that affect a flood peak at the catchment outlet at Konar catchment using HEC-HMS. The study showed considerable increase in rocky waste and decreases in the areas under paddy cultivation and open forest from 1976 to 2004. Peak discharge was 1023.3 $m^3 s^{-1}$ occurring on 1976 while the peak discharge increased to 1194.7 $m^3 s^{-1}$ for the year 2004.

Zhang (2013) investigated the performance of fully and semi-distributed hydrologic models in simulating the process of transformation from rainfall to runoff in mountain areas. The fully-distributed models Basin Pollution Calculation Center (BPCC) and HEC-HMS are calibrated for the Zhenjiangguan watershed located in the upper stream of Minjiang River Southwest China using stream- flow observations at the basin outlet. The analyses of the study indicated that the hydrographs simulated by the BPCC are relatively closer to the observed ones than those simulated by the HEC-HMS in view of the spatial heterogeneity in terrain, soil texture, land cover and meteorological conditions in mountain areas.

Suriya and Mudgal (2012) developed flood zone map of the Thirusoolam sub watershed using HEC-HMS. In the study, it was found that the flooded area has increased from 31.70 km^2 for 1976 land use condition to 36.61 km^2 for 2005 land use condition. The depth of flooding has increased from 3.71 m for 1976 land use condition to 4.55 m for 2005 land use condition. This indicates that the urbanization has increased the flooded area and flood depth.

Jinkang *et al*., (2012) developed and examined the effects of urbanization on annual runoff and flood events of the Qinhuai River watershed in Jiangsu Province, China. This study revealed that the watershed experienced conversion of approximately 17% non-urban area to urban area between 1988 and 2009. The urbanization scenarios for various years were developed by overlaying impervious surfaces of different land use maps to 1988 (as a reference year) map sequentially. When impervious ratios change from 3% (1988) to 31% (2018), the mean annual runoff would increase slightly and the annual runoff in the dry year would increase more than that in the wet year. The daily peak discharge of eight selected floods would increase from 2.3% to 13.9%.

Ali *et al*., (2011) simulated the impacts of land-use change on surface runoff of Lai Nullah Basin in Islamabad, Pakistan. The HEC-HMS rainfall-runoff model was calibrated and validated for 5 storm events in the study area, and the results showed good consistency between the simulated and measured hydrographs at the outlet (Katarian Bridge) of the basin with Nash–Sutcliffe efficiency ranging from 76 to 98%. The results indicated that the future land use as envisaged in the master plan is projected to increase the total runoff between 51.6 and 100.0% as well as the peak discharge between 45.4 and 83.3%, and that the magnitude of peak discharge increment relates to the expansion rate of built-up area.

James and Zhi-jia (2010) presented and examined the applicability, capability and suitability for flood forecasting in Misai and Wan'an catchments using HEC-HMS. The study had shown that simulated and observed peak discharges occurred on the same day and their time difference was one hour, which is acceptable for flood forecasting. The entire determination coefficient (DC) for the Misai Catchment was above 0.9, while in the Wan'an Catchment there were 0.74 and 0.76 DC values below the acceptable value.

Chen *et al., (*2009) studied the impacts of land use change scenarios on storm-runoff generation in Xitiaoxi basin, China. The HEC–HMS rainfall-runoff model is calibrated and validated for 7 storm events in the study area, and the results showed good consistency between the simulated and measured hydrographs at the outlet of the basin with Nash–Sutcliff efficiency ranging from 75% to 95%.

Lin *et al., (*2009) developed and compared optimal and empirical land-use models for the development of an urbanized watershed forest in Taiwan. Optimization was implemented using simulated annealing in a spatial pattern optimization model (OLPSIM), and developments predicted by the drivers of past land-use changes were modeled with the CLUE-s model. The landscapes simulated by the models were then input to a precipitation-runoff model (HEC-HMS) to assess the impact of land-use patterns on runoff in the watershed and sub-watershed scales. The results of hydrological simulations suggested that the three land-use strategies differ less in their total hydrological outputs, but more in their distribution of hydrological outputs across different sub-watersheds.

Khaliq (2004) evaluated the effect of land use change on hydrologic characteristics of surface waters, West of Azerbaijan province in Barandoz Chay basin HEC-HMS. The results showed that the because of the change occurred in the studied basins, flood peak flow increased more than of the flood volume and time focus and latency time reduced to the peak.

2.2 Soil Erosion

Soil erosion is one of the major problems in agriculture and natural resources management. It reduces soil productivity, pollutes the streams and fills the reservoirs (Fangmeier et al. 2006). Human activity such as construction of roads, highways, and dams, control works on streams and rivers, mining, and urbanization usually accelerate the process of erosion, transport, and sedimentation (Julien, 2010). Soil erosion by water involves the processes of detachment, transportation, and deposition of sediment by raindrop impact and flowing water (Foster and Meyer, 1977; Wischmeier and Smith, 1978). Water erosion is influenced by four factors namely, rainfall, soil type, slope gradient, and soil use/vegetation cover.

The mechanism of soil erosion is shown in Fig 1, in which water from sheet flow areas runs together under certain conditions and forms small rills. The rills make small channels. When the flow is concentrated, it can cause some erosion and much material can be transported within these small channels. A few soils are very susceptible to rill erosion. Rills gradually join together to form progressively larger channels, with the flow eventually proceeding to some established streambed. Some of this flow becomes great enough to create gullies. Soil erosion may be unnoticed on exposed soil surfaces even though raindrops are eroding large quantities of sediment, but erosion can be dramatic where concentrated flow creates extensive rill and gully systems. (Kim, 2006)

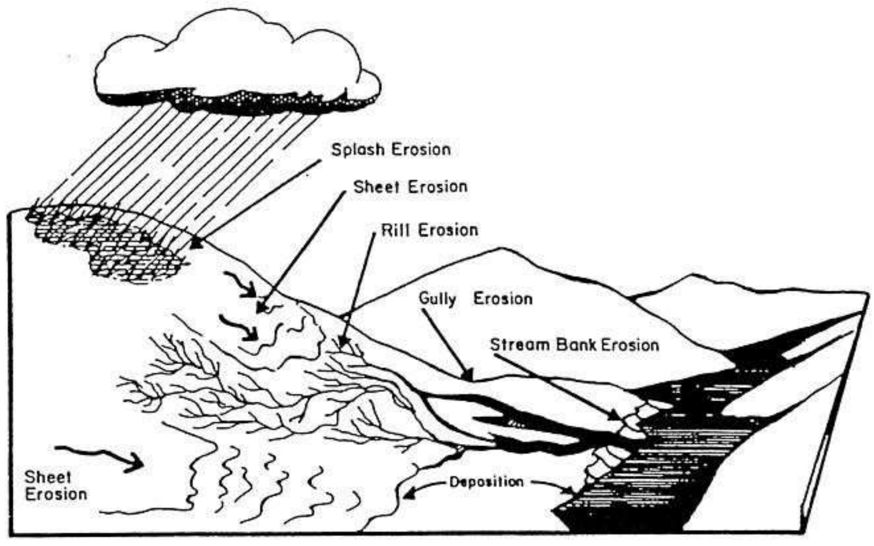

Fig. 2.2 The mechanisms of soil erosion (USACE, 1985)

2.2.1 Methods of estimating soil erosion

Existing soil erosion assessment methods include qualitative methods that identify erosion risk and quantitative methods that measure precise erosion rates. The qualitative methods include visual interpretation, index integration, and image classification. The quantitative methods include erosion model, digital elevation model, nuclear tracing, and neural network method.

The Universal Soil Loss Equation (USLE) model was suggested first based on the concept of the separation and transport of particles from rainfall by Wischmeier and Smith (1965) in order to calculate the amount of soil erosion in agricultural areas. It is the most widely used and accepted empirical soil erosion model developed for sheet and rill erosion based on a large set of experimental data from agricultural plots.

The USLE has been improved during the past 30 years by number of researchers. Modified Universal Soil Loss Equation (MUSLE) (Williams, 1975), Areal Nonpoint Source Watershed Environmental Resources Simulation (ANSWERS), the Guelph Model for evaluating the effects of Agriculture Management Systems on Erosion and Sedimentation (GAMES) (Rudra et al. 1986), the Unit Stream Power–

based Erosion Deposition (USPED) (Mitasova et al. 1996) and Revised Universal Soil Loss Equation RUSLE (Renard et al., 1997) are some of the models which estimate soil erosion.

2.2.2 Revised Universal Soil Loss Equation (RUSLE)

The USLE was revised in 1997 in effort to provide better estimate of the values of the various parameters in the USLE. There are five major factors that are used to calculate the soil loss for a given site. Each parameter is the arithmetic estimate of a specific condition that affects the severity of soil erosion at particular location. The calculated erosion values reflected by this model can vary significantly due to fluctuating weather conditions. Thus, the erosion values obtained from the RUSLE (Revised Universal Soil Loss Equation) more accurately represents long-term averages. (Kim, 2006)

The RUSLE uses the simple equation

$$A = R \times K \times LS \times C \times P$$

Where 'A' is the average annual potential soil loss in t ha^{-1} yr^{-1}

'R' is the rainfall-runoff erosivity factor

'K' is the soil erodibility factor

'LS' is the slope length and degree

'C' is the land-cover management factor

'P' is the conservation practice factor

2.2.3 Assessment of soil erosion using remote sensing and GIS

Rapid developments occurring in the technology of Remote Sensing (RS) and Geographic Information Systems (GIS) provide new approach to meet various demands related to the modeling of resources including soil and water conservation. Green (1992) stated that the integration of RS in a GIS database can reduce costs, and time as well as improve the detailed soil survey information. Therefore, the use of RS and GIS in watershed management would be very helpful to the managers in making the decisions.

Satellite data can be used for mapping, monitoring and estimation of soil erosion. The erosion mapping using GIS and RS has been conducted in many countries which combined GIS with RUSLE for soil erosion and loss assessment. Nevertheless due to limited data availability, highly variable and complex erosion processes in regional scale is difficult to estimate soil erosion by conventional method but can be done easily using remote sensing and GIS. The system is designed to capture, store, update, manipulate, analyze, and display studied data and used to perform analyses (ESRI, 2005).

There are some advantages of linking soil erosion models with a RS and GIS such as the following:

1) The data requirements are not too complex or unattainable. It is relatively easy to understand, and it is compatible with GIS.
2) The possibility of rapidly producing input data to simulate different scenarios. A GIS provides an important spatial/analytical function performing the time-consuming georeferencing and spatial overlays to develop the model input data at various spatial scales.
3) The ability to use very large catchments with many pixels, so the catchment can be simulated with more detail.
4) The facility of displaying the model outputs. Visualization can be used to display and animate sequences of model output images across time and space. Therefore, visualization enables objects to be viewed from all external perspectives, and to invoke insight into data through manipulable visual representations (Tim, 1996).

Chen *et al*., (2017) assessed the soil loss by using a scheme of alterative sub-models based on the RUSLE in a Karst Basin of Southwest China. The RUSLE gave a mean annual erosion rate of 30.24 MJ ha^{-1} yr^{-1} from the 1980s to 2000s. The mean annual erosion rate obtained using RUSLE is consistent with the result of previous research based on in situ measurement from 1980 to 2009. The result of the RUSLE model is sensitive to the slope steepness, slope length, vegetation and digital elevation model (DEM) resolution.

Napoli *et al.,* (2016) developed and assessed the long-term average annual soil loss in Chianti region, Italy by using RUSLE. The results of the study indicated that more than 29% of the Chianti territory was affected by values of soil loss which exceed the tolerable level. In addition, over 13% of the total area, corresponding to about 11,900 ha, was subjected to high and severe erosion processes with annual losses exceeding 22 t ha^{-1} yr^{-1}.

Habtamu and Amare (2016) estimated the mean annual soil loss by using RUSLE, GIS and Remote sensing techniques. The result revealed that the annual soil loss of the watershed extended from none in the lower and middle parts of the watershed to 265 t ha^{-1} yr^{-1} in the steeper slope part of the watershed with a mean annual soil loss of 47 t ha^{-1} yr^{-1}. The total annual soil loss in the watershed was 2,55,283 tons. About 181801 (71%) tons of soil erosion was occurred in about 6691 (24%) hectares of land. It was concluded that very severe soil loss was observed in the narrower steep slope upper part of the watershed at a rate that exceeded the tolerable soil loss limit.

Tanyaş *et al*., (2015) estimated cover-management factor of RUSLE and validation of RUSLE model in the watershed of Kartalkaya Dam. The study revealed that the input parameters of RUSLE require extensive filed and laboratory studies, so that in most of the cases, alternative approaches were used in the calculation of these parameters instead of original approaches.

Biswas *et al*., (2015) identified areas vulnerable to soil erosion risk in Telangana, India using GIS methods. The results revealed that around 69% of the state has a negligible risk of soil erosion above the tolerance limits, and did not call for immediate soil conservation measures. The remaining area (2.17 Mha) requires conservation planning. Four districts, viz. Adilabad, Warangal, Khammam, and Karimnagar are the most risk-prone areas with more than one-quarter of their total geographical area showing net positive soil erosion risk values.

Efthimiou *et al*., (2014) assessed the Venetikos River catchment, located at Western Macedonia, Northern Greece, using the RUSLE model and GIS. The results of the study revealed that the inter-annual implementation of the model, mean annual soil loss per unit area was calculated equal to 23.49 t ha^{-1} yr^{-1}. High risk erosion sites are located at the northern part of the catchment, while diffuse manifestations occur at its western and southern boundaries, as well as its lowlands (eastern part) near its outlet.

Ali (2012) mapped the spatial distribution of different erosion prone areas using USLE model by estimating the average annual soil losses of Mashhad plain, Northeast of Iran. The estimated annual soil loss values were subsequently grouped into five classes ranging from 0 to 0.25 t $ha^{-1}yr^{-1}$ around the trough line of the plain at Kashafrud river to 2–10 t ha^{-1} $year^{-1}$ at the hills and pediment plains. Over 5.6% and 34.8% of the plain area were found to be under critical erosion-prone area and under negligible and low soil loss classes respectively. Areas covered by moderate, relatively high, and high erosion potential zones were 42.6%, 17.2%, and 5.6% respectively.

Ishtiyaq and Verma (2013) assessed the soil erosion of Tandula Reservoir using USLE model and GIS. The result obtained from USLE model has been compared with the existing Nayak and Khosla models. The estimated soil loss using USLE with GIS, Nayak and Khosla methods were 490615 t ha^{-1}, 294588 t ha^{-1} and 396286.479 t ha^{-1} respectively. It was observed that USLE with GIS gave better result as compared to other two methods.

Naik *et al*., (2013) explored the erosion status in the eastern coastal region of India. The study was carried out to explore the existing characteristic features, problems and status of erosion and its remedial measures for the conservation and management of valuable coastal resources in respect of three states i.e. West Bengal, Odisha and Andhra Pradesh in the east coast. The potential soil loss reported for Andhra Pradesh, Odisha and West Bengal are 407, 144 and 17 and annual EI_{30} of 400 – 600, 600 – 800 and 600 – 800 MJ mm ha^{-1} h^{-1} respectively. Major portion of the coastal areas of West Bengal, Odisha and Andhra Pradesh falls in soil loss category of < 5 t $ha^{-1}yr^{-1}$.

Prasannakumar *et al*., (2012) estimated the soil erosion vulnerability of a forested mountainous sub-watershed in Kerala, India using RUSLE. The result of the study showed that maximum soil loss of 17.73 t h^{-1} yr^{-1} was found with a close relation to grass land areas, degraded forests and deciduous forests on the steep side-slopes (with high LS).

Reshma and Uday (2012) assessed the annual soil loss in Upper South Koel basin using Universal Soil Loss Equation (USLE) in GIS framework. The R-factor of the USLE was found as 546 MJ mm ha^{-1} h^{-1} yr^{-1}. The K-factor and LS factor varied from 0.23 - 0.37 and 0 – 21 respectively. The C factor was computed from NDVI values derived from Landsat-TM data. The P value was computed from existing cropping patterns in the catchment. The annual soil loss estimated in the watershed using USLE was 12.2 t ha^{-1} yr^{-1}. The study revealed that area covered under slight, moderate, high, very high, severe, very severe soil loss potential zones are 64.70%, 17.10%, 10.05%, 4.65%, 1.60% and 1.90% respectively.

Saleh *et al.*, (2010) estimated the soil loss and sediment yield using GIS and remote sensing of Ilam dam watershed, Iran. The study indicated the slope length and slope steepness of RUSLE were the most effective controlling parameter on soil erosion. The average annual soil loss and sediment yield was predicted upto 61.80 and 18.84 t ha^{-1} yr^{-1} respectively.

Terranova *et al*., (2009) identified areas highly affected by soil erosion by water (WSE) in Calabria by comparing the scenarios obtained by assuming control and preventive measures and actions, as well as actual conditions generated by forest fires, also in the presence of conditions of maximum rainfall erosion. GIS techniques had been adopted to treat data of reasonable spatial resolution obtained at a regional scale for application to the RUSLE model. The values obtained by the application of the RUSLE model have emphasized that land management by means of measures and actions for reducing WSE causes a notable reduction of the erosive rate decreasing from 30 to 12.3 MJ $ha^{-1} yr^{-1}$.

Krishna (2009) mapped the soil erosion susceptibility using remote sensing and GIS of the Upper Nam Wa Watershed, Nan Province, Thailand. The rate of potential soil erosion ranged as low as 0 to a maximum of more than 800 t ha^{-1} yr^{-1}. The analysis showed that most of the area has potential soil erosion rate of more than 800 t ha^{-1} yr^{-1}, followed by areas with 0–50 tons, 400–800 tons, and 50–400 tons.

Gregor and Matjaz (2004) estimated the R factor of RUSLE from daily rainfall data in the sub-Mediterranean climate of southwest Slovenia by using two models. A simple single-equation model was a good predictor on the annual scale. A more complex model gave good predictions for all months, including those with a low R factor. The overall efficiency coefficient (e) for the complex model was 0.879, which was slightly better than the first model.

Mazul *et al*., (2001) estimated the soil loss using remote sensing and GIS in Northern Thailand. The results indicated that the changes in agricultural pattern from traditional crops to orchard plantation and adoption of soil conservation decreased the annual soil erosion rate from 1.24 mm yr^{-1} in 1992 to 0.91 mm yr^{-1} in 1996.

2.2.4 Effect of land use land cover on soil erosion

Land use change may influence a variety of natural and ecological processes, including soil nutrient, soil moisture, soil erosion, land productivity and biodiversity (Fu *et al.*, 1999). It is very important that the studies of land use changes understand regional eco-environment and global environmental change. In recent years, the mutual impact of land use/cover change (LUCC) and soil erosion has become a major environmental concern, and strong influences of land use changes on soil erosion and sediment discharges have been identified. Among the factors explaining the intensity of soil erosion, plant cover and land uses are considered the most important, exceeding the influence of rainfall intensity and slope gradient (Thornes, 1990; Kosmas *et al.,* 1997; Wainwright and Thornes, 2004). Land use changes, especially physical expansion of urban areas and extensive use of land for agricultural purposes, may have positive or negative influence on soil erosion because of climatic, environmental and economic conditions

Li *et al.,* (2013) studied effects of land use changes of Guangdong, China, from 2002 to 2009 using remote sensing and estimated soil erosion using the Universal Soil Loss Equation. The results of the study showed that forest and wasteland land conversions induce substantial soil erosion, while transition from wasteland to forest retards soil loss. The average annual soil erosion amount was estimated about 21.86 t ha^{-1} yr^{-1} in 2009 comparing with 10.81 t ha^{-1} yr^{-1} in 2002.

Alkharabsheh *et al.,* (2013) assessed the impact of land cover change on the erosion in agricultural areas of northern Jordan using RUSLE. The study quantified and analyzed the soil erosion in the area between the years 1992 – 2009, and by comparing it with land cover changes. The mean soil loss in the study area was 9.53 t ha^{-1} and 8.97 t ha^{-1} in 1992 and 2009 respectively. The change of soil erosion between 1992 and 2009 was due to the change of the vegetation cover in this time period, as the other parameters were kept constant. The areas with mainly high soil erosion were located in the central and western parts of the study area, while the areas with decreased soil erosion were located in the north and southwest and were characterized by high slope and rainfall. The eastern part showed no major change between the two years, and was characterized with low rainfall, low slope and poor plant coverage.

Saowanee (2012) investigated the impacts of land use changes on soil erosion in Pa Deng sub-district, adjacent area of Kaeng Krachan National Park, Thailand, by applying remote sensing technique, geographical information system (GIS) and the Universal Soil Loss Equation (USLE). The study analyzed the land use changes in terms of area, size and pattern of the soil erosion risk in Pa Deng in the 1990–2010 period. According to the land use study of the two periods, it was found that in 2010, the community area and bare land significantly decreased to 86.04% and 69.14%, respectively while the forest and agricultural area slightly increased by 1.31% and 4.03%, respectively. The assessment of soil erosion risk in the study area revealed that the low soil erosion risk category (0–12.5 MJ ha^{-1} yr^{-1}) occupied most of the area in both 1990 and 2010 (approximately 85% of total area).

Roberto *et al*., (2012) predicted the possible impact of reservoirs and land use changes on sediment load in South East Asia using RUSLE and GIS framework. The mean annual simulated soil losses in basins prior to reservoirs operation are in good agreement with observations, with values ranging from 0.17 mm yr^{-1} to 0.34 mm yr^{-1} compared to the observed 0.19–0.35 mm yr^{-1} range. The result indicated that the land use change of 35% decrease in area resulted increased soil erosion upto 28%.

Wang *et al.,* (2012) evaluated the effect of land use changes on soil erosion and sediment yield using a grid-based distributed modelling approach. In this study, the total forested area dropped 10% from 1990 to 1995, whereas the areas of grassland and farmland increased by 6.7% and 3.3%, respectively. The total area where the land use changed between these 2 years was approximately 787.3 km^2. The results indicated that even relatively minor land use changes had a significant effect on regional soil erosion rates and sediment transport to rivers.

Arabinda and Kamlesh (2011) determined the influence of land use and land cover change (LUCC) on soil erosion potential of a reservoir catchment during the period 1989 to 2004. The results of the study showed that the mean soil erosion potential of the watershed was increased slightly from 12.11 t ha^{-1} yr^{-1} in the year 1989 to 13.21 t ha^{-1} yr^{-1} in the year 2004. Spatial analysis revealed that the disappearance of forest patches from relatively flat areas, increased in wasteland in steep slope, and intensification of cultivation practice in relatively more erosion- prone soil.

Chen and Peng (2000) studied the effect of land use changes on soil conditions in arid region of Korla City, China. The study revealed that the rate of vegetation cover in pasture, meadow, upland, crop rotation triennially, fallow land, and waste land is 90.0%, 74.0%, 49.0%, 54.0%, 42.0%, and 16.0% respectively. The rate of vegetation cover in desert is the lowest, only 10.0%.

2.3 Technological measures for efficient utilization of streamflow

In a natural environment, a small percentage of precipitation becomes surface runoff; however, as urbanization increases, the amount of surface runoff drastically increases. Surface runoff is created when pervious or impervious surfaces are saturated from precipitation or snow melt (Durrans, 2003). The utilization of remote sensing and GIS technology in streamflow management is constantly evolving, and GIS technologies are utilized to help decision-makers to determine the most efficient ways to manage streamflow, including the selection of capture measures based on criteria, and the evaluation of methods to capture urban runoff. However, as explained by Wang *et al.*, (2012), even in the most technically complex analysis, it is always necessary for the human element to select appropriate criteria and make other subjective decision. Recent streamflow management systems have largely focused on ecosystem-based approaches (instead of traditional approaches of moving the streamflow out of the affected area), which require groundwater recharge, maintenance of the natural flow regime, downstream impacts and water quality. Stormwater runoff management practices can be broadly classified into two categories. The first is the reduction of surface water runoff quantity, and the second is the improvement of storm water quality, before draining out in nearby water bodies or infiltrating into the ground. The storm water runoff management practices evolved with time, and new strategies have been developed to minimize the negative storm water runoff impacts.

Land use affects the hydrological characteristics of a catchment by reducing the infiltration of rainwater into the ground and thereby altering the volume and speed of surface runoff. Land cover change also affects the amount of soil erosion infiltration and transportation to the water body. Hence, it is necessary to understand the spatial distribution and long term dynamic principles of soil erosion prevention, understanding the interaction among hydrologic and geomorphic process, land use change on stream flow and soil erosion in order to address land degradation.

A check dam is a small barrier that is placed across a river or channel to slow the movement of water and sediments and to reduce channel erosion. In catchments with a high risk of soil erosion, check dams could trap sediments before they reach the dam storage or accumulate downstream. Although check dams are commonly used, to the best of our knowledge, few studies have focused on their effectiveness in controlling soil erosion (Castillo *et al.,* 2007; Romero-Díaz *et al.,* 2007). The use of check dams can have short-term and long-term benefits. Castillo *et al.,* (2007) concluded that check dams improve sediment storage and decrease vertical erosion in the upstream region, although the turbulence induced by them may cause erosion in the downstream region, which becomes a substitute for runoff energy and creates a sense of false stabilization when the induced erosion is high.

Percolation tanks are important structures for the conservation of runoff and groundwater recharge, a multipurpose structure for storing water for livestock, irrigation and recharge to groundwater. These are generally constructed across streams and bigger gullies in order to impound a part of the run-off water. They may be depression excavated to form a small reservoir an embankment across a natural ravine, or an impounded reservoir. Little can be found about the design of such structures though there are guidelines: Percolation tanks should not be located in heavy, impervious soils; suitable soils should be available for the embankment; an ideal location would be a narrow stream with high ground on either side; there should be some economic advantage (Srivastava, 2007).

Chapter -III

MATERIALS AND METHODS

This chapter deals with the detailed characteristics of the study area, materials and methodology adopted during the application of HEC-GeoHMS for estimation of streamflow and Revised Universal Soil Loss equation (RUSLE) method for modeling of soil erosion.

3.1 The Study Area

The Krishna lower basin of Andhra Pradesh was selected as a study area. It is located between the latitudes $15^{0}42'25''$ N and $17^{0}7'12''$ N and longitudes $79^{0}10'$ E and $81^{0}15'$ E which comprises parts of the Krishna and Guntur districts of Andhra Pradesh. It comprises 69 mandals. The catchment area is 11317.36 km^2. Erra Vagu, Naguleru Vagu, Eddu Vagu, Muneru river, Kotula river, Dandi Vagu, Ippala Vagu, and Uppu drain are the important tributaries of the Krishna lower river of Andhra Pradesh. The location map of the study area is depicted in the Fig. 3.1.

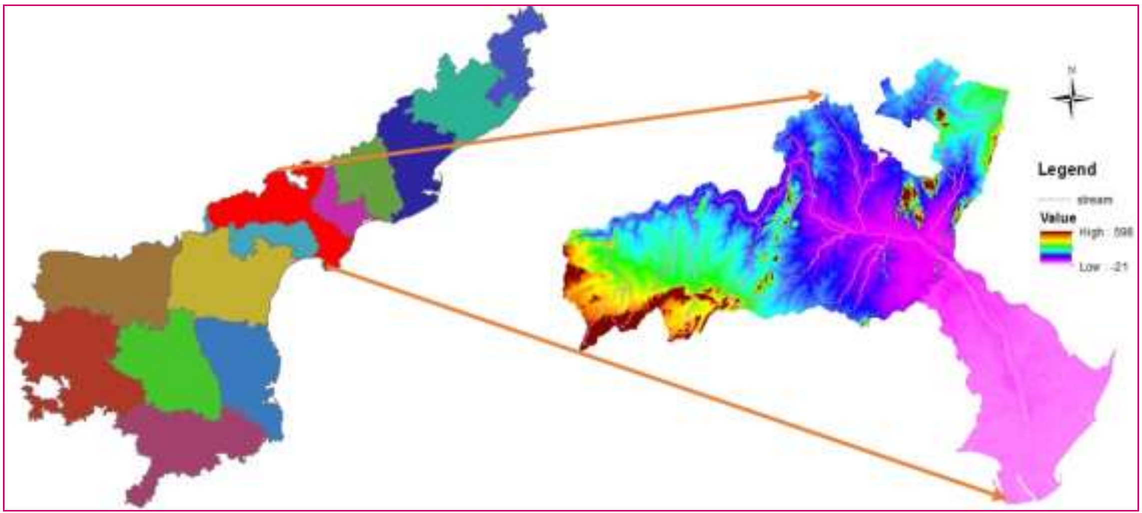

Fig. 3.1 Location map of Krishna lower sub basin, Andhra Pradesh

3.2 Data Acquisition

The data necessary for the study was comprised of

a) Digital elevation model (DEM): A DEM of the area of interest was extracted from SRTM.

b) Soil map (1:250,000): Soil map developed by National Bureau of Soil Survey and Land Use Planning (NBSSLUP) was taken as reference map and clipped to the study area to identify the type of soils.

c) The Land use land cover map (LULC): IRS P_6, LISS III image of December, 2014 and September, 2015 was downloaded from Bhuvan.

d) Daily and annual precipitation from 1993 to 2015: The precipitation data was obtained from the Directorate of Economics and Statistics (DES) and the Meteorological Department.

e) Weather data of different parameters, namely temperature, humidity, wind speed and solar radiation for the period of 1993 to 2015 was collected from LAM weather station, Guntur and ARS, Garikapadu.

f) Daily average flows and instantaneous maximum annual flows: Flow measurements were obtained from observed gauge data available at Prakasam barrage and Pulichintala project.

3.2.1 Digital Elevation Model

A DEM can be used to identify different basin characteristics such as drainage area, elevation, slope steepness, slope length, and streams relief ratio. The DEM has been downloaded from different sources to generate the correct stream network of the Krishna lower sub basin. Six tiles were required for the study area. The downloaded DEMs were mosaiced and rectified with the UTM projection, the spheroid type (WGS 1984) and Datum of WGS 84 and 44 N zone was applied. The sub-setting of image was performed for extracting study area by taking geo-referenced out line boundary of study area. Different DEMs and their specifications were presented in Table 3.1 and Fig. 3.2, Fig. 3.3, Fig. 3.4, Fig. 3.5 and Fig. 3.6.

Among these DEMs, SRTM 90 m produced correct stream network. The SRTM maintained Digital Elevation Data (DEM) on a near-global scale. The stream network generated from the SRTM DEM gave better results than that from the ASTER DEM

(Kulkarni *et al.*, 2014, Zope *et al.*, 2016). Therefore, DEM downloaded from SRTM with 90 m resolution has been utilized for the delineation of watershed.

Table 3.1: The Specifications of downloaded DEMs from different sources

S. No	Sources of DEM	Types	Year	Resolution	Sources
1	SRTM (Shuttle Radar Topography Mission)	1. SRTM non-void filled 2. SRTM void filled 3. SRTM 1 arc	2005 2012 2014	90 m 90 m 30 m	https://earthexplorer.usgs.gov/
2	ASTER (Advanced Spaceborne Thermal Emission and Reflection Radiometer)	ASTER GLOBAL DEM	2011	30 m	https://earthexplorer.usgs.gov/
3	CARTO	1. Version 1 2. Version 2 3. Version 3	2006-2008 2005-2014 2005-2014	30 m 30 m 30 m	http://bhuvan.nrsc.gov.in/bhuvan_links.php

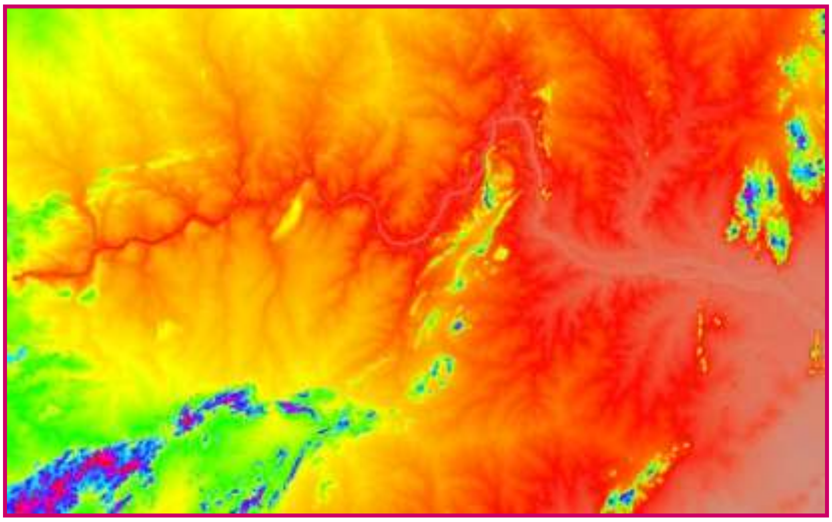

Fig. 3.2 Downloaded DEM from SRTM 1 arc

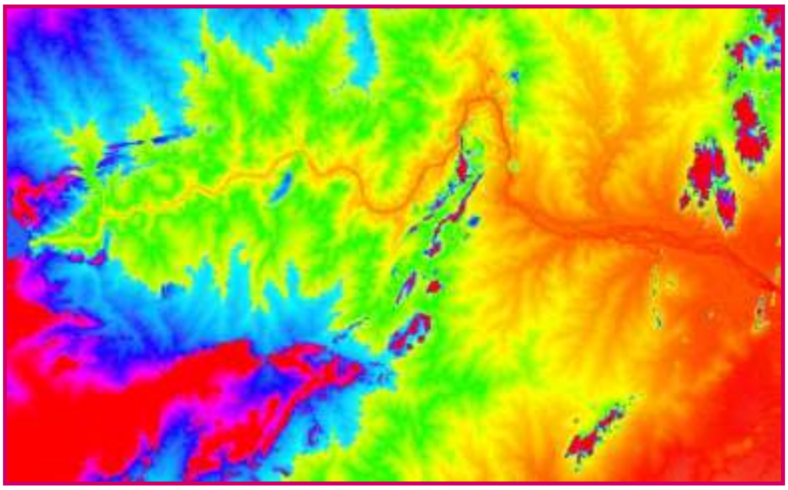

Fig. 3.3 Downloaded DEM from SRTM 3 arc

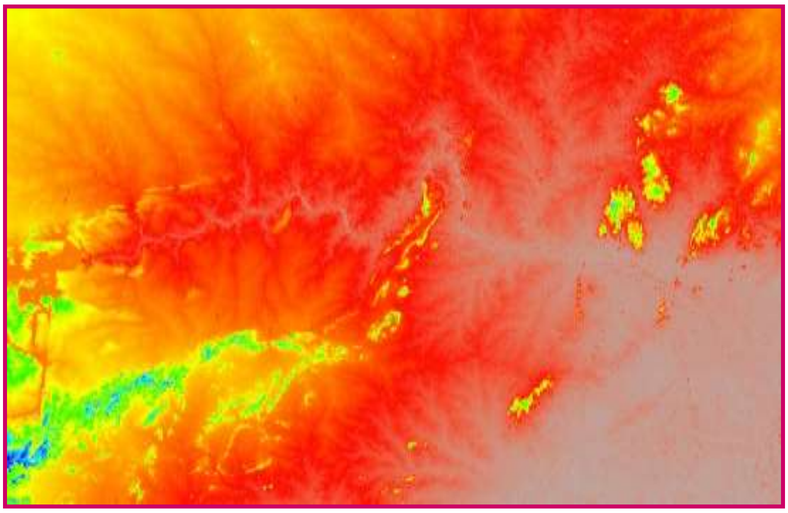

Fig. 3.4 Downloaded DEM from ASTER GLOBAL DEM

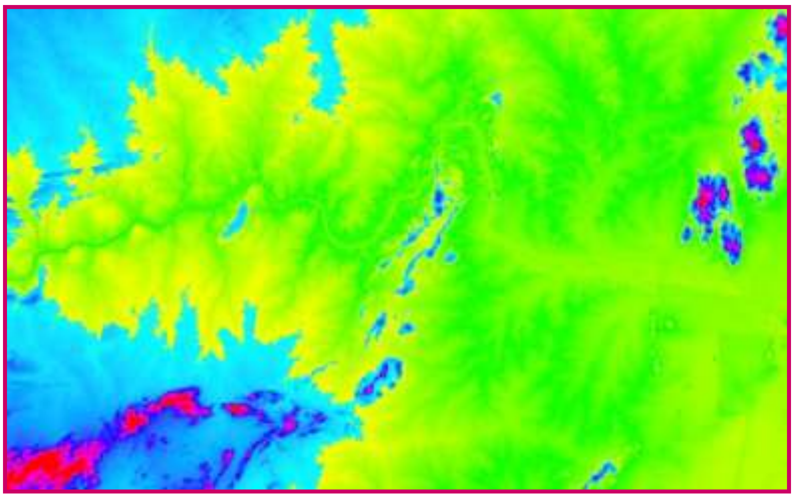

Fig. 3.5 Downloaded DEM from CARTO Version 1 DEM

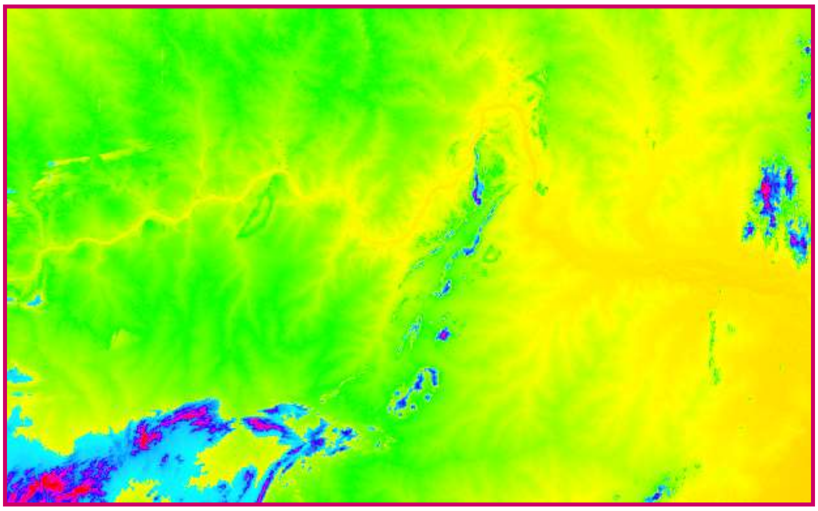

Fig. 3.6 Downloaded DEM from CARTO Version 3 DEM

3.2.2 Soil Classification Map

The Krishna lower sub-basin consists of mainly four types of soils. Majority of the area is under silt soils (46 percent) and clay soils (43 percent). Remaining 7 percent and 4 percent are under loam and water bodies. The details of different soil types were presented in Fig 3.7 and Table 3.2.

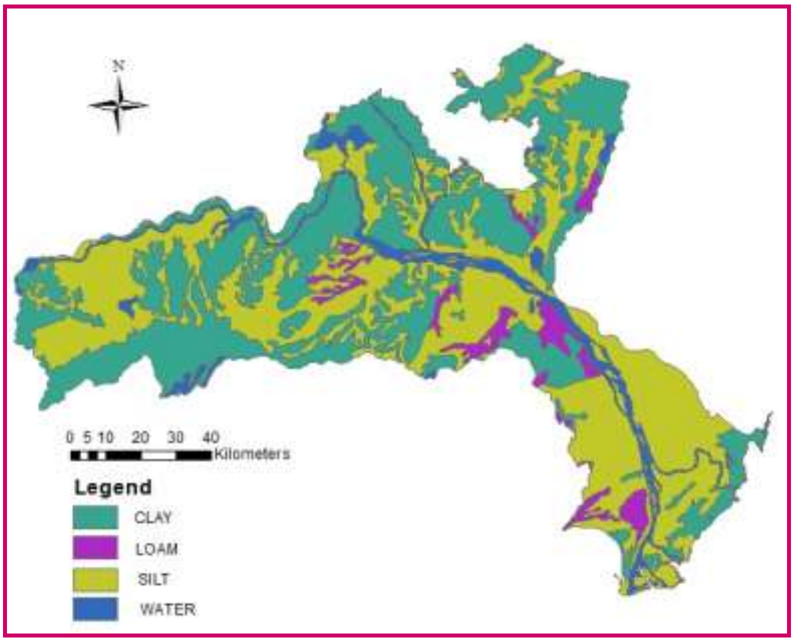

Fig. 3.7 Classification of soils of the study area

Table 3.2 Extent of different soils in the study area

S. No.	Description	Area (km^2)	Percentage (%)
1	Silt	5177.5	46
2	Clay	4832.51	43
3	Loam	506.57	4
4	Water bodies	800.78	7

3.2.3 Land use and Land cover (LULC)

Two different LULC maps were prepared for the study area using IRS P_6, LISS III image of December, 2011 and September, 2012 and December, 2014 and September, 2015 to analyze the change in LULC. The sub-setting of satellite images were performed from both images by taking geo-referenced out line boundary of Krishna lower sub basin as AOI. Individual agricultural land, water bodies, forest, scrub only, current fallow, other wasteland, build up and plantation shape files were created in the ERDAS Imagine by using the AOI (Area of interest) and signature editor tools. The area and percentage of different land uses in the year 2011-2012 and 2014-2015 were presented in Table 3.3 and Table 3.4 respectively. The classified LULC of 2011-2012 and 2014-2015 were shown in the Fig. 3.8 and Fig. 3.9 respectively.

Table 3.3 Land use of the study area during the year 2011-2012

S. No.	Land use	Area (km^2)	Percentage covered (%)
1	Current fallow	107223.2	9.41
2	Built-Up Land	26123.3	2.29
3	Plantation	36054.3	3.16
4	Forest	95943.3	8.42
5	Double Crop	386137.4	33.9
6	Scrub land	82547.2	7.24
7	Kharif only	166131.6	14.6
8	Waste Land	25524.6	2.24
9	Rabi only	131588	11.5
10	Water	82540.6	7.24

Table 3.4 Land use of the study area during the year 2014-2015

S. No.	Land use	Area (km^2)	Percentage covered (%)
1	Current fallow	73916.03	6.48
2	Built-Up Land	26266.53	2.3
3	Plantation	35473.18	3.11
4	Forest	94627.85	8.3
5	Double Crop	457162	40.1
6	Scrub land	76856.16	6.74
7	Kharif only	168486.70	14.8[
8	Waste Land	21126.35	1.85
9	Rabi only	92884.62	8.15
10	Water	93115.76	8.17

Major land use in the study area was double crop followed by kharif only, rabi only and the current fallow. Therefore, agriculture occupy maximum area in the Krishna lower sub basin. There was a variation in the LULC of the study area during year 2014-2015. Double cropped area has been increased which lead to decrease in current fallow. The area under rabi only has been decreased. There is very little change in the remaining land uses.

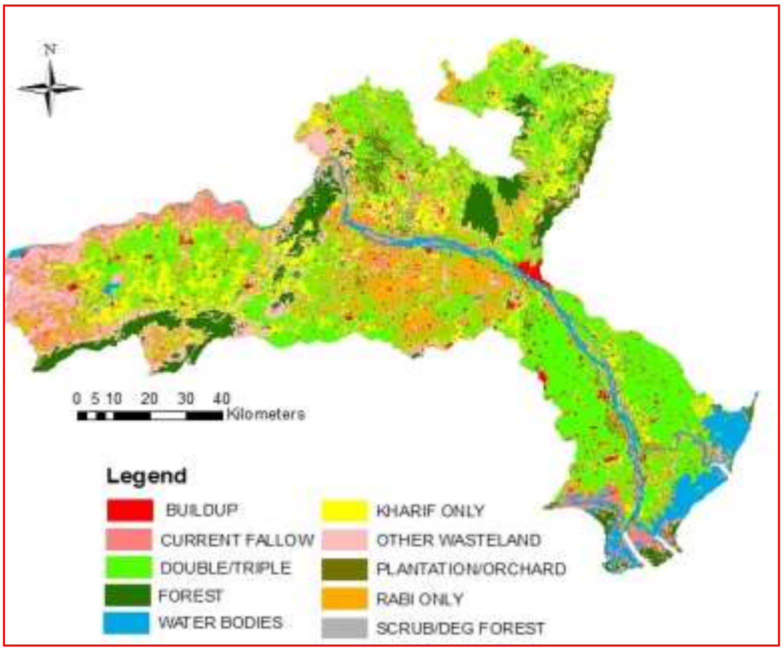

Fig. 3.8 Land use land cover map during the year 2011-2012

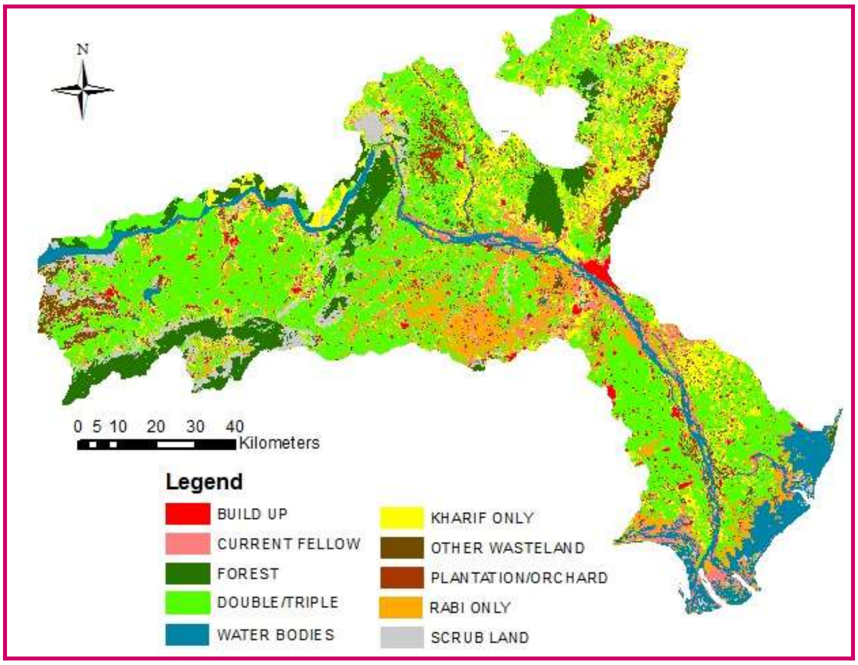

Fig. 3.9 Land use land cover map during the year 2014-2015

3.2.4 Climatic Data

Climate of the study area is semi-arid with distinct summer, winter and rainy seasons. The major amount of rainfall is received during the South-West monsoon. The rainfall distribution is observed as seasonal with more than 75 percent of rainfall received during the south-west monsoon period. North-East monsoon and summer showers constitute remaining 25 percent of rainfall.

The average annual rainfall of study area for 23 years from 1993 to 2015 was 979.60 mm. The average annual rainfall received in study area from 1993-2015 is presented in Table 3.5 and Fig 3.10. The highest amount of rainfall was recorded in 2010 as 1620.71 mm and the lowest amount of rainfall was recorded in 2009 as 566.54 mm.

The study area covers 69 mandals and every mandal has one rain gauge station. The 69 rain gauge stations data was used to simulate runoff and soil erosion. The point map of rain gauge of study area has been shown in Fig. 3.11.

The mean maximum and minimum temperature of the study area was 41.18 ^{0}C and 16.81^{0}C respectively and the average relative humidity was 74.22% (Table 3.6 and Fig. 3.12).

Table 3.5 Annual rainfall data of the study area from 1993 to 2015

Year	Annual rainfall (mm)
1993	736.27
1994	1009.22
1995	923.48
1996	1028.69
1997	865.47
1998	959.05
1999	710.19
2000	1033.23
2001	844.61
2002	588.54
2003	950.55
2004	675.29
2005	1032.04
2006	991.82
2007	992.52
2008	1158.25
2009	566.54
2010	1620.71
2011	747.36
2012	1303.13
2013	1265.72
2014	671.37
2015	768.73

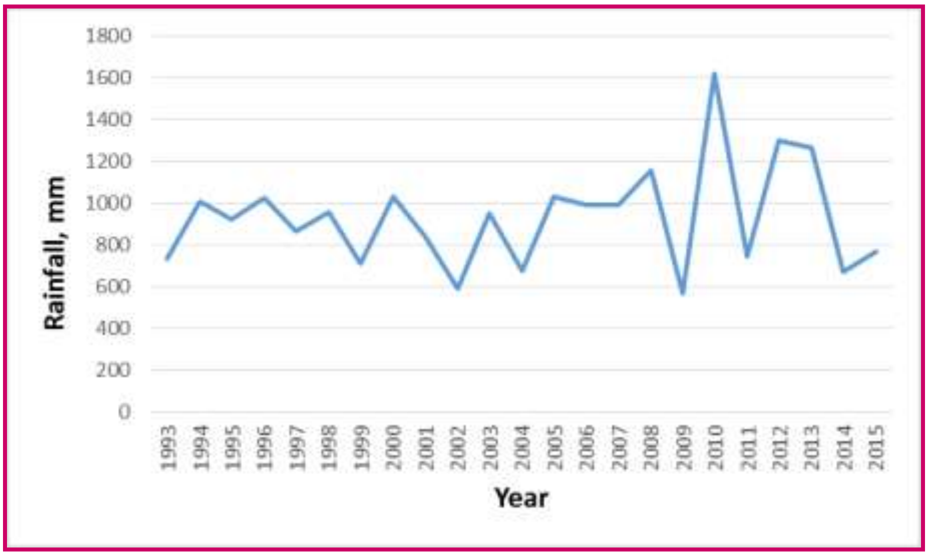

Fig. 3.10 Variation of annual rainfall data of the study area from 1993 to 2015

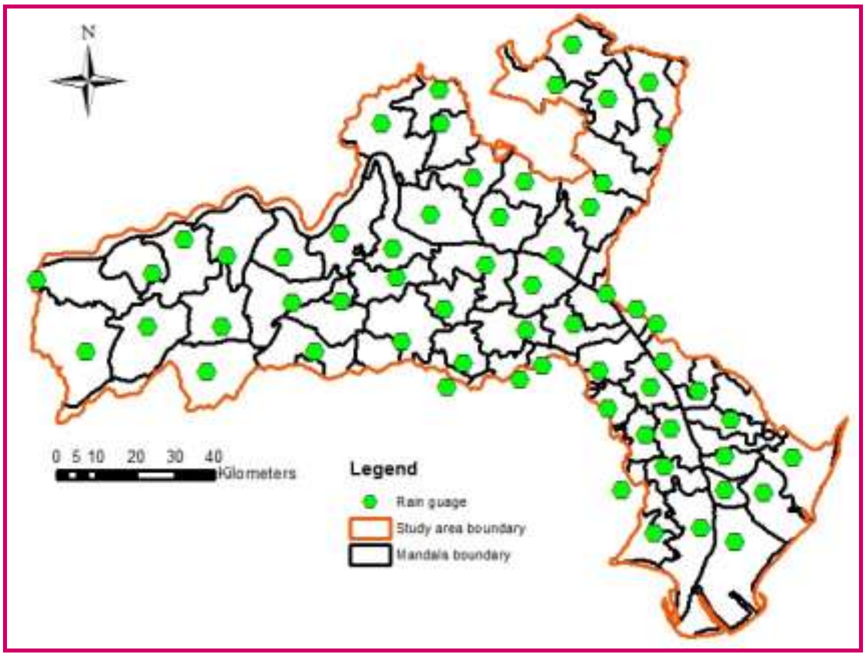

Fig. 3.11 Rain gauge network map of the study area

Table 3.6 Monthly average maximum and minimum temperature, relative humidity of the study area from 1993 to 2015

S. No.	Month	Mean maximum temperature (^0C)	Mean minimum temperature (^0C)	Mean relative humidity (%)
1	January	30.56	16.81	72.27
2	February	32.15	18.49	70.86
3	March	35.33	21.06	66.33
4	April	38.23	24.49	64.07
5	May	41.18	26.93	50.38
6	June	37.84	25.90	60.90
7	July	34.56	24.80	67.23
8	August	33.37	23.96	71.25
9	September	33.54	23.84	74.22
10	October	32.99	22.57	73.05
11	November	31.28	20.36	72.39
12	December	30.34	17.20	71.03

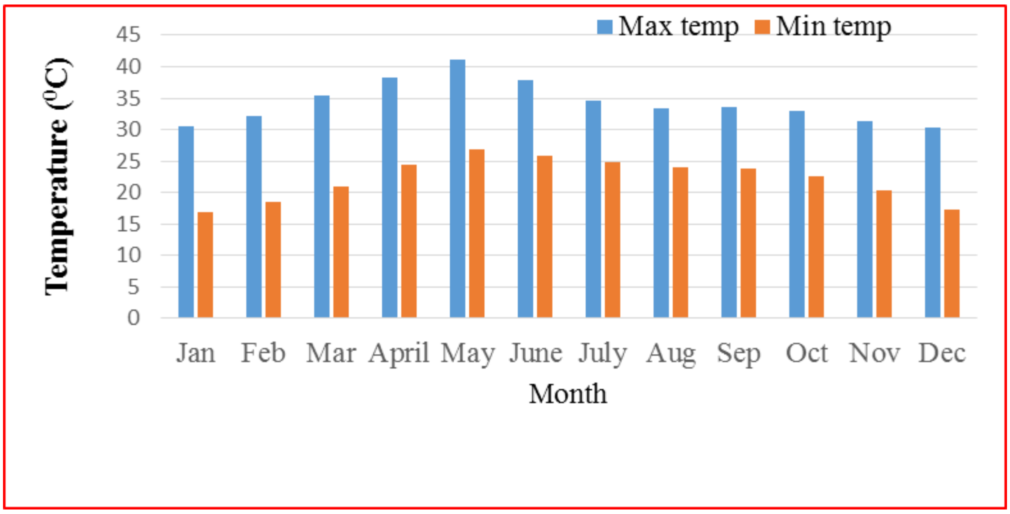

Fig. 3.12 Monthly average maximum and minimum temperature from 1993-2015

3.2.5 Physiography

The physiography of the area is undulating having a land slope of 1 to 44%, varying from nearly level to steep slope. About 91 percent of the area is nearly level and remaining 8 percent of the area occupied moderate slope to steep slope (Table 3.7).

Table 3.7 Classification of land slope of the study area

S. No	Land slope (%)	Area (km^2)	Area (%)
1	0-5	10402.92	91.92
2	5-10	475.32	4.20
3	10-15	216.16	1.91
4	>15	222.95	1.97

3.2.6 Hydraulic particulars of reservoirs in the study area

Pulichintala project and Prakasam Dam are the important reservoirs constructed across the Lower Krishna River. Pulichintala is a multi-purpose project serving irrigation needs, hydro power generation and flood control. It was constructed on 13 November 1988. It started functioning from 7 December 2013. Prakasam barrage was constructed on 1954 and started functioning from 1957. The details of the above reservoirs were presented in the Table 3.8.

Table 3.8 Technical details of the dams

Pulichintala Project			
1	Location of Dam	:	latitude = 16° 46' 14" N longitude = 80° 03' 33"E
2	Command area	:	13.08 lakh acres in Guntur, Krishna, West Godavari and Prakasam District
3	T. B. L.	:	+ 58.24 M
4	Maximum Water Level	:	+ 53.34 M
5	Maximum designed flood discharge	:	57,700 cumecs
6	Crest of Spillway	:	36.34 M
7	Size and No of gates		18.50 M X 17.00 M & 24 Nos
Prakasam Dam			
1	Location of Dam	:	latitude = 16°30'N longitude = 80°37'E
2	Command area	:	13.08 lakh acres in four District Viz. Krishna, West Godavari, Guntur and Prakasam
3	T. B. L.	:	+ 17.39 M
4	Maximum Water Level	:	+ 22.13 M
5	Maximum designed flood discharge	:	33, 697 cumecs
6	Crest of Spillway	:	12.21 M
7	Size and No of gates	:	12.19 M X 3.66 M & 70 Nos.

3.2.7 Crops and cropping pattern in study area

The major crops grown in the study area are paddy, maize, green gram, black gram, groundnut, sesame, cotton, chillies and vegetables respectively. Other crops are also grown but not in significant area. The details of different crops grown in the study area were presented in the Table 3.9.

Table 3.9 Details of planting time and maximum root zone depth of different crops grown in study area

S. No	Name of the Crop	*Kharif*		Maximum root zone depth (cm)
		Planting Date	Harvesting Date	
1	Paddy	July	November	60
2	Maize	July	October	100

3	Green gram	June	September	25
4	Black gram	July	September	25
5	Groundnut	October	March	30
6	Sesame	June	October	40
7	Cotton	June	January	120
8	Chillies	July	October	80
	Rabi			
9	Paddy	November	April	60
10	Maize	October	February	100
11	Sesame	August	December	40
12	Green gram	October	January	25
13	Black gram	October	March	25
14	Pulses	October	March	30
15	Groundnut	November	February	30

3.3 Details of different software models used for the study

3.3.1. Arc GIS 10.1

ArcGIS is a software, developed by Environmental Systems Research Institute (ESRI) of Redlands, California. It is a Geographic Information System (GIS) for working with maps and geographic information. It is a computer software capable of assembling, storing, manipulating, displaying geographically referenced information i.e. data identified according to their locations. GIS is capable of displaying data spatially than temporally. It has become a useful and important tool in hydrology and hydrologists in the scientific study and management of water resources.

In the present study, HEC-GeoHMS is used as extension of ArcGIS for generating watershed characteristics, perform spatial analysis, delineate sub-basins and streams, construct inputs for HEC-HMS model. Spatial maps of different input and output data has been prepared using GIS.

3.3.2 ERDAS IMAGINE 9.3

The ERDAS IMAGINE software was designed to process satellite imagery from AVHRR, Landsat MSS and TM, and Spot Image into land cover, land use maps, map deforestation, and assist in locating oil reserves under the product name ERDAS. It is a remote sensing application with raster graphics editor abilities designed by ERDAS for geospatial applications. Imagine is aimed mainly at geospatial raster data processing and allows users to prepare, display and enhance digital images for mapping use in geographic information system (GIS) and computer-aided design (CAD) software. It is a toolbox allowing the user to perform numerous operations on an image and generate an answer to specific geographical questions.

In the present study, the satellite remote sensing data has been used for updating of drainage and surface water bodies and changes in land use. Erdas 9.3 version software was utilized for processing of images (rectification, sub setting and classification) in order to prepare land use land cover of the study area.

3.3.3 HEC-GeoHMS 10.1

The Hydrologic Engineers Center's Geospatial Hydrologic Modelling Extension, HEC-GeoHMS 10.1 is public domain extension to ESRI's ArcGIS 10.1 software and the Spatial Analyst extension. It is a geospatial hydrology toolkit designed for engineers and hydrologists. The program allows users to visualize spatial information, document watershed characteristics, perform spatial analysis, delineate sub-basins and streams, construct inputs to hydrologic models and assist with report preparations. Using DEM terrain data, HEC-GeoHMS produces HMS input files, a stream network, sub-basin boundaries, and connectivity of various hydrologic elements in an ArcView GIS environment via a series of steps called terrain pre-processing and basin processing. The physical representation of catchments and rivers was configured in the basin models, and hydrologic elements were linked.

Determination of a hydrologically correct DEM and its derivatives, mainly the flow direction and flow accumulation grids, often demands some iteration of drainage path calculations in order to precisely depict the flow of water through the catchment. The hydrologically correct DEM must have a resolution sufficient to capture the details of surface flow. Problems often arise when the drainage area has a coarse resolution. These problems can be overcome if proper care is taken in the terrain pre-processing stage to produce a fine resolution of the drainage area. The DEM with 90 m x 90 m resolution downloaded from SRTM was used to derive parameters for the hydrological modeling. The terrain preprocessing was the first step in using HEC Geo-HMS. Terrain preprocessing includes Fill Sinks, Flow Direction, Flow Accumulation, Stream Delineation, Stream Segmentation, Catchment Grid Delineation, Catchment Polygon Processing, and Drainage line processing. The following steps were used in HEC-

GeoHMS to obtain the DEM in order to delineate various components of the catchment. The main window view of HEC-GeoHMS displaying the steps and derived stream network were shown in Fig 3.13 and Fig 3.14 respectively.

1. “Raw” DEM from terrain dataset was generated.
2. Fill sinks: The flow direction developed on the initial DEM derived from terrain dataset had sinks, hence filling was needed. After filling, flow direction was calculated. If the paths did not match the digitized lines indicated the need for stream burning was required.
3. Burn streams: Streams provided by SRTM were burned in.
4. Flow direction of the reconditioned DEM was generated.
5. Flow accumulation was computed
6. Stream definition: The threshold of 50 km^2 was given.
7. Stream segmentation has been done.
8. Catchment grid delineation was completed.
9. Processing of delineating catchment polygon was carried out.
10. Processing of drainage line was done.
11. Processing of adjoint catchment was completed.

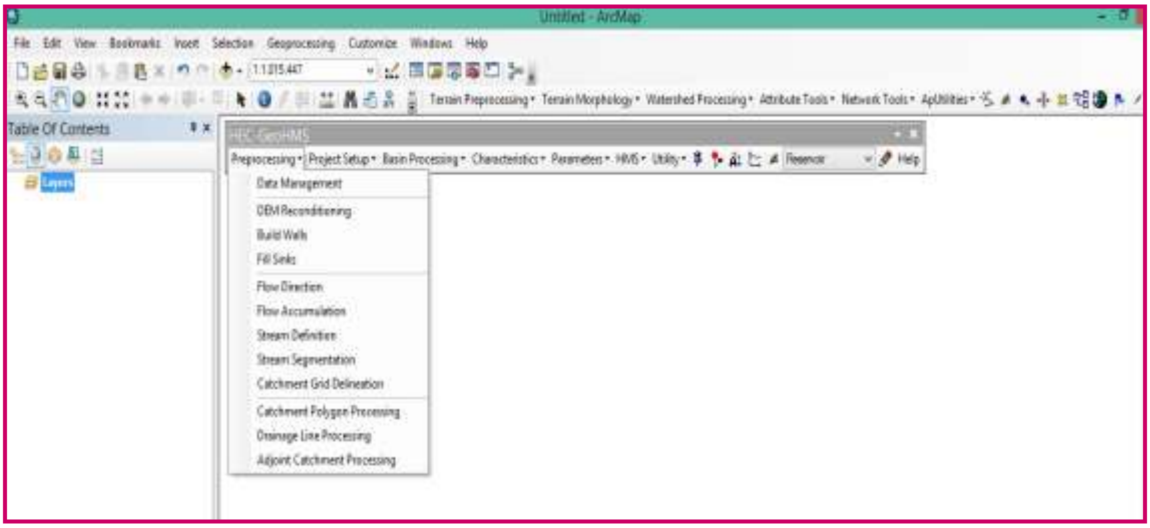

Fig. 3.13 Main window of HEC-GeoHMS extension in Arcmap

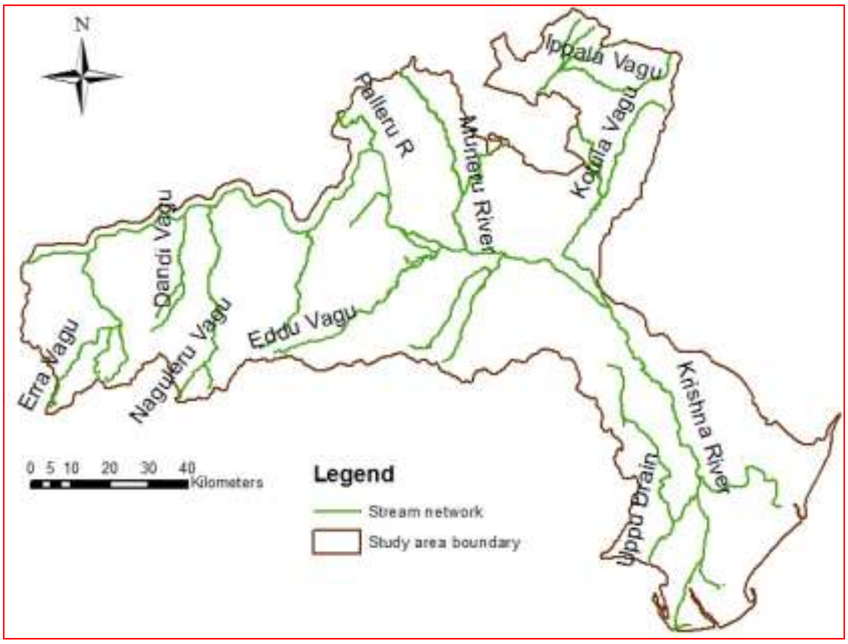

Fig. 3.14 Derived stream network from HEC-GeoHMS using SRTM DEM

3.34 Development of project in GeoHMS environment

After the terrain processing, line project was created to set up the simulation and procedure to create the project were given below. Additionally, parameters like river slope, river length, watershed centroid, and longest and centroidal flow path were also determined. The results acquired using Geo-HMS were the catchment area of each sub-basin, slope of each sub-basin, flow length, which will in turn used for the calculation of "Time of Concentration". The screenshot of creation of project in HEC-GeoHMS were shown in Fig. 3.15.

This section covers preliminary work on getting the good DEM and its derivatives as foundation for development of GeoHMS model.

1) GeoHMS "Project Setup -> Start New Project" function was run.
    a. Project name was defined as Krishna Lower sub basin
    b. Description was specified as HEC-HMS project
    c. "Original Stream Definition" as extraction method was selected
    d. Type date of the project files for metadata
    e. "Outside MainView Geodatabase" as project data location was selected
    f. Default target location was selected.

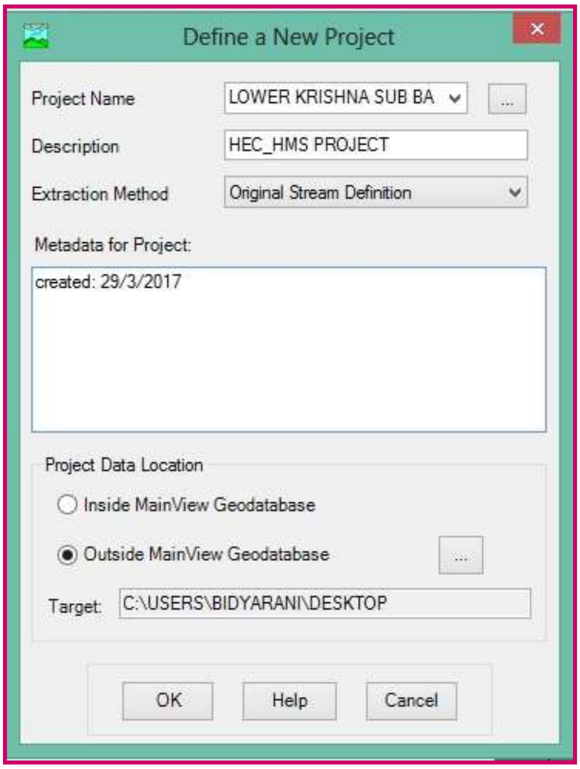

Fig. 3.15 Creation of project in HEC-GeoHMS

2) This generated a new directory to store the new project.

3) Zoom in to the outlet of the dataset (most downstream DEM cell).

4) “Add Project Points” GeoHMS tool ( ) was clicked on.

5) Click on the most downstream cell of the DEM.
   a. Specify point name and description (can keep defaults)

6) GeoHMS “Project Setup -> Generate Project” function was run
   a. Verify that all input layers were pointing to the right data particularly “Raw DEM”.
   b. Specify output layers (can keep defaults)

7) When the watershed was delineated, said “Yes” to create the project for the area shown.
   a. Default names for layers was accepted and generated for the HEC-GeoHMS project.
   b. A new data frame was added to the ArcMap with the name of the HEC-GeoHMS project and a number of layers was added to it.

Spatial input layers were prepared in HEC-GeoHMS environment and HEC-HMS was used for modelling. The delineated watershed was shown in Fig. 3.16.

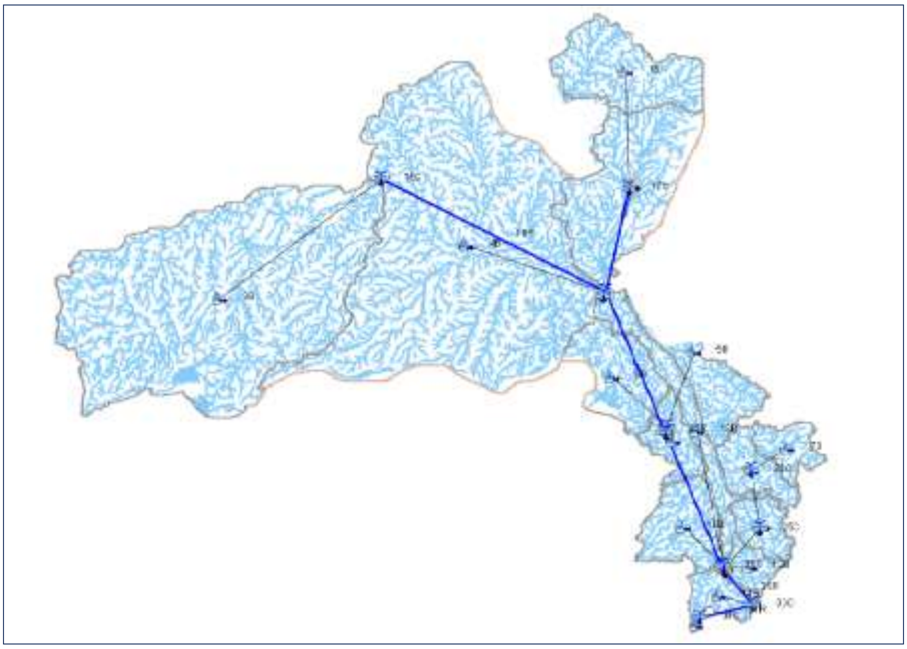

Fig. 3.16 Delineated watershed with basin centroid

3.3.4 HEC-HMS model setup

HEC-HMS Model setup consists of four main model components: basin model, meteorological model, control specifications, and input data (time series, paired data, and gridded data).The Basin model for instance, contains the hydrologic element and their connectivity that represent the movement of water through the drainage system. The meteorological component is also the first computational element by means of which precipitation input is spatially and temporally distributed over the river basin. The spatio-temporal precipitation distribution was accomplished by the gauge weight method. The Thiessen polygon technique was used to determine the gauge weights and the following input data used like daily precipitation, daily temperature, elevation, and long term mean monthly actual potential evapotranspiration. (Sintayehu, 2015)

The purpose of using the HEC-HMS model in this study was to assess the streamflow of 23 years.

3.4 Computation of basin parameters

Watershed analysis includes initial parameter estimation for rainfall-runoff modeling and determination of DEM derivatives for further analysis and simulation.

HEC-HMS categorizes all land types and water in a watershed as either directly connected impervious surface or pervious surface. Precipitation on directly connected impervious surface runs off with no volume losses. Precipitation on the pervious surfaces is subject to losses. The SCS-CN loss model was used in the present study.

The SCS-CN method was developed by the Soil Conservation Service (SCS) of USA which estimates precipitation excess as a function of cumulative precipitation, soil cover, land use, and antecedent moisture. It can predict surface runoff from daily rainfall data. Let I_a is the initial loss of rain water by interception, infiltration through the soil, depression storage etc. The ratio of direct runoff (surface runoff) (Q) to the rainfall depth minus the initial losses (P- I_a) is equal to the ratio of the retention of rainfall. It is given by the formula

$$Q = \frac{(P - I_a)^2}{P - I_a + S}$$

Where Q = Accumulated precipitation excess at time t,

P = Accumulated rainfall depth at time t,

I_a = Initial abstraction (initial loss), and

S = Potential maximum retention, a measure of the ability of a watershed to abstract and retain storm precipitation.

The SCS developed an empirical relationship between I_a and S as I_a = 0.3S. Therefore, the cumulative excess at time t is given as:

$$Q = \frac{(P - 0.3S)^2}{P + 0.7S}$$

The maximum retention (S) is determined using the following equation (SI system):

$$S = \frac{25400 - 254CN}{CN}$$

Where CN = curve number.

3.4.1.1 Curve number (CN)

CN is a computed variable which is based on the Antecedent Moisture Condition (AMC), land use /land cover class and hydrological soil group. It is an index that represents the combination of hydrologic soil group, land use classes, and antecedent moisture conditions. CN value varies from 0 to 100. It depends on land use pattern, treatment, hydrologic condition, and hydrologic soil of watershed. The classification details of hydrologic soil groups were presented in Table 3.10.

For Indian conditions, Dhruvanarayana (1993) has reported the value for I_a as follows

- Black soil regions, AMC II and III $I_a = 0.1S$
- Black soil regions, AMC I $I_a = 0.3S$
- All other regions, $I_a = 0.3S$

Table 3.10 Classification of hydrologic soil group

S. No	Hydrologic soil group	Type of Infiltration	Infiltration Rate	Type of soils
1	A	High infiltration	>25 mm/hr	Deep sand
2	B	Moderate infiltration	12.5-25 mm/h	Deep coarse sand
3	C	Low infiltration	2.5 -12.5 mm/h	Shallow fine soil
4	D	Very low infiltration	<2.5 mm/h	Clayey shallow soil

3.4.1.2 Antecedent moisture condition (AMC)

AMC is defined as the summation of 5-day precipitation before the runoff-producing storm. It is used as the wetness index of soil. It changes continuously and can have a very significant effect on the flow during wet weather, and thus affect the CN number in hydrological modeling. The effect is evident in most hydrologic systems including storm water runoff and sanitary sewers with inflow and infiltration. It has three levels

AMC I: Having lowest runoff potential because of the soils are dry enough for satisfactory

AMC II: Average or normal condition of the soil regarding runoff generating potential

AMC III: The features favourable to develop highest runoff potential of the soil, when areas of watershed are saturated from antecedent rains.

The limits of estimating the antecedent moisture condition in different crop growing seasons were presented in the Table. 3.11

Table 3.11 Seasonal Rainfall limits for estimation of antecedent moisture condition

AMC	5 days total antecedent rainfall (mm)		Runoff producing condition
	Dormant season	Growing season	
I	<12.7	<35.6	Lowest runoff potential
II	12.7-27.9	35.6-53.3	Moderate runoff potential
III	Over 27.9	Over 53.3	Highest runoff potential

CN for various soil types with the associated percent of imperviousness was given in the Table 3.12. The curve number can be found from the table as a function of hydrologic soil group and antecedent moisture content.

Table 3.12 CN values for various soil types with the associated percent of imperviousness

S. No	Land use	Hydrologic group		
		B	C	D
1	Double crop	95	95	95
2	Kharif	69	76	79
3	Rabi	81	88	91
4	Water bodies	98	98	98
5	Forest	58	68	75
6	Scrub only	80	80	85
7	Current fallow	80	80	85
8	Other wasteland	80	80	88
9	Build-up	80	81	91
10	Plantation	55	71	73

Runoff depth was computed using the above mention SCS-CN loss method. The time to peak and peak runoff rate were estimated using the equations given below

Time of concentration

Time of Concentration is the time required for rainfall to reach the watershed lowest elevation from the highest elevation of the watershed. It is used as the duration of the storm for calculating quantity of surface runoff. It is given by equation

$$T_c = 0.01947 L^{0.77} S^{-0.385}$$

where T_c = Time of concentration, minute

L = Length of travel from the remotest point of the watershed to the outlet, m

S = Watershed gradient (m/m)

Lag time

The lag time is defined as the length of time between the centroid of precipitation mass and the peak flow of the hydrograph. It can be calculated from the equation given below

$$T_p = 0.6T + \sqrt{T_c}$$

where T_p = Time to peak of the basin

T_c = Time of concentration, h

Peak runoff rate

The peak runoff rate of the basin can be determined using equation given below

$$Q_p = \frac{2.089QA}{T_p}$$

where Q_p = Peak discharge, m^3s^{-1}

T_p = Lag time of the basin

Q = Direct runoff, m

A = Area of watershed, km^2

The runoff volume was estimated for Krishna Lower sub basin of Andhra Pradesh during the years 1993-2015. Rate runoff was calculated for significant rainfall events during the year 2015 and compared with the observed value at Pulichintala project.

3.5 Calculation of RUSLE parameters

The Universal Soil Loss Equation (USLE) was first developed in the 1960s by Wischmeier and Smith of the United States Department of Agriculture as a field scale model. It was later revised in 1997 in an effort to better estimate the values of the various parameters in the USLE. There are five major factors that are used to calculate the soil loss for a given site. Each parameter is the arithmetic estimate of a specific condition that affects the severity of soil erosion at a particular location. The calculated erosion values reflected by this model can vary significantly due to fluctuating weather conditions. Thus, the erosion values obtained from the RUSLE more accurately represents long-term averages. The RUSLE uses the following equation

$$A = R \times K \times LS \times C \times P$$

Where 'A' is the average annual potential soil loss in tons ha^{-1} $year^{-1}$

'R' is the rainfall-runoff erosivity factor

'K' is the soil erodibility factor

'LS' is the topographic factor

'C' is the land-cover management factor

'P' is the conservation practice factor

The overview of RUSLE methodology to estimate soil erosion was shown in the Fig. 3.17

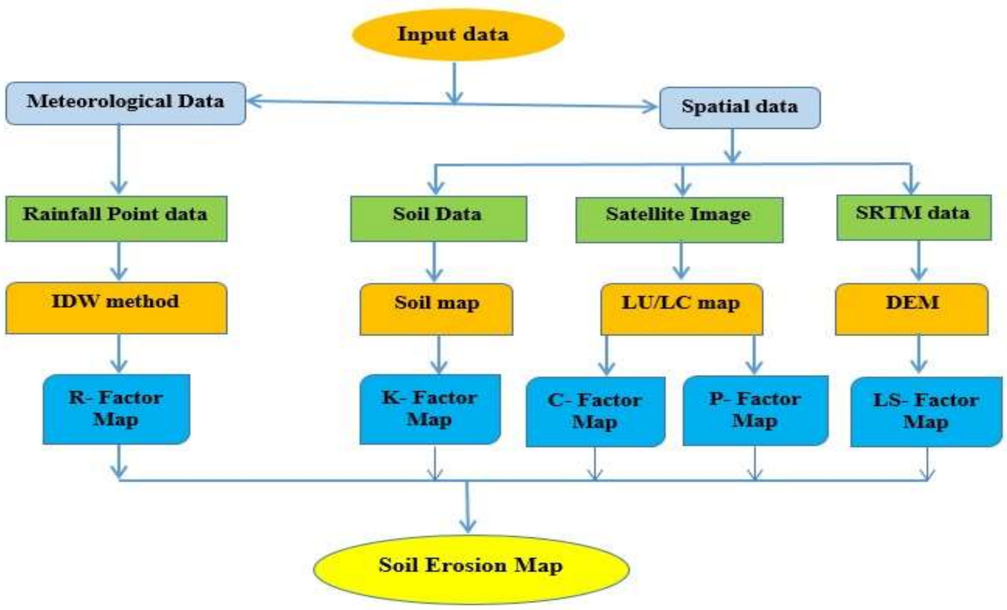

Fig. 3.17 Overview of RUSLE methodology

3.5.1 Rainfall erosivity factor (R)

Rainfall erosivity depends on amount, intensity and distributions of rainfall. The soil loss is closely related to rainfall partly through the detaching power of raindrop striking the soil surface and partly through the contribution of rain to runoff (Morgan, 1994). Though there are a number of ways of analyzing the rainfall erosivity depending on the local condition of the place, the values of R factor for this study was estimated according to the equation adopted by Singh, *et al.*, (1981) for the entire India.

$$R = 79 + 0.363 * AAP \qquad \ldots(2)$$

Where AAP = Average annual precipitation, mm

Wischmeier and Smith (1978) recommended that at least 20 years of rainfall data is required to capture the natural climatic variation. Mean annual rainfall was calculated using the data from 69 rainguage stations from 1993 to 2015. The R factor was computed using the above formula and converted in to raster surface using IDW (Inverse Distance Weighted) interpolation method in ArcGIS 10.1 software.

3.5.2 Soil erodibility factor (K)

Soil erodability (K) is defined as mean annual rainfall soil loss per unit of R for a standard condition of bare soil, recently tilled up and down with slope with no conservation practices and on a slope of 5^o and 22 m length (Morgan, 1994). It is based on soil texture, structure, organic matter and even permeability. The corresponding value of K for the soil types were taken from Soil erosion, Andhra Pradesh given by NBSSLUP.

3.5.3 Topographic factor (LS factor)

The slope length and slope steepness factors are commonly combined in a single index as LS and refer to as the topographic factor. Slope length is defined as the distance from the point of origin of overland flow to the point where either the slope gradient decreases enough that deposition begins or the runoff water enters a well-defined channel that may be part of a drainage network (Tadesse, 2014). The steeper and longer the slope, the higher the risk for erosion. For the calculation of LS factor, there are several equations given by different researchers. Some of the equation were listed in the Table 3.13.

Table 3.13 Different equations for estimation of LS factor

S. No.	Researchers	Equations
1	Unit Stream Power Erosion and Deposition (USPED)	LS = Power("flow accumulation"*(cell resolution)/ 22.1,0.4) * Power(Sin("slope in degree" * 0.01745))/ 0.09,1.4) *1.4
2	Moore and Burch, 1986	LS= ("Flow accumulation" * (cell resolution) $22.1)^{0.4}$ * (Sin("slope of degree")/$0.0896)^{1.3}$
3	Griffin *et al.*, 1988	LS= Power("flow accumulation" * (cell resolution)/ 22.1,0.6) * Power(Sin("slope in degree" * 0.01745))/ 0.09,1.3)
4	Morgan, 1979	LS= $(L/100)^{0.5} * (0.136 + 0.097\ S + 0.0139\ S^2)$
5	Mc Cool *et al.*, 1987	L= $(\lambda/22.1)^m$ S= 10.8 sin θ + 0.03, s < 9% S= 10.8 sin θ - 0.05, s ≥ 9%
Where, L = slope length in m, S= slope steepness (S) in percent, λ= field slope length, m= dimensionless exponent that depends on slope steepness		
Source: Through the Review of Literature		

The LS factor for this study was computed using equation suggested by Morgan, 1979 which was used in Soil erosion Andhra Pradesh, Bulletin by NBSSLUP. It ranged from 0.85 to 13 for the study area.

3.5.4 Cover management factor (C)

Cover management factor is defined as the ratio of soil loss from land cropped under specific conditions to the corresponding loss from clean-tilled, continuous fallow (Wischmeier and Smith, 1978). C-factor represents the effect of soil- disturbing activities, plant, crop sequence and productivity level, soil cover and subsurface bio-mass on soil erosion. Vegetation indices generally the normalized differences vegetation index (NDVI) is used to derive the cover factor used in erosion modelling (Suriyapasit and Shrestha, 2008). For calculating C-factor, the following equation was used

$$C = exp\left[-\alpha \frac{NDVI}{\beta - NDVI}\right]$$

Where: α, β are parameters that determine the shape of the NDVI-C curve. They suggested values of 2 and 1 for α and β respectively. Van der Knijff, *et al*. (1999) also proven that the equation seems to produce more realistic C values than those estimated assuming a linear relationship. The value of C basically depends on the vegetation's cover percentage and growth stage. The C-factor ranges from 0 (meaning full very strong cover effect resulting in no erosion) to 1 (represents no vegetation cover effect), however the NDVI values range from 1 (full cover) to 0 (bare land).

3.5.5 Conservation practice factor (P)

Conservation practice factor (P) is the ratio of soil loss with a specific support practice to corresponding soil loss with upslope and downslope tillage. These practices essentially effect erosion by adjusting the flow pattern, steepness, or direction of surface runoff and by reducing the amount and rate of runoff. The support practices for cultivable lands are including contouring, strip-cropping, terracing, and subsurface drainage. While on dryland or rangeland area, soil disturbing practices to result storage of moisture and reduction of runoff considered to be as support practices mechanisms. The value of P-factors were taken from Soil erosion, Andhra Pradesh given by NBSSLUP. The P factor for different land uses was presented in Table 3.14.

Table 3.14 P factor for different land use land cover

S. No	Land use land cover	P – factor
1	Agricultural land	0.23
2	Water bodies	1
3	Forest	0.6
4	Scrub only	1
5	Current fallow	1
6	Other wasteland	1
7	Build-up	1
8	Plantation	0.5

3.5.6 Estimation of soil loss rate

RUSLE model was integrated with GIS and RS techniques to estimate the annual average soil loss rate (t ha^{-1} yr^{-1}) and to identify soil erosion risk areas in Krishna lower sub basin. The RUSLE model uses six parameters including rainfall runoff erosivity (R), soil erodibility (K), slope length and steepness (LS), cover management (C), and support practice factor (P).

3.6 Identification of technological measures for efficient utilization of streamflow

The procedures used to fulfill the third objective of the study was presented in this section. Soil and water conservation measures were planned for catchment area treatment based on estimated soil erosion data. Site selection for soil and water conservation measures was carried out by overlying the slope, soil, land use/land cover and stream order maps. The multi-layer integration of land use/ land cover, soil, slope, flow direction, drainage and settlement gave the suitability units for identifying sites for percolation tanks and check dams. Factor layers (maps) were incorporated in ArcMap multi criteria evaluation analysis, using the weighted overlay function in the ArcGIS analyst. Finally, a suitability map was developed that showed the potential sites for different conservation structures in study area.

The criterion has been decided for identifying the suitable sites for conservation measures, namely check dams and percolation tanks. The site for check dam can be selected on 2^{nd} /3^{rd} order streams in moderate to well drained conditions with slope < 10% and land use may be agricultural areas/Waste land/Forest areas. Criteria for selection of site for Percolation tank is 2^{nd} /3^{rd} order streams on well drained to excessively drained conditions with slope < 3 % and land use may be waste land.

Chapter IV

RESULTS AND DISCUSSION

This chapter presents results of the application of hydrological model and RUSLE model to the Krishna lower sub basin of Andhra Pradesh. The spatial and temporal variation of stream flow and soil erosion has been presented under the following categories.

4.1 Simulation of stream flow

4.1.1 Spatio-temporal variation of rainfall data in Krishna lower sub basin

Rainfall spatial variability exerts a considerable influence on the space-time distribution of state variables of a hydrological system. It influences considerably the volume of runoff, peak runoff and time to peak. Its impact depends on factors such as basin scale, precipitation type and predominant hydrological partitioning processes. The spatial distribution of the average annual rainfall from 1993 to 2015 was shown in the Figure 4.1. This map clearly depicted the decreasing trend of rainfall from eastern part to western part of the basin. The eastern part of the study area received more rainfall.

The average annual precipitation in the study area ranged from 609.05 mm to 1350.16 mm. The highest amount of rainfall events were recorded during the years 2013, 2010, 2008, 1994 and 1995. The spatial variation of rainfall for wet and dry years was also shown in Fig. 4.2 and 4.3. Highest amount of rainfall was received in the eastern part of the study area even in dry and wet years also. The amount of rainfall varied temporally. The rainfall occurred during the dry year (2009) varied from 372.63 mm to 691.89 mm. Similarly, the rainfall received during the wet year (2013) ranged from 1205.95 mm to 2204.74 mm. The spatial maps have clearly shown the wide variation of rainfall spatially and temporally in the study area. Accordingly, there will be variation in depth of runoff.

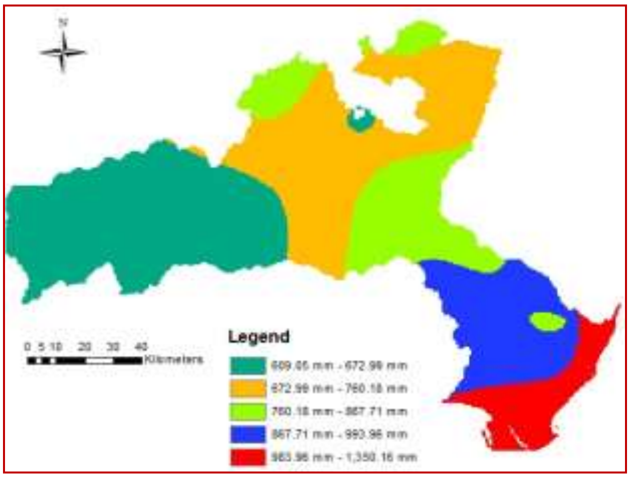

Fig. 4.1 Spatial variation of average annual rainfall (mm) in the study area

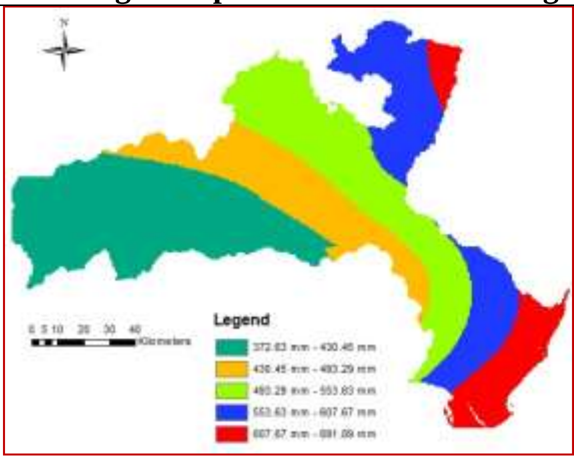

Fig. 4.2 Spatial variation of rainfall (mm) during dry year (2009)

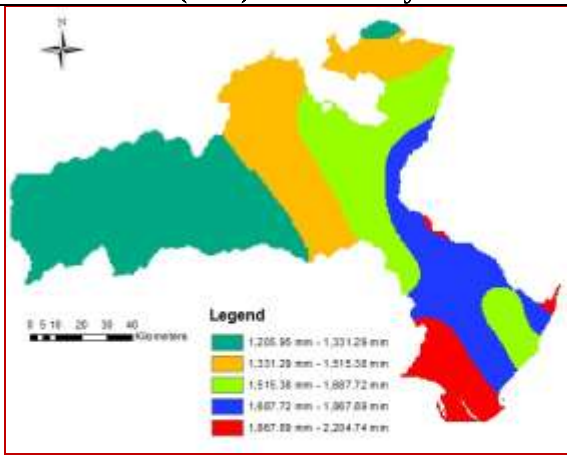

Fig. 4.3 Spatial variation of rainfall (mm) during wet year (2010)

4.1.2 Generation of characteristics of watershed and development of CN method for Krishna lower sub basin

Hydrological parameters have been computed from the delineated catchment and provided as input into the HEC-HMS hydrological models. The study area has been divided into 15 sub watersheds. The physical catchment characteristics of sub watersheds such as catchment area, perimeter, catchment length and slope were automatically calculated in HEC-GeoHMS (Table 4.1). Data of Hydrologic soil group and land use map were used to define CN for each land use type in sub basin. A good condition refers to lightly grazed with 75% or more land covered with plants. If the area consists of patches of land then a composite curve number (CN) for the watershed was obtained by weighing them in proportion of the area. The value of CN varies between

64.67 and 98.0. It means that around 64.67% to 98% from rainfall will transform into runoff. The composite CN map of each sub basin is shown in the Fig. 4.4

Table 4.1 Physical characteristics of study area

S. No.	Sub-watersheds	Area (km^2)	Mean elevation (m)	Basin slope	Longest flow length (m)	Curve number	Time of concentration (min)
1	1B	578.10	98.47	0.00419	36596.27	88.34	36.50
2	2B	3159.53	135.89	0.00762	97659.44	74.51	75.89
3	3B	864.76	72.74	0.00718	44906.84	81.78	40.59
4	4B	3820.72	52.54	0.00362	88974.92	77.68	83.96
5	5B	356.15	9.32	0.00037	38041.42	77.58	153.29
6	6B	396.64	13.66	0.00053	30645.48	66.92	113.07
7	7B	150.32	5.33	0.00013	17593.90	69.50	183.34
8	8B	206.54	7.93	0.00036	24111.29	64.67	87.98
9	9B	229.80	6.02	0.00034	25241.32	70.70	133.65
10	10B	361.90	4.12	0.00013	26276.14	71.35	224.03
11	11B	184.59	4.25	0.00014	20463.08	71.57	262.93
12	12B	126.87	3.38	0.00014	14944.77	79.82	137.90
13	13B	365.75	7.50	0.00101	76701.46	88.61	128.47
14	14B	160.92	2.56	0.00036	17852.75	85.86	116.57
15	15B	50.78	0.63	0.00073	3143.59	98.00	6.80

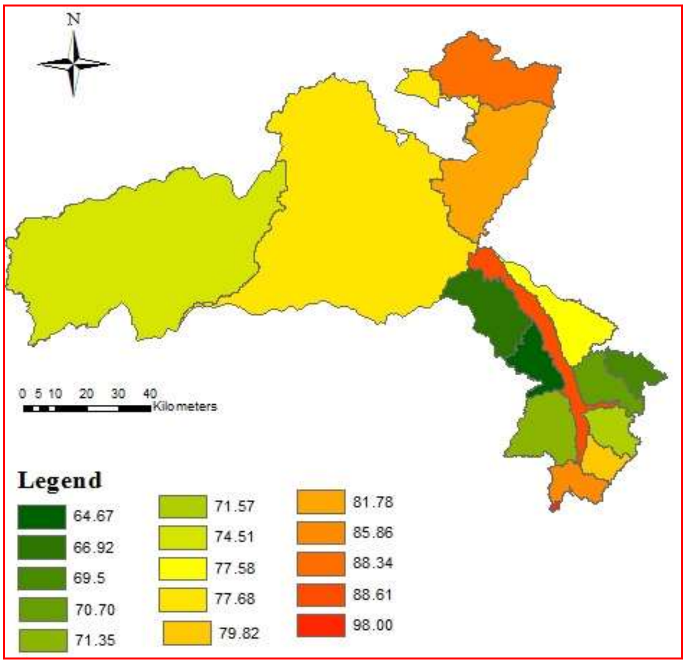

Fig. 4.4 Composite curve number map of study area

4.1.3 Simulation of stream flow in study area from 1993-2015

HEC-HMS provides various methods including SCS-CN technique for simulating surface runoff. The Soil Conservation Service Curve Number (SCS-CN) approach was used for predicting direct runoff volume for a given rainfall event in the study area. The volume of runoff predicted can be used for the planning of land use and the careful management of soil, water and vegetation resources, through the use of appropriate conservation practices and structural works that can retard runoff, increase the infiltration rate, improve production and enhance the productivity and sustainability of the land. The simulated runoff for the lower Krishna sub basin from 1993-2015 was presented in depth units (mm) in the Table 4.1 and depicted in Fig.4.5. The same was converted to volume in million cubic metres (MCM).

Table 4.2 Simulated annual runoff depth from 1993-2015 for lower Krishna sub basin

S. No.	Year	Runoff depth (mm)
1	1993	416.86
2	1994	963.93
3	1995	920.75
4	1996	778.91
5	1997	565.33
6	1998	621.28

7	1999	359.31
8	2000	878.39
9	2001	594.47
10	2002	261.97
11	2003	625.64
12	2004	328.84
13	2005	805.67
14	2006	578.89
15	2007	682.63
16	2008	1004.3
17	2009	288.02
18	2010	1383.50
19	2011	479.26
20	2012	1029.10
21	2013	1116.40
22	2014	328.65
23	2015	365.68

The maximum amount of surface runoff was simulated during the year 2010 coincided with the highest amount of rainfall recorded during year. Similarly, less amount of runoff was simulated in the year 2002. The runoff was analysed further preparing graphs which had shown (Fig 4.6) linear variation of rainfall- runoff. The scattered graph has been drawn with data was pertaining to 23 years annual rainfall (mm) on X axis and annual runoff (mm) on Y axis and with the correlation coefficient of 0.9. It clearly indicated that the runoff is highly correlated with rainfall events.

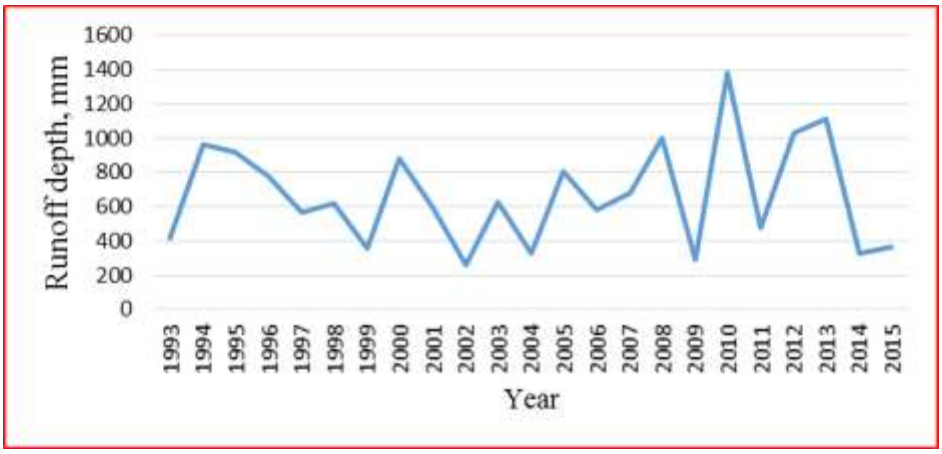

Fig. 4.5 Simulated average annual runoff depth from 1993-2015

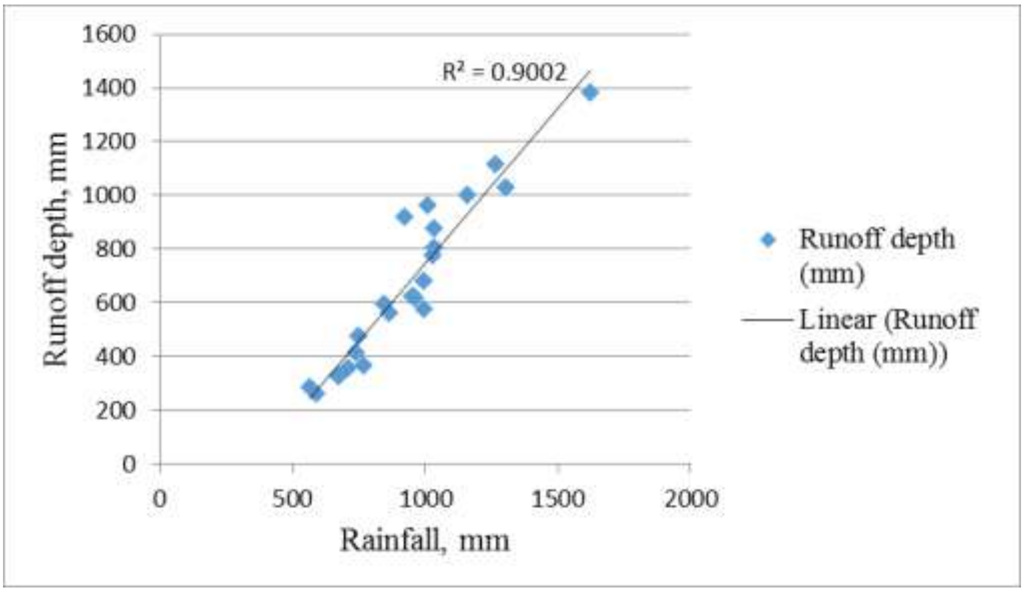

Fig. 4.6 Scattered diagram for yearly rainfall-runoff series

The area near the output point of the basin play the highest role in flood development and should be placed in the first priority of initiating management measures. The runoff from peak rainfall events during high rainfall years were calculated to know the impact of heavy rainfall and were presented in the Table 4.3.

Table 4.3 Simulated runoff depth for the heavy rainfall events

Events	Days	Rainfall depth (mm)	Runoff depth (mm)
1995	16th Oct to 18th Oct	70.66	12.18
2000	22nd Aug to 24th Aug	170.52	122.96
2005	20th Sep to 21th Sep	158.62	73.99
2009	30th Sep to 2nd Oct	138.80	80.56
2010	20th May to 22ndMay	159.98	82.19
2015	18th Jun to 20thJun	106.60	62.07

There was a variation in conversion of rainfall into runoff depth in different rainfall events. The effects of spatial rainfall on runoff are likely to vary depending on the effect of antecedent catchment conditions. More runoff was obtained with spatially averaged rainfall input under wet conditions. However, for dry catchment conditions, the runoff prediction was seen to be considerably less than for the wet conditions. This result indicated that there is an interaction between the spatial rainfall and the spatial distribution of soil moisture which controls runoff prediction.

The runoff depth and peak runoff rate were simulated for different rainfall events in the year 2015(Table 4.4a) and compared with the inflow discharge that are available at Pulichintala project.

Table 4.4a. Simulated runoff depth and rate of runoff at Pulichintala during the year 2015

Date	Runoff depth (mm)	Time of concentration (h)	Time to peak (h)	Simulated peak discharge (m^3/s)	Observed peak discharge (m^3/s)
19th June	0.72	23.38	18.87	25.24	45.02
20th June	1.69	23.38	18.87	59.23	85.00
21st August	2.90	23.38	18.87	101.77	96.29
22th August	3.50	23.38	18.87	122.67	125.41
29th August	0.45	23.38	18.87	15.859	21.70
31st August	0.49	23.38	18.87	17.50	55.00

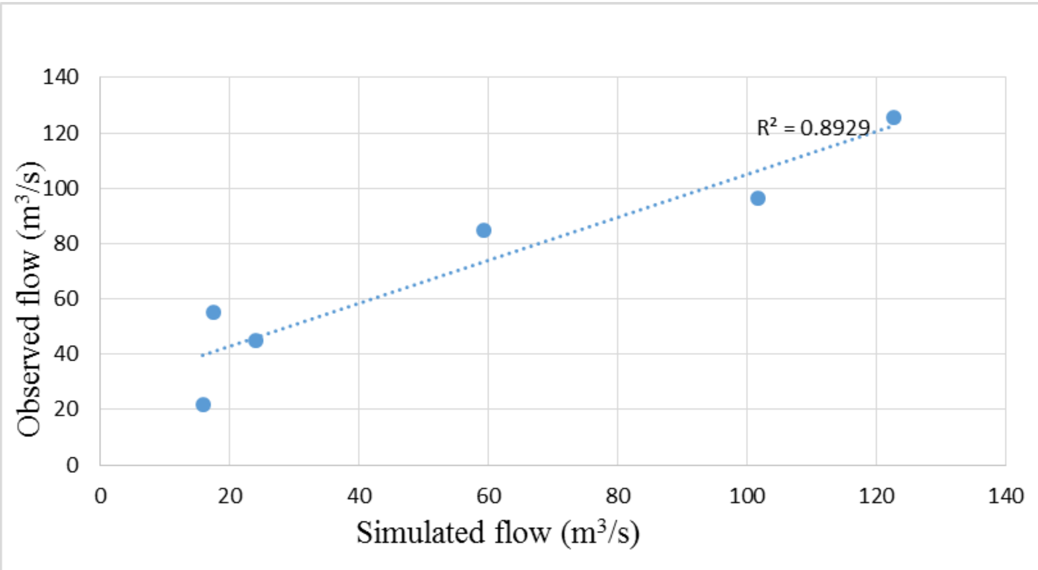

Fig. 4.7 Comparison of observed Vs simulated rate of runoff

The simulated peak runoff rates are close to the observed inflows. The graph has clearly shown in Fig. 4.7. The results obtained in the present study were in good agreement R^2=0.89. The HEC-HMS models calibrated for even based simulation.

Despite difficulties, limitations and uncertainties associated with obtaining observations and measured parameters, this study ended up with satisfactory results for the simulation of rainfall-runoff process**.**

Table 4.4b Simulated peak discharge for the rainfall events during the year 2015

Date	**Runoff (mm)**	**Time of concentration (h)**	**Time to peak (h)**	**Peak discharge, (m^3/s)**
13th June	1.348	61.34	44.64	71.41
15th June	0.570	61.34	44.64	30.19
16th June	0.157	61.34	44.64	8.32
6th July	7.628	61.34	44.64	404.08
7th July	1.547	61.34	44.64	81.95
11th July	2.783	61.34	44.64	147.42
12th July	3.748	61.34	44.64	198.54
26th August	1.528	61.34	44.64	80.94
27th August	2.542	61.34	44.64	134.66
28th August	2.270	61.34	44.64	120.25
29th August	27.094	61.34	44.64	1435.26
31st August	0.640	61.34	44.64	33.90

The simulated peaks for different rainfall events for the year 2015 were presented in the Table 4.4b. The computed discharges provide insight about peak runoff rates and volumes that can be obtained in the Krishna lower sub basin of Andhra Pradesh. But calibration and validation are needed to be carried out at the downstream of the basin for accurate results.

4.1.4 Runoff depth in different types of soils in Krishna lower sub basin

A detailed land use land cover and soil map using GIS and RS tools showed that the catchment is dominated by silt soils coupled with agricultural area. The Group C was covering the major portion of the study area. The proportion of rainfall becoming direct runoff is also controlled by the permeability of the catchment and can mask the impact of spatial rainfall. The runoff was high in clay soil and followed by silt soil. It was very less in loam soil. The result indicated the impact of soil type on runoff and confirmed the strong correlation between the CN values and runoff depth. The value of CN is lower for soils with high infiltration.

Table 4.5 Volume of runoff in different types of soil of study area

Runoff volume in MCM			
Year	**Clay**	**Silt**	**Loam**
1993	792.16	651.55	79.33
1994	1835.05	1574.15	156.17
1995	1944.29	1423.05	148.12
1996	1496.39	1265.29	131.68
1997	1064.06	968.74	93.11
1998	1203.72	1055.09	104.03
1999	804.73	599.60	53.48
2000	1654.49	1491.02	136.00
2001	1133.74	999.67	98.62
2002	493.77	427.40	48.92
2003	1247.31	1038.74	101.02
2004	671.21	634.46	46.95
2005	1593.43	1456.47	116.74
2006	1306.09	632.18	111.28
2007	1330.88	1137.95	113.16
2008	1928.01	1692.90	157.15
2009	504.05	596.29	41.74
2010	2626.91	2358.81	222.14
2011	925.12	874.57	72.46
2012	1965.21	1826.10	158.35
2013	2226.74	1948.47	162.72
2014	645.71	516.64	60.68
2015	779.65	616.78	55.48

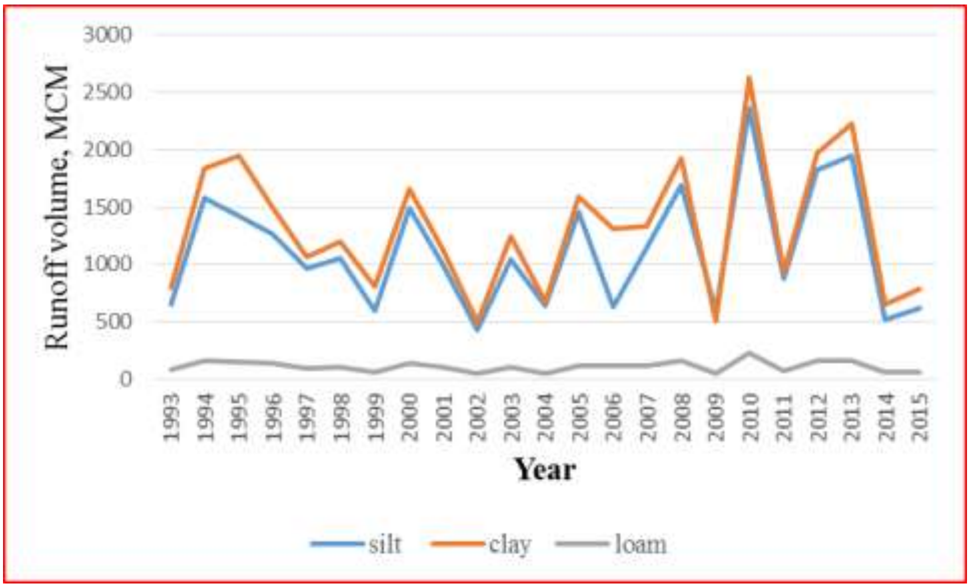

Fig. 4.8 Runoff volume in different types of soil of study area

4.1.5 Effect of land use land cover on stream flow

Land use plays an important role in controlling hydrologic response of catchment, particularly in terms of the nature and magnitude of surface water and ground water interactions and surface water availability. The change in land use controls the water yield of surface streams and groundwater aquifers and thus the amount of water available in a watershed. It effect the generation of land flow, soil water storage, water demand for irrigation etc. The LULC maps for two different years have been prepared from IRS P_6, LISS III (Table 4.6). The maps were used to check the effect of change in land use on stream flow of the Krishna lower sub basin.

Table 4.6 Spatial change in land use land cover from year 2011 to 2015

S. No.	Land use land cover	Type of LULC in percentage		Rate of change in LULC
		2011-2012	2014-2015	
1	Current fallow	9.41	6.48	+2.92
2	Built-Up Land	2.29	2.30	-0.01
3	Plantation	3.16	3.11	+0.05
4	Forest	8.42	8.30	+0.12
5	Double Crop	33.90	40.10	-6.23
6	Scrub land	7.24	6.74	+0.5
7	Kharif only	14.60	14.80	-0.21

8	Waste Land	2.24	1.85	+0.39
9	Rabi only	11.50	8.15	+3.4
10	Water	7.24	8.17	-0.93

There was not much change in land use land cover of sub basin except double cropped area, current fallow land and rabi cropped area. Double crop area has been increased which directly contributed to decrease in current fallow area due to intensive cropping. Rabi cropped area has been decreased due to unavailability of water.

The spatial maps of runoff depth for the year 2011-12 and 2014-15 have been presented in Fig 4.9 and Fig 4.10 respectively. A poor condition refers to heavily grazed pastures with almost no vegetation. Bare land has a high runoff potential. Urbanisation has a great effect on runoff generation. Even though built-up area amounts to only 2.29% in 2011-2012 and 2.3% in 2014-2015, there was a considerable amount of runoff. The runoff has increased from 33.9% to 40% with the increase in double cropped area, the runoff has been reduced. The current fallow area was reduced to 6.48% from 9.41%. Accordingly, the runoff has been decreased in the year 2014-2015. The area under rabi crop has been reduced. The simulated runoff was also decreased.

From the above results, it can be concluded that built area produced more runoff followed by scrub land, wasteland, fallow land, rabi only, kharif only, forest, plantation and double cropped area.

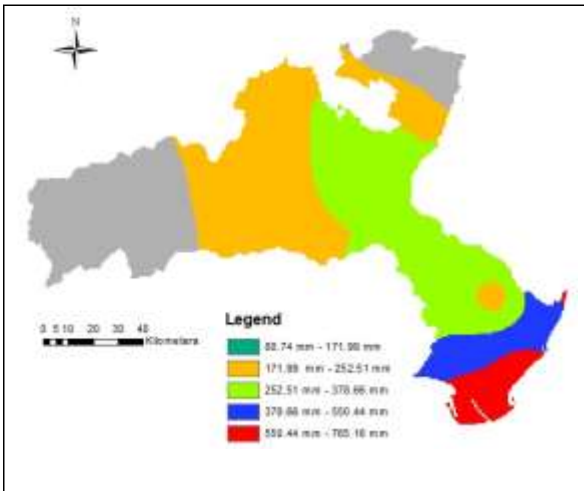

Fig. 4.9 Spatial variation of runoff depth (mm) of 2011-2012

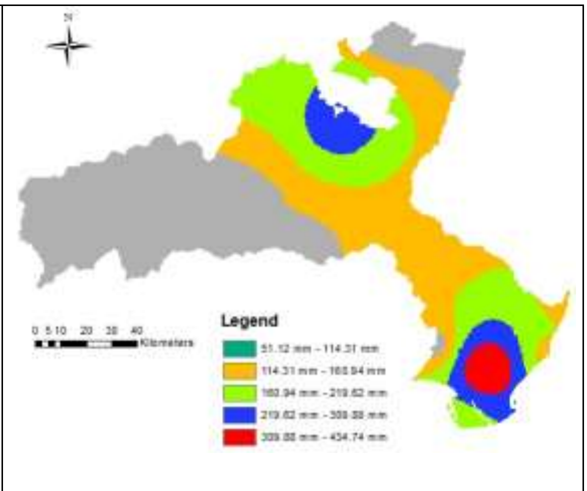

Fig. 4.10 Spatial variation of runoff depth (mm) of 2014-2015

On pervious catchment areas, rainfall variations are damped by the integrating reaction of the catchment, whereas on impervious areas a high proportion of precipitation becomes effective rainfall. Impervious catchments are fast responding and studies showed that a high density rain gauge network is required for runoff modelling.

4.1.6 Volume of flow in Krishna lower sub basin

The volume of flow of water in Krishna lower sub basin was simulated using SCS-CN method for a period of 1993 to 2015 to estimate amount of runoff contributing from different land use land cover. The volume of runoff in Krishna lower sub basin was presented in Table 4.7.

Table 4.7 Volume of runoff in Krishna lower sub basin

S. No.	Year	Total flow, MCM
1	1993	1523.03
2	1994	3565.37
3	1995	3515.46
4	1996	2893.36
5	1997	2125.90
6	1998	2362.84
7	1999	1457.81
8	2000	3281.52
9	2001	2232.03
10	2002	970.09
11	2003	2387.08
12	2004	1352.62
13	2005	3166.64
14	2006	2049.56
15	2007	2581.98
16	2008	3778.06
17	2009	1142.07
18	2010	5207.85
19	2011	1872.15
20	2012	3949.66
21	2013	4337.93
22	2014	1223.03
23	2015	1451.91

4.2 The Annual Average Soil Loss Rate (A)

In this study, RUSLE model was integrated with GIS and RS techniques to estimate the annual average soil loss rate (t ha^{-1} $year^{-1}$), and to identify soil erosion risk areas in lower Krishna sub basin. The RUSLE model uses six parameters including rainfall runoff erosivity (R), soil erodibility (K), slope length and steepness (LS), cover management (C), and support practice factor (P). Raster map of each RUSLE parameters derived from different data sources were presented and analysed.

4.2.1 Rainfall erosivity factor (R)

Many studies (Jain *et al.*, 2001; Dabral *et al.*, 2008; Ganasri *et al.*, 2016) revealed that the soil erosion rate in the catchment is more sensitive to rainfall. The daily rainfall is a better indicator of variation in the rate of soil erosion to characterize the seasonal distribution of sediment yield. The erosivity factor (R) was estimated and the values were presented in the Table 4.8. The spatial maps of R-factor were presented in Fig 4.11 to Fig. 4.16. The value of R factor for 23 years is given in appendix.

Table 4.8 R factor values for different years of rainfall in the study area

Sl. No.	Year	R Factor
1	1995	425.00 - 688.95
2	2000	313.16 - 629.32
3	2005	336.40 - 574.99
4	2009	163.09 - 484.89
5	2010	458.93 - 1039.08
6	Average of 23 years	235.50 - 573.08

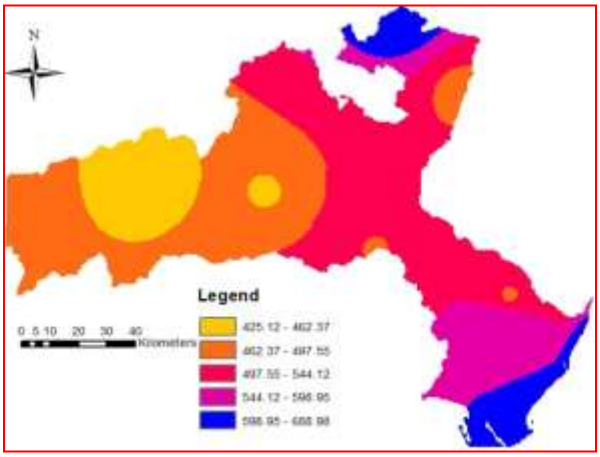

Fig. 4.11 Spatial variation of R-factor map of 1995

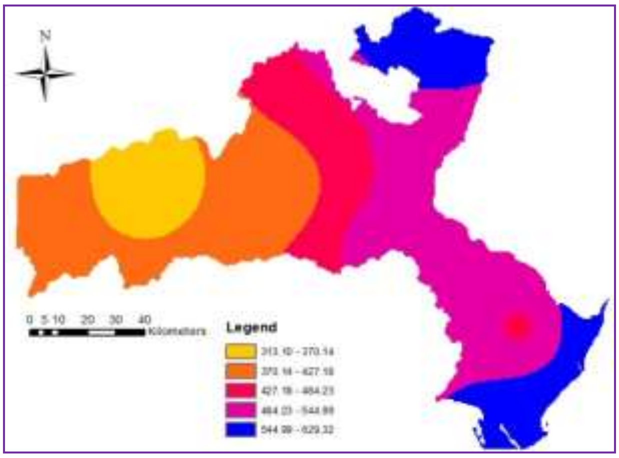

Fig. 4.12 Spatial variation of R-factor map of 2000

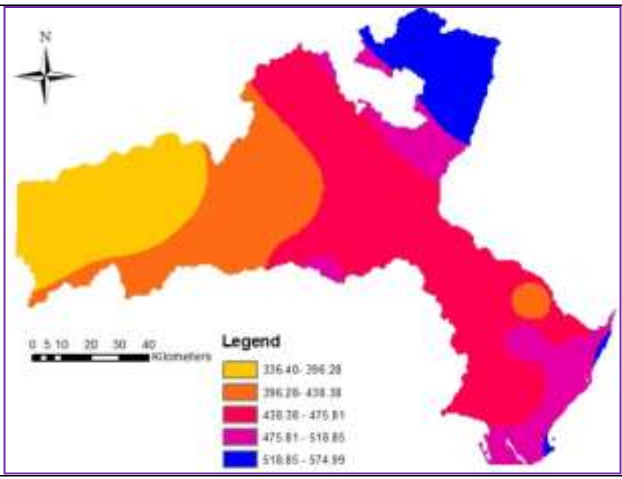

Fig. 4.13 Spatial variation of R-factor map of 2005

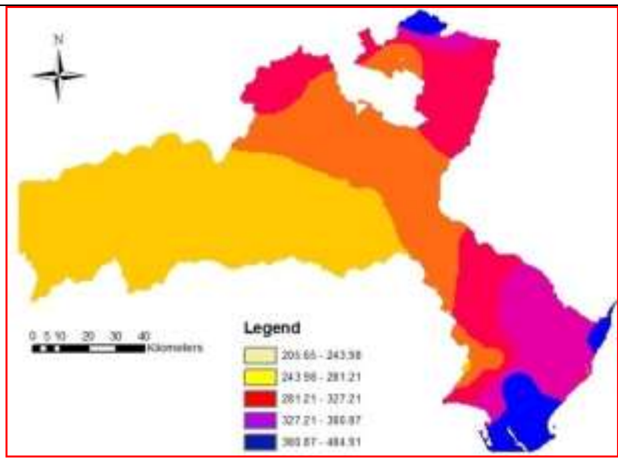

Fig. 4.14 Spatial variation of R-factor map of 2009

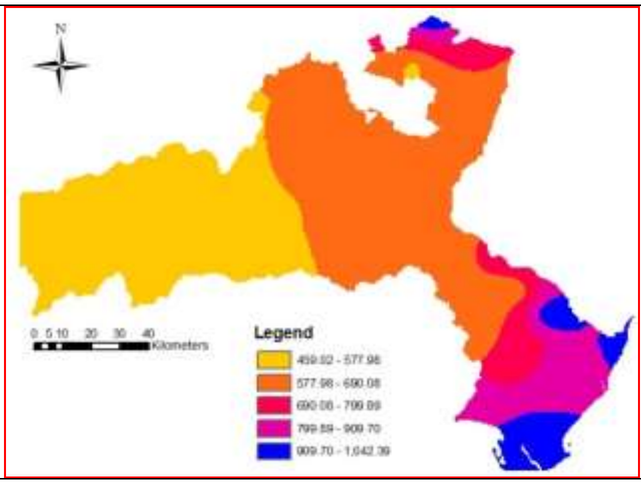

Fig. 4.15 Spatial variation of R-factor map of 2010

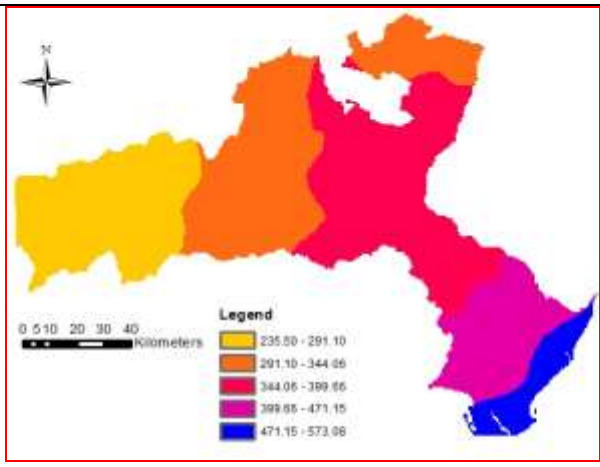

Fig. 4.16 Spatial variation of R-factor map for 23 years

4.2.2 Soil erodibility factor (K)

K factor values were assigned to respective soil types in soil map to generate the soil erodibility map. The corresponding value of K for the soil types were taken from Soil erosion, Andhra Pradesh given by NBSSLUP. The estimated K values for the textural groups vary from 0.15 t ha h ha^{-1} MJ^{-1} mm^{-1} (clay), 0.29 t ha h ha^{-1} MJ^{-1} mm^{-1} (loam), 0.35 t ha h ha^{-1} MJ^{-1} mm^{-1} for silt and zero has taken for water. The spatial map of K- factor for the study area was depicted in Fig. 4.17.

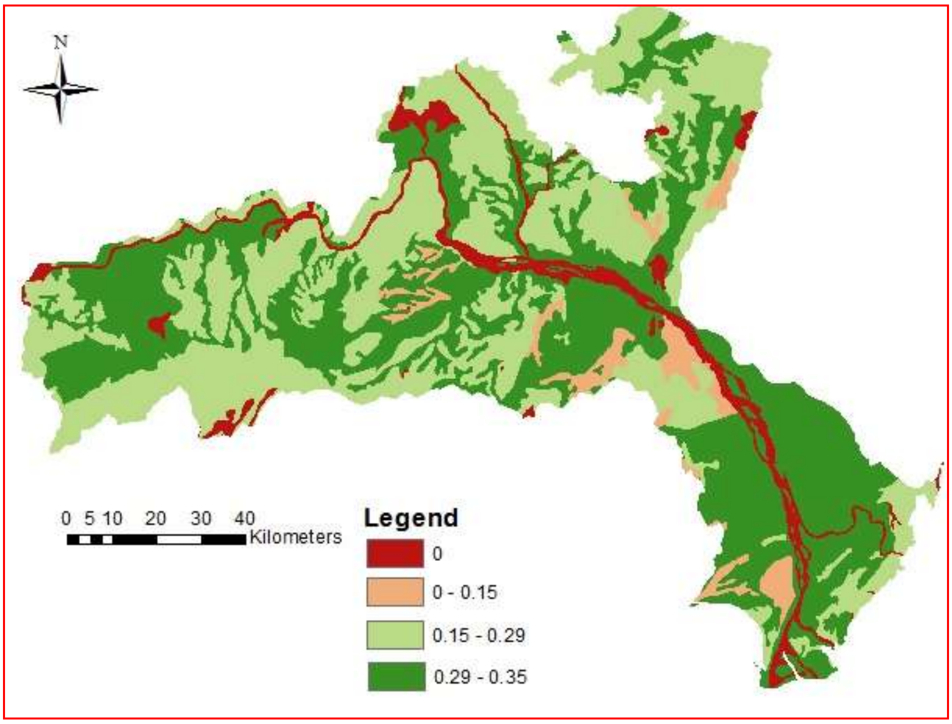

Fig. 4.17 Spatial variation of K-factor map

4.2.3 Topographic factor (LS)

Topographic factor represents the influence of slope length and slope steepness on erosion process. The topographic component of RUSLE was computed using equation suggested by Morgan, (1994). LS factor was calculated by considering the flow accumulation and slope in percentage as an input. From the analysis, it is observed that the value of topographic factor increases in a range of as the flow accumulation and slope increases. It ranged from 0.85 to 13 for the study area (Fig.4.18).

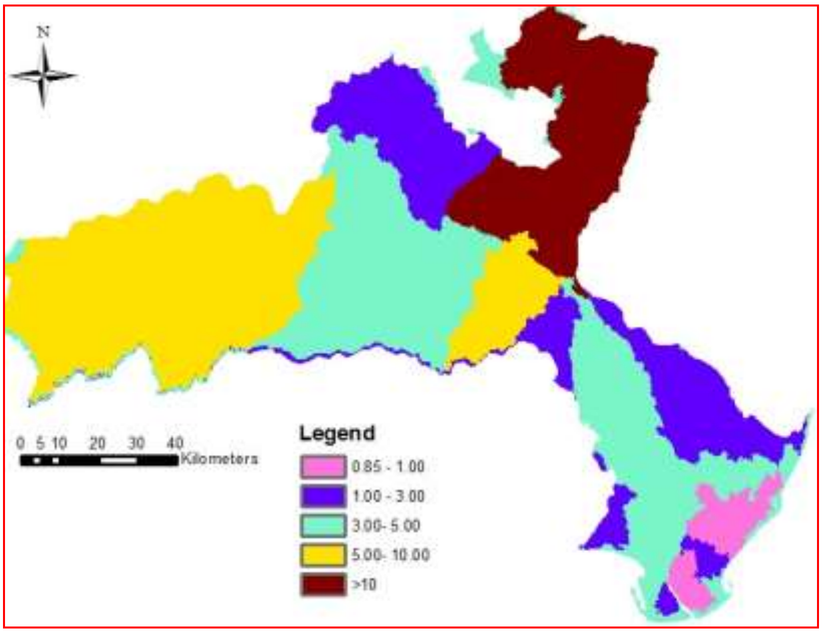

Fig. 4.18 Spatial variation of LS-factor map

4.2.4 Crop management factor (C)

It is defined as the ratio of soil loss under a given crop to that from bare soil. Generally the C-factor will range between 1 and almost 0. Hereby C=1 means no cover effect and a soil loss comparable to that from a tilled bare fallow. C=0 means a very strong cover effect resulting in no erosion. Information on land use permits a better understanding of the land utilization aspects of cropping pattern, fallow land, forest, wasteland and surface water bodies, which are vital for developmental planning/erosion studies. For this study, the value of C was obtained from NDVI was used and shown in the Fig.4.19.

4.2.5 Conservation practice factor (P)

P is the support practice factor. It reflects the effects of practices that will reduce the amount and rate of the water runoff and thus reduce the amount of erosion. In the present study the P-factor map was derived from the land use/land cover and slope (Fig.20). The P factor classes range from 0.23 to 1.00. The highest value of P factor is assigned to areas with no conservation practices (deciduous forest, wasteland, scrubland); the minimum values correspond to build up, agriculture land and plantation area with strip and contour cropping. The lower the P value, the more effective the conservation practices (Prasannakumar, 2012).

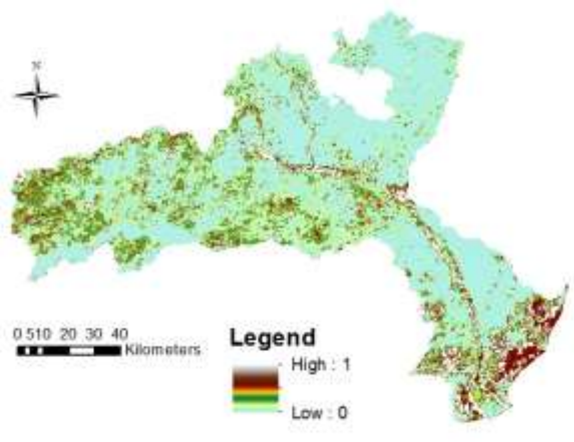

Fig. 4.19 Spatial variation of C-factor map

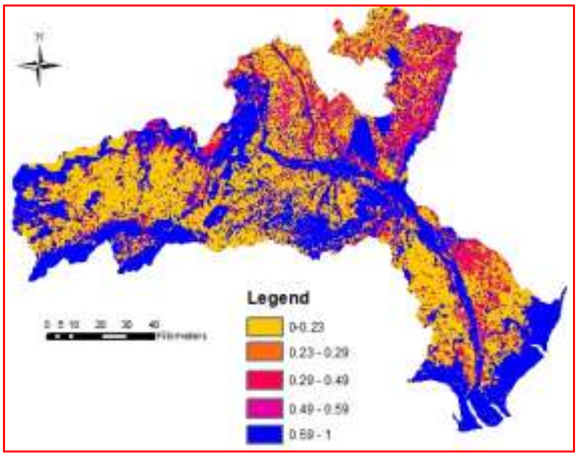

Fig. 4.20 Spatial variation of P-factor map

4.3 Estimation of annual soil erosion

The GIS analysis has been carried out for RUSLE to estimate annual soil loss on the spatial distribution of the soil erosion in the study area. In order to estimate the annual average soil loss rate for the basin, the above six parameters were multiplied using the raster calculator tool. Accordingly the catchment has been classified into five classes of soil loss starting from slight erosion to severe erosion as given below.

1. Slight (<5 t $ha^{-1}yr^{-1}$)
2. Moderate (5-10 t $ha^{-1}yr^{-1}$)
3. Strong (10-15 t $ha^{-1}yr^{-1}$)
4. Severe (15-20 t $ha^{-1}yr^{-1}$)
5. Very severe (20-40 t $ha^{-1}yr^{-1}$)

Soil erosion is highly variable in the spatial as well as temporal domain. The temporal variation of soil loss has been estimated during 1993 to 2015 to study the impact of rainfall amount and intensity on soil loss. The soil loss for different years of annual rainfall for study area has been calculated and presented in the Table 4.9a and 4.9b in terms of area (km^2) and percentage respectively. It can be observed from the table that about 16 percent of total area of catchment was found under slight risk of erosion. Around 43.02% of catchment lies in slight erosion. About 42.41% of area shows moderate soil erosion. Strong to severe erosion occurs around 12.45% to 1.3%. Very severe erosion occur 0.8% which is very less compared to other classes. The highest average annual soil erosion for the year 1993 to 2015 was computed as 28.69 t $ha^{-1}yr^{-1}$.

The results have clearly indicated the effect of rainfall on erosion. Soil erosion was more during the years of high rainfall compared to the years of low rainfall.

Table 4.9a. The areal extent of annual soil loss for different years in study area

Area (km^2)					
Year	**Slight**	**Moderate**	**Strong**	**Severe**	**Very severe**
1993	5544.23	3960.28	1603.25	57.89	151.7
1994	3184.45	5319.05	2440.97	206.02	166.88
1995	4944.33	5314.58	854.99	167.83	35.616
1996	6089.23	4494.48	550.25	117.78	65.618
1997	4829.85	5086.67	1208.03	125.24	67.554
1998	7031.79	3472.12	671.92	103.78	103.78
1999	5445.12	4744.29	926.97	122.52	78.457
2000	5325.55	4398.40	1392.63	163.68	37.098
2001	4753.91	5384.34	989.33	157.55	32.229
2002	4430.64	5601.16	1095.43	145.64	44.493
2003	4369.65	4795.30	1911.62	74.09	166.7
2004	4788.55	5049.48	1289.08	139.94	50.309
2005	3348.02	5516.23	2132.76	162.9	157.45
2006	5089.60	5050.89	928.31	141.34	107.22
2007	3577.55	5354.95	2090.42	115.15	179.28
2008	4299.00	5315.81	1489.06	175.44	38.046
2009	8764.22	2329.99	160.71	52.26	10.166
2010	2810.15	3406.22	4290.93	600.32	209.73
2011	4234.44	5373.70	1497.89	97.27	114.06
2012	4230.94	5374.17	1493.53	96.95	113.12
2013	4515.59	5246.44	1346.72	145.24	63.358
2014	4889.10	5005.82	1232.39	130.32	59.576
2015	5503.61	4804.09	810.13	151.89	23.812

Table 4.9b. The areal extent of annual soil loss for different years in study area

Area (%)					
Year	**Slight**	**Moderate**	**Strong**	**Severe**	**Very severe**
1993	48.99	34.99	14.17	0.51	1.34
1994	28.14	47	21.57	1.82	1.47
1995	43.69	46.96	7.555	1.48	0.31
1996	53.8	39.71	4.862	1.04	0.58
1997	42.68	44.95	10.67	1.11	0.6
1998	61.77	30.5	5.903	0.91	0.91
1999	48.11	41.92	8.191	1.08	0.69
2000	47.06	38.86	12.31	1.45	0.33
2001	42.01	47.58	8.742	1.39	0.28
2002	39.15	49.49	9.679	1.29	0.39
2003	38.61	42.37	16.89	0.65	1.47
2004	42.31	44.62	11.39	1.24	0.44
2005	29.58	48.74	18.85	1.44	1.39
2006	44.97	44.63	8.203	1.25	0.95
2007	31.61	47.32	18.47	1.02	1.58
2008	37.99	46.97	13.16	1.55	0.34
2009	77.44	20.59	1.42	0.46	0.09
2010	24.83	30.10	37.91	5.30	1.85
2011	37.42	47.48	13.24	0.86	1.01
2012	37.41	47.52	13.21	0.86	1.00
2013	39.90	46.36	11.9	1.28	0.56
2014	43.20	44.23	10.89	1.15	0.53
2015	48.73	42.54	7.173	1.34	0.21

The mandals are categorised as per the classes of soil erosion (Table 4.10). All most all mandals are prone to slight to moderate soil erosion. About 17 mandals are subjected to very severe erosion which needs immediate attention in terms of watershed management.

Table 4.10 Mandals under different classes of soil erosion

S. No.	Soil erosion class	Affected mandals
1	Very severe (20-40 t $ha^{-1}yr^{-1}$)	Parts of Veldhurthy, Macherla, Rentachinthala, Dachepalle, Machavaram, Belamkonda, Amaravathi, Thadepalle, Kollur, Repalle, Nijampatnam, Nagayalanka, Koduru, Machilipatnam, Vijayawada Urban, Ibrahimpatnam, Kanchikacherla,
2	Severe (15-20 t $ha^{-1}yr^{-1}$)	Parts of Veldhurthy, Macherla, Rentachinthala, Dachepalle, Machavaram, Durgi, Gurazala, Repalle, Nijampatnam, Ibrahimpatnam, Jaggayyapet, Vijayawada Urban, Nagayalanka.
3	Strong (10-15 t $ha^{-1}yr^{-1}$)	Parts of Bollapalli, Veldhurthy, Macherla, Rentachinthala, Belamkonda, Tadikonda, Tadepalle, Repalle, A Konduru, Verullapadu, Kanchikacharla, Ibrahimpatnam, Nagayalanka, Machilipatnam.
4	Moderate (5-10 t $ha^{-1}yr^{-1}$)	Almost all mandals
5	Slight (<5 t $ha^{-1}yr^{-1}$)	Almost all mandals

4.4 Effect of land use land cover on soil loss

Soil loss has a close relationship with land use and land cover. An attempt was made to analyse the effect of land use land cover on erosion rate. Among the various land use and land cover, very severe erosion occurred in build-up area, Severe to strong erosion occurred in scrubland and wasteland. Moderate erosion occurred in double/triple cropping area and slight erosion was observed in forest and kharif cropped area. About 13.45% (262.66 km^2) of build-up and 9.28% (21.65 km^2) of wasteland were affected by very severe erosion. Severe erosion occurred in 38.77% (768.561 km^2) of scrubland, in 18.62% (233.26 km^2) and 4.73% (43.93 km^2) of rabi crop area and waste land respectively. The spatial map of soil erosion for the years 1995, 2000, 2005, 2009 and 2010 were shown in Fig. 4.21 to 4.26.

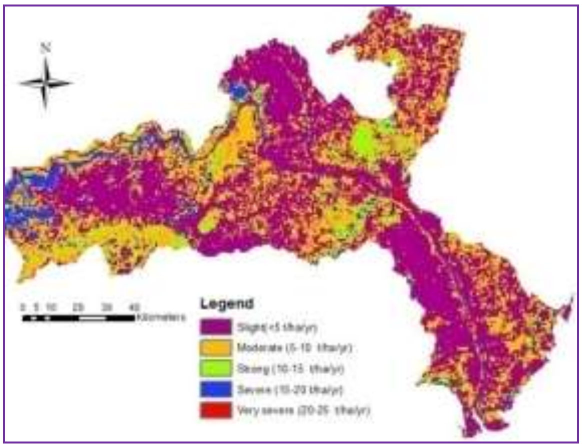

Fig. 4.21 Spatial variation of soil erosion during the year1995

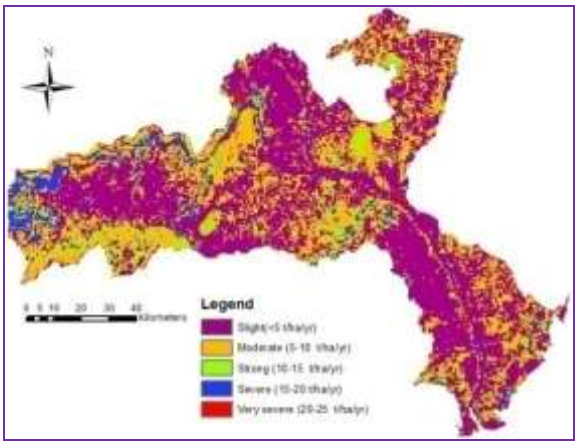

Fig. 4.22 Spatial variation of soil erosion during the year 2000

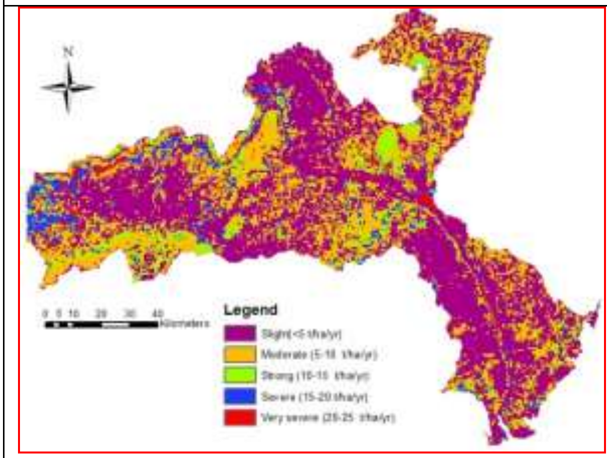

Fig. 4.23 Spatial variation of soil erosion during the year 2005

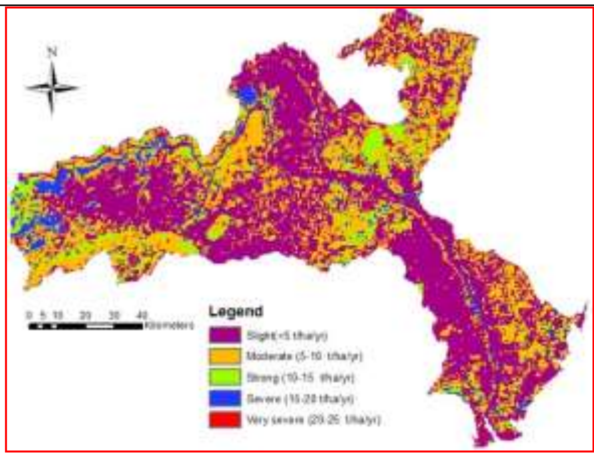

Fig. 4.24 Spatial variation of soil erosion during the year 2009

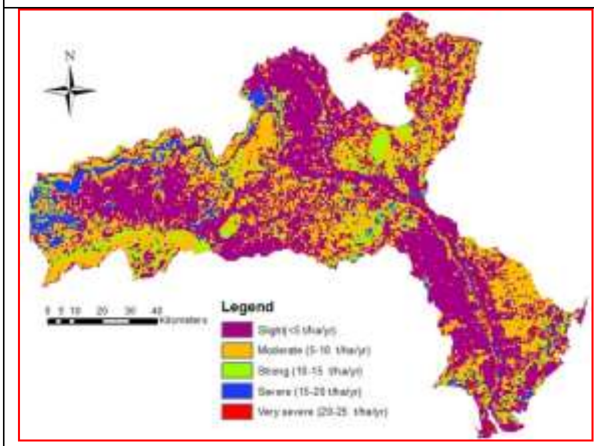

Fig. 4.25 Spatial variation of soil erosion during the year 2010

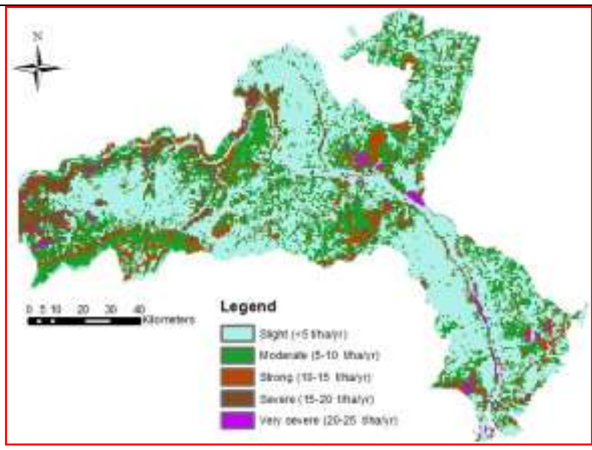

Fig.4.26 Spatial variation map of average soil erosion during 1993-2015

According to Wishmeier and Smith (1978), the maximum tolerable soil loss (12 t ha^{-1} yr^{-1}) is defined as "the maximum level of soil erosion that will permit a level of crop productivity to be sustained economically and indefinitely". Soil loss in excess of 12.5 t ha^{-1} yr^{-1} affect the effectiveness of soil conservation structures, as at this stage gully formation starts which in turn hampers the cultural operations (Gurmel Singh *et al*., 1981). Therefore, if a soil loss of about 12 t ha^{-1} yr^{-1} is considered as tolerable limit, then 13.75 percent of the total area of study area is predicted to be vulnerable to strong to very severe soil erosion risk class. Thus, those sub basin needs to be planned for soil conservation measures.

4.5 Technological measures for efficient utilization of streamflow

The reduction of surface runoff can be achieved by constructing suitable structures or by changes in land management. Further, this reduction of surface runoff will increase infiltration and help in water conservation. Water conservation structures are extremely important to conserve precious natural resources like, soil and water, which is depleting day by day at alarming rate. The surface runoff can be checked by constructing structures like check dams, farm ponds, nala bunds, percolation tanks, contour trenches etc. These structures may differ with different parameters viz., location, slope, soil type, rainfall intensity, land cover and settlement. Depending on these parameters, the construction of check dams, percolation tanks are to be proposed at appropriate sites in the study area.

The overlay operation of land use map, soil map, stream order map and slope map was carried out according to the criterion for identifying suitable sites for check dams, percolation tanks. As per guidelines suitable sites were proposed to construct the check dam since it is located in suitable land classes (barren land, agricultural, forest), slope (less than 10%) and soil type (sandy clay loam). Check dams are recommended for drainage line treatment. The identified sites for check dams were Fig 4.27.

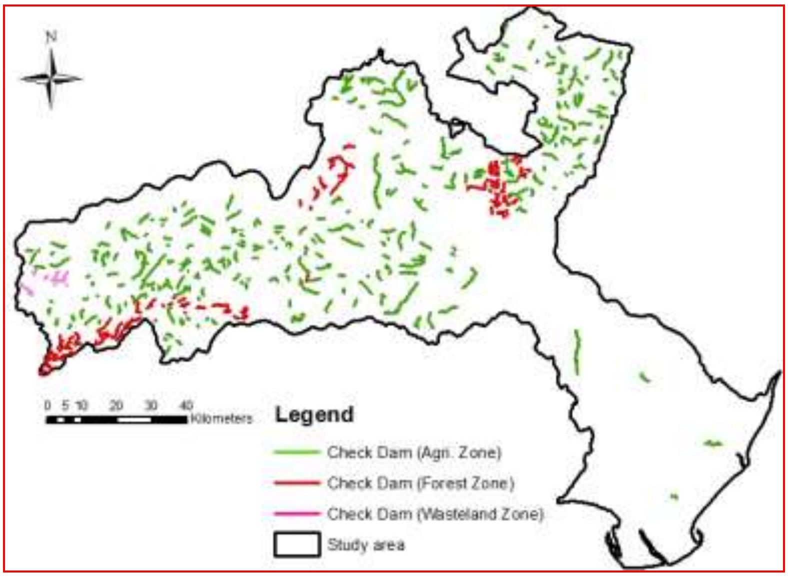

Fig. 4.27 Suitable sites for check dams

The suitability of percolation tanks sites confirmed as the site is located on second and third order drainage and satisfies the conditions of land use (barren land), soil type (sandy clay loam) and slope (less than 3%). For the study area, around 1452.92 km^2 was covered as wasteland and 27 percolation tanks can be constructed. Every 53.81 km^2 of wasteland can have one percolation tank. The identified sites percolation tanks were Fig. 4.28.

This structure helps in reducing velocity of runoff water, water harvesting and also ground water recharge. Percolation tanks are suggested across streams and bigger gullies to impound part of runoff water and thereby recharging of ground water.

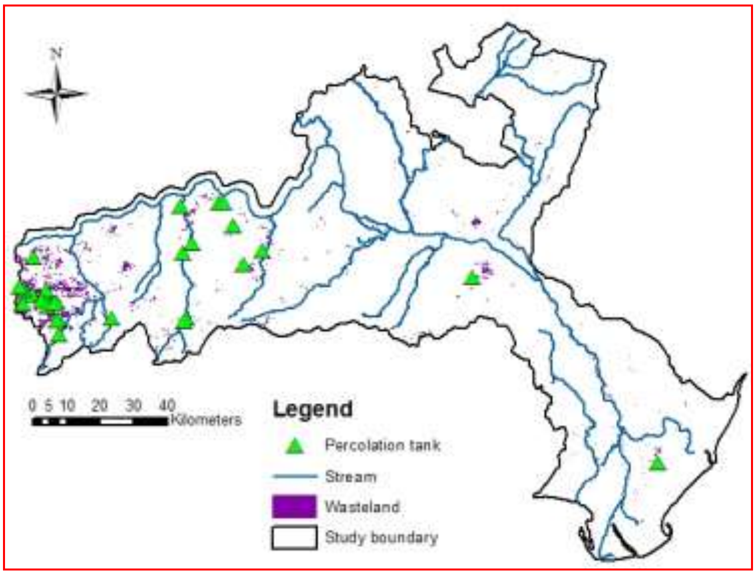

Fig. 4.28 Suitable sites for percolation tank

Hence, hydrological models HEC-HMS and RUSLE can be used to simulate runoff and rate of soil loss in a Krishna lower sub basin of Andhra Pradesh. The models can help in save time and money in obtaining runoff and soil erosion data rather than measurement in the watershed. Moreover, it may help to simulate runoff and erosion in ungauged watershed, where there is no gauging station to measure hydrologic data.

Chapter V

SUMMARY AND CONCLUSIONS

This chapter presents a summary of the research findings, conclusions and recommendations made towards enhancing conservation and effective management of water resources of Krishna lower sub basin. The conclusions were drawn from the research findings and discussions. Areas for further research have also been proposed for the purpose of exploring problems facing in the catchments so that they can be addressed appropriately.

The Krishna lower sub basin was selected for simulating stream flow and soil erosion. Different DEMs were downloaded to generate basin characteristics namely drainage area, elevation, slope steepness, slope length, and streams relief ratio. Among three DEMs, SRTM 90 m produced correct stream network. The catchment area was delineated using the hydrological model HEC-HMS. The catchment area of Krishna lower sub basin of Andhra Pradesh was 11317.36 km^2. The IRS P_6, LISS III images of December (2011), September (2012), December (2014) and September (2015) were downloaded from Bhuvan. The LULC maps were prepared for the study area. The basic classes were kharif only, double/triple crop, rabi only, build up, water bodies, forest, plantation, current fallow, wasteland and scrub land. Soil map developed by National Bureau of Soil Survey and Land Use Planning (NBSSLUP) was taken as reference map and clipped to the study area to identify the type of soils. The study area consisted of mainly four types of soils. Majority of the area is under silt soils (46 percent) and clay soils (43 percent). Remaining 7 percent and 4 percent are under loam and water bodies. Climatic data of different parameters temperature, humidity, wind speed and cropping pattern for the period of 1993 to 2015 were collected from LAM weather station, Guntur and ARS Garikapadu.

Daily and annual total precipitation from 1993 to 2015 pertaining to the study area was obtained from the Directorate of Economics and Statistics (DES) and the Meteorological Department. The average annual rainfall of study area for 23 years from 1993 to 2015 was 931.31 mm. The highest amount of rainfall was recorded in 2010 as 1620.71 mm and the lowest amount of rainfall was recorded in 2009 as 566.54 mm. The mean maximum and minimum temperature were ranged between 41.18 ^{0}C and 16.81^{0}C respectively and the average relative humidity was 74.22%. The physiography of the area is undulating having a slope of 1-44%, varying from nearly level to steep slope. Flow measurements were obtained from observed gauge data available at Prakasam barrage and Pulichintala project. The major crops grown in the study area were paddy, maize, green gram, black gram, groundnut, sesame, cotton, chillies and vegetables respectively.

Arc GIS 10.1 was used for creating spatial maps. HEC-GeoHMS was used as extension of ArcGIS for generating watershed characteristics, perform spatial analysis, delineate sub-basins and streams. Additionally, parameters like river slope, river length, watershed centroid, and longest and centroid flow path were also determined. The results acquired using HEC-HMS were the catchment area of each sub-basin, slope of each sub-basin, flow length and time of concentration. The stream flow was simulated for 23 years of rainfall of Krishna lower sub basin using SCS-CN technique. The time to peak and peak runoff rate was estimated for different rainfall events in the study area.

RUSLE model integrated with GIS and RS techniques was used for estimation of annual average soil loss rate (t ha^{-1} yr^{-1}). The RUSLE model used five parameters including rainfall runoff erosivity (R), soil erodibility (K), slope length and steepness (LS), cover management (C), and support practice factor (P). Raster map of each RUSLE parameters derived from different data source were integrated to obtain soil loss rate. The values of R factor were estimated according to the equation adopted by Singh (1981). The erosivity factor (R) was ranged from 163.095-484.898 (2009) for dry year, 458.935-1039.085 (2010) for wet year and 235.50-573.08 (2015) for normal year. The K factor for the soil types were taken from Soil erosion, Andhra Pradesh given by NBSSLUP. The estimated K values for the textural groups vary from 0.15 t ha h ha^{-1} MJ^{-1} mm^{-1} (clay), 0.29 t ha h ha^{-1} MJ^{-1} mm^{-1} (loam), 0.35 t ha h ha^{-1} MJ^{-1} mm^{-1} for silt and zero has taken for water. The LS factor for this study was computed using equation suggested by Morgan, 1979. It ranged from 0.85 to 13. The value of C basically depends on the vegetation’s cover percentage and growth stage. The C-factor ranged from 0 (meaning full strong cover effect resulting in no erosion) to 1 (represents no vegetation cover effect). The P-factor map was derived from the land use land cover and slope map. The P factor classes ranged from 0.23 to 1.00.

The following conclusions were drawn from the study:

- HEC-GeoHMS generated various basin parameters namely, basin slope, basin elevation, area of each watershed and time of concentration and delineated the watershed.
- There was a decreasing trend of rainfall amount received from eastern part to western part of the basin. The eastern part of the study area received more rainfall.
- Composite Curve number of the sub basins ranged from 71.66 and 98.0. The basin with highest composite curve number produced more runoff.
- Simulated runoff was more for the years with high rainfall. The annual runoff is highly correlated with annual rainfall with coefficient of 0.9.
- The simulated runoff depth was 1383.5 mm in the year 2010. It was only 261.97 mm in the year 2002. The average annual runoff depth during the period of 1993 to 2015 was 668.59 mm.
- The simulated peak runoff rates were matched well with the inflow discharges that are available at Pulichintala project for different storm events and were in good agreement with R^2=0.89. Hence, the model HEC- HMS can be used to predict runoff rate to plan flood mitigation measures.
- The intensity of runoff was based on antecedent moisture condition (AMC) of the catchment. The catchment with more AMC produced more runoff.
- The amount of runoff depth varied from 80.74 to 765.16 mm during the year 2011-12. There was decrease in runoff depth 51.12 to 434.74 mm with increase in double cropped area and decrease in current fallow during the year 2014-15.
- Build up areas have produced more runoff followed by scrub land, current fallow, rabi crop, kharif crop, forest, plantation and double crop/triple crop areas.
- Clay soils produced more runoff followed by silt and loam soils. However, type of soil coupled with landuse determines the amount of runoff.
- The potential soil erosion of Krishna lower sub basin in Andhra Pradesh from 1993-2015 were mapped and quantified using RUSLE model.
- The maximum annual average soil loss rate of the Krishna lower sub basin for the year 1993 to 2015 was computed as 28.69 t $ha^{-1}yr^{-1}$.

- Around 43.02% of catchment was prone to slight erosion. About 42.41% of area showed moderate soil erosion. Strong to severe erosion occurred in 12.45% and 1.3% of area. Very severe erosion occurred in 0.8% of area which was very less compared to other classes.

- The study revealed that the average annual soil loss was sensitive to rainfall factor, R and type of land use.

- The very severe erosion was affected in 13.45% (262.66 km^2) of build-up and 9.28% (21.65 km^2) of wasteland. Severe erosion occurred in 38.77% (768.561 km^2) percent of scrubland, in 18.62% (233.26 km^2) and 4.73% (43.93 km^2) of rabi crop and wasteland area respectively. Moderate erosion occurred in double/triple cropping area and slight erosion occurred in forest and kharif crop.

- Percolation tank and check dams were suggested as conservation measure in severe eroded areas.

- Waste land occupied 1452.92 km^2 area and 27 percolation tanks are proposed to augment water resources by retarding runoff.

- The hydrological model HEC-HMS can be used for event based simulation of rainfall events in lower Krishna sub basin of Andhra Pradesh. RUSLE erosion model integrated with GIS and remote sensing can be used to map the soil loss in lower Krishna sub basin of Andhra Pradesh.

Scope for future work

- Sensitivity analysis for different parameters namely curve number, lag time, recession constant and threshold flow is to be carried out to provide insight about response of the watersheds.
- Effect of land use land cover, soil type, antecedent moisture condition and slope on volume and rate of runoff will be needed to study independently rather than integrated.
- The calibration and validation has to be carried out at downstream of the catchment for accurate simulation of peak discharges.
- Simulation of stream flow with actual duration of storms is very important.

LITERATURE CITED

Alexakis, D.D., Grillakis, M.G., Koutroulis, A.G., Agapiou, A., Themistocleous, K., Tsanis, I.K., Michaelides, S., Pashiardis, S., Demetriou, C., Aristeidou, K., Retalis, A., Tymvios, F and Hadjimitsis, D.G. 2014. GIS and Remote sensing techniques for the assessment of land use change impact on flood hydrology: the case study of Yialias basin in Cyprus. *Natural Hazards Earth System Science.* 14: 413–426.

Ali, B. 2012. Estimation of soil losses by USLE model using GIS at Mashhad plain, Northeast of Iran. *Arabian Journal of Geosciences*. 7: 211–220.

Ali, M., Sher, J.K., Aslam, I and Zahiruddin, K. 2011. Simulation of the impacts of land-use change on surface runoff of Lai Nullah Basin in Islamabad, Pakistan basin in Islamabad, Pakistan. *Landscape and Urban Planning.* 102: 271– 279.

Alkharabsheha, M.M., Alexandridisa, T.K., Bilasb, G., Misopolinosb, N and Silleosa, N. 2013. Impact of land cover change on soil erosion hazard in northern Jordan using remote sensing and GIS. *Procedia Environmental Sciences*. 19: 912 – 921.

Amin, A., and Singh, S.k. 2012. Study of urban land use dynamics in Srinagar city using geospatial approach. Bull. *Environmental Science and Research.* 1(2): 18-24.

Amin, A, Baharak, M., and Abolfazl, M. 2015. Monitoring and forecasting the land use change using HEC-HMS model and Remote Sensing techniques GIS (Case Study: Ardabil 1984-2024). *Biological Forum.* 7(2): 63-68.

Arabinda, S., Kamlesh, N. T and Bhadoria, P.B.S. 2011. Effect of land use land cover change on soil erosion potential in an agricultural watershed. *Environmental Monitoring and Assessment.* 173(1-4): 789-801.

Asgari, H and Hosseinzade, A. 2008. Hydrological modeling of shrivan dam watershed using HEC-HMS model in GIS environment. *3rd conference of water management*, Iran.

Azam, M., Hyung, S.K and Seung, J., M.2017. Development of flood alert application in Mushim stream watershed Korea. *International Journal of Disaster Risk Reduction.* 21:11-26.

Betts, R.A., Boucher, O., Collins, M., Cox, P. M., Falloon, P.D., Gedney, N., Hemming, D. L., Huntingford, C., Jones, C.D., Sexton, D.M.H and Webb, M.J. 2007. Projected increase in continental runoff due to plant responses to increasing carbon dioxide. *Nature*. 448:1037-1041.

Biswas, H., Raizada1, A., Mandal, D., Kumar, S., Srinivas, S and Mishra, P. K. 2015. Identification of areas vulnerable to soil erosion risk in India using GIS methods. *Solid Earth.* 6:1257-1257.

Castillo, V.M., Mosch, W.M., Garcia, C.C., Barbera, G.G., Cano, J.A.N and Lopez-Bermudez, F. 2007. Effectiveness and geomorphological impact of check dams for soil erosion control in a semiarid Mediterranean catchment: EI C'arcavo (Murcia, Spain). *Catena.* 70: 416–427.

Chen, H., Takashi, O., and Wu, P. 2017. Assessment for soil loss by using a scheme of alterative sub-models based on the RUSLE in a Karst Basin of Southwest China. *Journal of Integrative Agriculture.* 16(2): 377–388.

Chen, F and Peng, B. 2000. The effect of land use changes on soil conditions in arid region. *Chinese Geographical Science.* 10(3): 226 – 230.

Chen, X., Tian, C., Meng, X., Xu, Q., Cui, G., Zhang, Q and Xiang, L. 2015. Analyzing the effect of urbanization on flood characteristics at catchment levels. *The International Association of Hydrological Sciences*. 370: 33–38.

Chen, Y., Xu, Y and Yin, Y. 2009. Impacts of land use change scenarios on storm-runoff generation in Xitiaoxi basin, China. *Quaternary International*. 208: 121–128.

Christopherson, R. W. 2010. *Elements of Geosystems*. Pearson Publishers.

Dabral, P.P., Baithuri, N., Pandey, A., 2008. Soil erosion assessment in a hilly catchment of North Eastern India using USLE, GIS and remote sensing. *Water Resources Management.* 22(12):1783-1798.

Devakota, L.P and Dhiraj, R.G. 2015. Impacts of climate change on hydrological regime and water resources management of the Koshi River Basin, Nepal. *Journal of Hydrology: Regional Studies.* 502-515.

Devries, J.J and Hromadka, T.V. 1993. *Computer Models for Surface Water Handbook of Hydrology*. McGraw-Hill, New York.

Dhruvanarayana, V.V. 1993. *Soil and Water Conservation Research in India*, Indian Council of Agriculture Research, Krishi Anusadhan Bhavan, Pusa, New Delhi.

Durrans, S.R. 2003. Stormwater Conveyance Modeling and Design. Waterbury, CT: Haested Press.

Dwarakish, G.S and Ganasri, B.P. 2015. Impact of land use change on hydrological systems: A review of current modeling approaches. *Cogent Geoscience.* 1(1): 1-18.

ESRI. 2005. Annual Report and Review of Research. Visited date: 02/03/2017 https://www.esri.ie/publications/esri-annual-report-and-review-of-research-2005/

Efthimiou, N., Lykoudi, E and Karavitis, C. 2014. Soil erosion assessment using the RUSLE model and GIS. *European Water*. 47: 15-30.

Fangmeier, D.D.E., Workman, W.J., Huffman, S.R., R.L and Schwab, G. O. 2006. *Soil erosion by water*. Soil and Water Conservation Engineering, 5th ed. Thomson Delmar Learning, New York. 134-158.

Feldman, A. D. 2000. *Hydrologic Modeling System HEC-HMS*. Technical Reference Manual. US Army Corps of Engineers (USACE), Hydrologic Engineering Center, HEC. Davis, CA, USA.

Foster, G.R and Meyer, L.D. 1977. Soil erosion and sedimentation by water- an overview. *In proceedings of the National Symposium on Soil Erosion and Sedimentation by Water*, Chicago, 12-13 December 1977.

Fu, B., Ma, K., Zhou, H., and Chen, L. 1999. The effect of land use structure on the distribution of soil nutrients in the hilly area of the Loess Plateau, China. *Chinese Science Bulletin.* 44:732–736.

Ganasri, B.P and Ramesh, H. 2016. Assessment of soil erosion by RUSLE model using remote sensing and GIS - A case study of Nethravathi Basin. *Geoscience Frontiers*. 7: 953-961.

Graffin, S. D., Wade, J. B., Porac, J. F. and McNamee, R. C. 2008. The Impact of CEO Status Diffusion on the Economic Outcomes of Other Senior Managers. *Organization Science*. 19: 457–74.

Gregor, P and Matjaz, M. 2004. Estimating the R factor from daily rainfall data in the sub-Mediterranean climate of southwest Slovenia. *Hydrological Sciences Journal.* 49(5): 269-277.

Gurmel Singh, Joshi, B. P and Singh, P. N. 1981. Water management for high rainfall and seasonally dry region (North Western Hilly regions), Bulletin No. R-9/D-7, CSWCRTI, Dehradun.

Habtamu, S.G and Amare, S.M. 2016. Soil loss estimation using GIS and Remote sensing techniques: A case of Koga watershed, Northwestern Ethiopia. *International Soil and Water Conservation Research.* 4(2): 126-136.

Ishtiyaq, A and Verma, M.K. 2013. Application of USLE model & GIS in estimation of soil erosion for Tandula reservoir. *International Journal of Emerging Technology and Advanced Engineering*. 3(4): 570-576.

Jain, S.K., Kumar, S and Varghese, J. 2001. Estimation of soil erosion for a Himalayan watershed using GIS technique. *Water Resources Management*. 15(1): 41-54.

James, O.O and Zhi-jia L. 2010. Application of HEC-HMS for flood forecasting in Misai and Wan'an catchments in China. *Water Science and Engineering.* 3(1): 14-22.

Jiang, T., Chen, D. Y., Xu, C., Chen, X and Singh, V. P. 2014. Comparison of hydrological impacts of climate change simulated by six hydrological models in the Dongjiang Basin, south China. *Journal of Hydrology*. 336: 316-333.

Jinkang, D, Qian, L., Hanyi, R., Tianhui, Z., Dapeng, Z., Xu, Youpeng, X and Xu, C.Y. 2012. Assessing the effects of urbanization on annual runoff and flood events using an integrated hydrological modeling system for Qinhuai river basin, China. *Journal of Hydrology*. 464-465: 127–139.

Joy, S., Alexander, L.D and Patrice, C. 2014. Analysing the effect of land-use and cover changes at sub-catchment levels on downstream flood peaks: A semi-distributed modelling approach with sparse data. *Catena.* 118: 28-40.

Julien, P.Y. 2010. *Erosion and Sedimentation.* 2nd ed. Cambridge University Press, Cambridge.

Kathol, J. P., Werner, H. D and Trooen, T. P. 2003. Predicting runoff for frequency based storm using a prediction- runoff model. *American Society of Agricultural Engineers*, South Dakota, USA.

Kim, H.S. 2006. Soil Erosion Modeling Using RUSLE and GIS on the IMHA Watershed, South Korea. M.Sc. Thesis. Colorado State University, USA.

Kishor, C., Panigrahi, B and Jagadish, C.P. 2014. Simulation of rainfall-runoff process using HEC-HMS model for Balijore Nala watershed, Odisha, India. *International Journal of Geomatics and Geosciences*. 5(2): 253-265.

Khaliq, S. 2004. The impact of land use change and hydraulic characteristics of surface water, tea Barandvz areas of West Azarbaijan province. Ph.D. thesis. Watershed Mangement, Tehran University.

Kosmas, C., Danalatos, N., Cammeraat, L.H., Chabart, M., Diamantopoulos, J., Farand, R., Gutiérrez, L., Jacob, A., Marques, H., Martínez-Fernández, J., Mizara, A., Moutakas, N., Nicolau, J.M., Oliveros, C., Pinna, G., Puddu, R., Puigdefábregas, J., Roxo, M., Simao, A., Stamou, G., Tomasi, N., Usai, D., Vacca, A., 1997. The effect of land use on runoff and soil erosion rates under Mediterranean conditions. *Catena* 29: 45–59.

Krishna, K.C. 2009. Mapping soil erosion susceptibility using remote sensing and GIS: A case of the upper Nam Wa watershed, Nan province, Thailand. *Environmental Geology*. 57: 695–705.

Kumar, P., Sharma, L.K., Pandey, P.C., Sinha, S and Nathawat, M.S. 2013. Geospatial strategy for tropical forest- wildlife reserve biomass estimation. *International Journal of Earth Observations and Remote Sensing.* 6(2): 917-923.

Kulkarni, A.T., Bodke, S.S., Rao, E.P., and Eldho, T. I. 2014. Hydrological impact on change in Land use land cover in an urbanizing catchment of Mumbai: A case study, ISH Journal Hydraulic Engineering. 20(3): 314-325

Li, L., Wang, Y and Liu, C. 2013. Effects of land use changes on soil erosion in a fast developing area. *International Journal of Environmental Science and Technology*. 11(6): 1549-1562.

Lin, Y.P., Verburg, P.H., Chang, C.R., Chen, M.H.Y and Chen, M.H. 2009. Developing and comparing optimal and empirical land-use models for the development of an urbanized watershed forest in Taiwan. *Landscape and Urban Planning.* 92: 242–254.

Majidi, A and Shahedi, K. 2012. Simulation of rainfall-runoff process using Green-Ampt method and HEC-HMS model (Case Study: Abnama Watershed, Iran), *International Journal of Hydraulic Engineering.* 1(1): 5-9.

Mangolika, C., Rumpa, D., Debasri, R., Subhasish, D and Mazumdar, A. 2014. Hydrological modeling studies with HEC-HMS for Damodar basin, India. *World Applied Sciences Journal*. 31(12): 2148-2154.

Mansell, M. G. (2003). *Rural & Urban Hydrology*. Thomas Telford Ltd, London.

Markus, M., James, R.A., Lin, Y and Mohamad, I.H. 2007. Changing estimates of design precipitation in Northeastern Illinois: Comparison between different sources and sensitivity analysis. *Journal of Hydrology*. 347:211– 222.

Mazul, K. H. and Kayoshi, H. 2001. Estimation of soil erosion using remote sensing and GIS, its valuation and economic implications on agricultural production. *International Soil Conservation Organization Meeting.* 1090-1093.

McColl, C and Aggett, G. 2006. Land-use forecasting and hydrologic model integration for improved land-use decision support. *Journal for Environment Management.* 84(4): 494-512.

Mehta, A., Sinha, V.K and Ayachit, G. 2012. Land use/ land cover study using remote sensing and GIS in an arid environment. *Bulletin of Environmental and Scientific Research*. 1(3-4): 4-8.

Mitasova, H., Hofierka, J., Zlocha, M and Iverson, R. 1996. Modeling Topographic Potential for Erosion and Deposition using GIS. *International Journal of Geographical Information Science.* 10(5): 629-641.

Moore, I.D and Burch, G.J. 1986. Physical basis of the length slope factor in the Universal Soil Loss Equation. *Soil Science Society of America*. 50 (5):1294-1298.

Morgan, R. 1994. Soil Erosion and Conservation. Silsoe College, Cranfield University, Cranfield.

Naik, B.S., Panda, R.K., Praveen, J., Anchal, D and Madhu, M. 2013. Appraisal of the erosion status in the eastern coastal region of India. *Indian Journal of Soil Conservation.* 41(2): 121-126.

Napoli, M., Stefano, C., Simone, O., Gabriele, M and Camillo, A. 2016. *Catena.* 145: 246–256.

Narayan, G. H. 2010. Water Scarcity and Security in India. *Centre for International Trade in Agriculture & Agro-based Industries*, Pune: 18-20.

Prasannakumar, V., Vijith, H., Abinod, S and Geetha, N. 2012. Estimation of soil erosion risk within a small mountainous sub-watershed in Kerala, India, using Revised Universal Soil Loss Equation (RUSLE) and geo-information technology. *Geoscience Frontiers*. 3(2): 209-215.

Price, K. 2011. Effects of watershed topography, soils, land use, and climate on base flow hydrology in humid regions: a review. *Progress in Physical Geography*. 35(4): 465-492.

Quintero, M., Wunder, S and Estrada, R.D. 2009. Modeling hydrology and livelihoods in Andean payments for environmental services schemes. *Forest Ecology and Management*. 258: 1871-1880.

Radmanesh, F., Por, H.J., Behnia, A., Khond, A., Ali, M.B. 2006. Calibration and assessment of HEC-HMS model in Roodzard watershed. *17th international conference of river engineering*, university of Shahid Chamran, Ahvaz. 24-32.

Renard, K., Foster, G., Weesies, G., McDool, D., & Yoder, D. (1997). *Predicting Soil Erosion by Water: A Guide to Conservation Planning with the Revised Universal Soil Loss Equation (RUSLE)*. Agricultural Handbook 703, USDA-ARS.

Reshma, P and Uday, K. 2012. Integrated approach of Universal Soil Loss Equation (USLE) and Geographical Information System (GIS) for soil loss risk assessment in Upper South Koel Basin, Jharkhand. *Journal of Geographic Information System.* 4: 588-596.

Romero-Díaz, A., Alonso-Sarriá, F and Martínez-Lloris, M. 2007. Erosion rates obtained from check-dam sedimentation (SE Spain). A multi-method comparison. *Catena.* 71:172–178.

Roberto, R., Thanh, H.L and Maria, C., R. 2012. A RUSLE approach to model suspended sediment load in the Lo river (Vietnam): Effects of reservoirs and land use changes. *Journal of Hydrology*. 422-423:17-31.

Rudra, R.P., Dickinson, W.T and Wall, G.J. 1986. GAMES – a screening model of soil erosion and fluvial sedimentation on agricultural watersheds. *Canadian Water Research Journal.* 11(4): 58–71.

Saleh, A., Niazi, Y and Amiri, F. 2010. Spatial distribution of soil loss and sediment yield based on SATEEC GIS system and Remote Sensing (Case Study, Ham Dam Watershed-Lower Part, Iran). *World Applied Sciences Journal*. 9(8): 860-872.

Saowanee, W. 2012. Impacts of land use changes on soil erosion in Pa Deng sub-district, adjacent area of Kaeng Krachan national park, Thailand. *Soil and Water Resource.* 7(1): 10–17.

Singh, G., V.V. Rambabu and S. Chandra. 1981. Soil Loss Prediction Research in India. ICAR Bullet, T12/D9, CS WCTRI, Dehradun.

Sintayehu, L.G. 2015. Application of the HEC-HMS model for runoff simulation of upper blue Nile river basin. *Hydrology: Current Research.* 6:199-216.

Srivastava, R.C., Verma, H.C., Nanda, B.K and Mohanty, S. 2007. 'SODEPT' A software for design of percolation tank. *Water Resource Management*. 21:1955–1972.

Suriya, S and Mudgal, B.V. 2012. Impact of urbanization on flooding: The Thirusoolam sub watershed – A case study. *Journal of Hydrology*.412-413:210–221.

Suriyaprasita, M and Shresthab, D.P. 2008. Deriving Land Use and Canopy Cover Factor from Remote Sensing and Field Data in Inaccessible Mountainous Terrain for Use in Soil Erosion Modelling. *The International Archives of the Photogrammetry, Remote Sensing and Spatial Information Sciences* 37: 1747-1750.

Tadesse, A and Abebe, M. 2014. GIS based soil loss estimation using RUSLE model: The case of Jabi Tehinan Woreda, ANRS. Ethiopia. *Natural Resources*. 5: 616-626.

Tanyas, H., Kolat, C and Suzen, M.L. 2015. A new approach to estimate cover-management factor of RUSLE and validation of RUSLE model in the watershed of Kartalkaya Dam. *Journal of Hydrology*. 528: 584-598.

Terranova, O., Antronico, L., Coscarelli, R and Iaquinta, P. 2009. Soil erosion risk scenarios in the Mediterranean environment using RUSLE and GIS: An application model for Calabria (southern Italy). *Geomorphology.* 112(3-4): 228-245.

Thornes, J.B. 1990. The interaction f erosional and vegetational dynamics in land degradation: Spatial outcomes, in vegetation and erosion, edited by J.B. Thrones, pp. 41-23, John Wiley, Hoboken, N.J.

USACE. 1985. "National engineering handbook (2nd edition)." Washington, DC: US Department of Agriculture.

Van. D.K.J.M., Jones, R.J.A and Montanarella, L. 1999. Soil erosion risk assessment in Italy, European Soil Bureau, *European Commission.*

Wainwright, J., and Thornes, J.B., 2004. Environmental Issues in the Mediterranean. Processes and Perspectives from the Past and Present. Routledge, London.

Wang, G., Jiang, H., Xu, Z., Wang, L and Yue, W. 2012. Evaluating the effect of land use changes on soil erosion and sediment yield using a grid-based distributed modelling approach. *Hydrological Processes.* 26: 3579-3592.

Williams, J. 1975. *Sediment Yield Prediction with Universal Equation using Runoff Energy Factor*. Agricultural Research Service Report ARS-S-40, U.S. Department of Agriculture.

Wischmeier, W.H and Smith, D.D. 1965. *Predicting rainfall-erosion losses from cropland east of the Rocky Mountains: Guide for selection of practices for soil and water conservation.* Agricultural Research Service, US Department of Agriculture, Washington.

Wischmeier, W.H and Smith, D.D. 1978. *Predicting Rainfall Erosion Losses- A Guide to Conservation Planning*. U.S. Department of Agriculture Handbook No.537.

Yener, M. K., 2006. *Semi-distributed Hydrologic Modeling Studies in Yuvacık Basin*, M. Sc. Thesis, Civil Engineering Department, Middle East Technical University, September.

Zhang, H. 2013. Quantitative comparison of semi- and fully-distributed hydrologic models in simulating flood hydrographs on a mountain watershed in southwest China. *Journal of Hydrodynamics*. 25(6): 877-885.

Zope, P.E., Eldho, T. A, and Jothi, P. 2016. Impacts of land use land cover change and urbanization on flooding: A case study of Oshiwara River Basin in Mumbai, India. *Catena.* 145: 142-154.

APPENDIX – I

S. No	Mandals	Daily rainfall data (mm)											
		1993	1994	1995	1996	1997	1998	1999	2000	2001	2002	2003	2004
1	Veerullapadu	1025.6	1122.1	0.0	861.7	690.3	1059.6	1039.2	1049.4	684.2	693.8	693.8	596.4
2	G Konduru	677.1	893.9	2603.9	747.7	957.0	969.3	981.6	956.3	919.5	647.2	1068.2	414.7
3	Mylavaram	501.7	1044.5	1130.8	1075.0	963.4	1170.6	335.0	735.4	866.7	747.7	850.6	413.6
4	A Konduru	736.1	1114.9	1008.4	984.6	812.1	1212.2	321.6	1087.7	582.6	521.6	768.2	563.9
5	Gampalagudem	742.7	1211.1	1059.7	1045.0	803.6	1034.6	1000.6	1394.0	774.2	845.0	1067.2	892.6
6	Vissannapet	704.2	1142.2	1224.2	1230.9	953.2	1228.1	747.2	1197.2	706.3	732.8	1032.2	745.5
7	Reddigudem	529.8	1026.9	1094.8	1081.8	749.6	866.0	604.0	1203.2	526.9	601.4	672.1	571.0
8	Vijawada (R)	0.0	0.0	0.0	0.0	0.0	968.9	808.7	1017.2	1144.8	583.4	918.6	646.7
9	Vijawada (U)	0.0	1080.0	0.0	973.7	842.7	978.9	818.7	1007.2	1134.8	573.4	938.6	666.7
10	Kankipadu	0.0	0.0	0.0	0.0	0.0	941.2	765.9	869.0	1021.0	629.8	1092.2	732.1
11	Chatrai	654.9	1212.2	0.0	1104.1	879.5	963.0	241.2	1017.4	678.0	675.2	849.8	670.8
12	Pamidimukkala	741.7	1261.8	1360.3	1346.3	1185.4	915.3	709.1	1028.1	954.6	602.6	885.4	612.1
13	Jaggayyapeta	669.5	1104.7	897.3	1023.5	651.0	950.2	683.8	1393.9	650.5	366.9	994.0	504.1
14	Vatsavai	866.4	1112.3	1088.6	939.1	809.0	1091.5	944.2	1239.9	706.4	644.0	1003.5	629.4
15	Penuganchiprolu	792.4	1226.7	796.1	994.7	781.5	1242.4	929.8	1175.6	639.4	606.8	965.1	486.2
16	Nandigama	726.2	1056.5	1105.9	768.8	777.1	1329.2	962.0	1215.2	745.8	526.2	1050.8	732.2
17	Ghantasala	612.1	1119.1	1147.7	1501.4	869.5	826.1	434.0	1175.6	830.2	492.4	628.6	317.8
18	Challapalle	894.0	1239.1	1417.4	1902.3	984.9	925.9	943.4	1062.1	888.4	814.6	1005.4	644.6
19	Mopidevi	0.0	0.0	0.0	1386.4	986.4	884.4	808.1	1042.6	1053.4	701.1	1160.9	560.6
20	Movva	907.3	1287.4	0.0	853.1	572.2	665.2	747.2	1214.9	705.8	370.8	629.4	441.5
21	Koduru	658.5	1025.5	807.7	1288.9	820.4	967.4	1090.8	984.8	1109.0	636.7	1746.8	505.5
22	Avanigadda	600.2	959.4	563.3	1269.2	796.2	910.2	837.7	1159.0	890.7	551.8	1088.9	541.2

S. No.	Mandals	**Daily rainfall data (mm)**										
		2005	**2006**	**2007**	**2008**	**2009**	**2010**	**2011**	**2012**	**2013**	**2014**	**2015**
1	Veerullapadu	1166.2	895.4	1015.8	1223.6	507.0	893.2	898.8	904.4	910.0	915.6	921.3
2	G Konduru	964.2	906.0	895.4	1325.5	841.3	834.3	817.4	800.5	783.6	766.7	749.8
3	Mylavaram	1103.8	896.0	831.4	1505.6	1107.4	1002.8	1014.4	1025.9	1037.5	1049.0	1060.6
4	A Konduru	965.8	578.6	763.0	1096.4	565.8	672.6	657.9	643.2	628.5	613.8	599.1
5	Gampalagudem	1395.8	1131.2	1097.0	1440.8	453.4	1055.4	1059.0	1062.6	1066.2	1069.9	1073.5
6	Vissannapet	1070.8	928.2	1242.9	1904.6	1033.5	1174.2	1188.1	1202.1	1216.1	1230.0	1244.0
7	Reddigudem	1353.2	954.8	798.8	1388.2	662.0	913.2	918.7	924.2	929.7	935.2	940.6
8	Vijawada(R)	1100.2	997.2	1223.0	1493.2	1048.6	1464.0	1548.4	1632.8	1717.2	1801.7	1886.1
9	Vijawada (U)	1100.2	997.2	1223.0	1493.2	1048.6	1285.8	1331.5	1377.2	1422.9	1468.6	1514.3
10	Kankipadu	1084.4	1176.5	825.2	1003.8	640.8	1232.3	1298.7	1365.1	1431.6	1498.0	1564.5
11	Chatrai	1225.4	1020.8	856.8	1240.4	674.2	963.9	979.7	995.5	1011.3	1027.2	1043.0
12	Pamidimukkala	1185.6	1625.6	757.7	838.8	609.6	818.4	800.7	783.0	765.3	747.6	730.0
13	Jaggayyapeta	1092.6	823.8	760.0	1247.8	614.1	821.3	818.2	815.2	812.2	809.1	806.1
14	Vatsavai	1142.3	975.8	779.6	1202.8	936.0	925.4	922.9	920.5	918.0	915.5	913.0
15	Penuganchiprolu	1105.6	742.7	914.6	1086.8	689.6	808.4	799.1	789.7	780.3	771.0	761.6
16	Nandigama	1166.8	886.0	954.8	905.0	751.0	878.7	873.9	869.2	864.5	859.8	855.0
17	Ghantasala	700.9	1176.7	923.0	1200.0	465.7	714.4	699.5	684.6	669.8	654.9	640.0
18	Challapalle	1150.2	1542.4	1214.6	1558.9	764.9	1068.2	1063.0	1057.8	1052.6	1047.4	1042.3
19	Mopidevi	1037.7	1598.9	1000.5	1358.8	579.9	1292.1	1343.1	1394.1	1445.1	1496.1	1547.1
20	Movva	903.3	1599.8	976.4	1279.6	773.9	996.7	1016.4	1036.1	1055.9	1075.6	1095.3
21	Koduru	1077.7	1671.6	1558.7	1456.2	697.4	1293.3	1318.7	1344.0	1369.4	1394.8	1420.2
22	Avanigadda	1026.2	1467.3	1071.9	1223.3	679.3	1057.2	1072.5	1087.8	1103.0	1118.3	1133.6

S. No	Mandals	Daily rainfall data (mm)											
		1993	1994	1995	1996	1997	1998	1999	2000	2001	2002	2003	2004
23	Nagayalanka	1066.6	1356.0	1059.0	1350.4	1114.6	997.6	901.7	1132.8	993.5	972.2	945.1	917.9
24	Machilipatnam	654.8	1683.2	0.0	1379.9	1356.8	882.8	749.9	1333.0	912.9	1076.8	1093.3	1109.6
25	Kanchikacherla	0.0	0.0	853.2	930.4	831.6	1237.2	815.1	1083.8	914.8	1335.8	1454.7	1573.8
26	Chandarlapadu	745.6	967.4	1966.1	958.6	751.8	1050.5	299.2	1116.2	520.0	622.4	560.8	499.2
27	Tiruvuru	649.0	1218.1	1197.8	1187.4	683.8	1052.6	978.7	1031.8	730.8	902.9	889.5	876.1
28	Penamaluru	853.0	1073.7	1802.0	899.1	818.2	0.0	0.0	0.0	0.0	322.9	508.5	694.1
29	Thotlavalluru	0.0	0.0	0.0	674.6	972.2	1055.6	907.6	1208.8	953.4	1444.4	1605.0	1765.5
30	Ibrahimpatnam	259.2	318.5	1092.8	664.1	696.7	642.9	476.2	630.9	413.6	602.3	607.3	612.3
31	Macherla	182.2	173.2	1120.3	566.5	637.7	579.4	429.2	542.0	337.5	537.3	543.4	549.3
32	Rentachintala	105.3	27.9	1147.9	468.9	578.7	516.0	382.1	453.1	261.5	472.5	479.5	486.4
33	Gurazala	28.4	117.5	1175.5	371.3	519.6	452.5	334.9	364.1	185.4	407.6	415.6	423.4
34	Dachepalli	48.5	262.8	1203.3	273.7	460.6	389.1	287.9	275.2	109.3	342.8	351.7	360.5
35	Machavaram	125.4	408.1	1230.6	176.2	401.7	325.7	240.8	186.3	33.2	278.0	287.8	297.6
36	Bellamkonda	202.4	553.4	1258.2	78.6	342.6	262.3	193.7	97.3	42.8	213.1	223.9	234.6
37	Atchempet	279.3	698.7	1285.7	18.9	283.6	198.8	146.6	8.4	118.9	148.3	160.0	171.7
38	Krosur	356.3	844.0	1313.3	116.5	224.6	135.4	99.5	55.5	195.0	83.4	96.1	108.8
39	Amaravathi	433.2	989.4	1340.8	214.1	165.6	72.0	52.4	169.4	271.1	18.6	32.2	45.8
40	Thullur	510.2	1134.7	1368.4	311.7	106.6	8.5	5.4	258.4	347.1	46.3	31.7	17.1
41	Tadepalli	587.1	1280.0	1395.9	409.2	47.6	54.9	41.7	347.3	423.2	111.2	95.6	80.1
42	Mangalagiri	664.0	1425.3	1423.5	506.8	11.4	118.4	88.8	436.2	499.3	176.0	159.5	143.0
43	Tadikonda	741.0	1570.6	1451.1	604.4	70.4	181.8	135.9	525.2	575.4	240.9	223.4	205.9
44	Pedakurapadu	817.9	1716.0	1478.6	701.9	129.4	245.2	183.0	614.1	651.4	305.7	287.3	268.9

S. No.	Mandals	Daily rainfall data (mm)										
		2005	2006	2007	2008	2009	2010	2011	2012	2013	2014	2015
23	Nagayalanka	1000.9	1528.8	1346.0	1637.0	1809.6	1982.1	2154.7	2327.2	2499.8	2672.3	2844.9
24	Machilipatnam	1024.5	1683.3	923.6	1109.6	1059.1	1008.7	958.2	907.8	857.3	806.9	756.4
25	Kanchikacherla	1049.6	840.0	1004.4	919.5	896.9	874.3	851.7	829.1	806.5	783.9	761.3
26	Chandarlapadu	1196.2	723.3	956.2	718.6	598.6	478.6	358.6	238.6	118.6	1.4	121.4
27	Tiruvuru	1506.0	1168.2	1152.6	922.2	745.5	568.8	392.1	215.4	38.7	138.0	314.7
28	Penamaluru	0.0	1231.0	1509.0	2422.3	3176.8	3931.3	4685.8	5440.3	6194.8	6949.3	7703.8
29	Thotlavalluru	1210.3	1420.4	951.4	935.1	805.7	676.2	546.8	417.3	287.9	158.4	29.0
30	Ibrahimpatnam	1251.6	1025.6	1130.6	1014.9	954.4	893.9	833.4	772.9	712.4	651.9	591.4
31	Macherla	933.8	544.3	584.6	338.4	163.8	10.8	185.4	360.0	534.6	709.2	883.8
32	Rentachintala	972.9	459.2	927.3	740.9	718.1	695.3	672.5	649.7	626.9	604.1	581.3
33	Gurazala	803.5	532.7	990.3	962.3	1055.7	1149.1	1242.5	1335.9	1429.3	1522.7	1616.1
34	Dachepalli	709.1	973.7	954.1	1124.0	1246.5	1369.0	1491.5	1614.0	1736.5	1859.0	1981.5
35	Machavaram	995.2	582.4	1003.6	868.8	873.0	877.2	881.4	885.6	889.8	894.0	898.2
36	Bellamkonda	831.5	594.8	763.6	662.1	628.1	594.2	560.2	526.3	492.3	458.4	424.4
37	Atchempet	933.8	522.5	968.6	843.1	860.5	877.9	895.3	912.7	930.1	947.5	964.9
38	Krosur	897.3	562.2	923.9	821.1	834.4	847.7	861.1	874.4	887.7	901.0	914.3
39	Amaravathi	1010.1	726.1	1249.8	1235.0	1354.9	1474.7	1594.6	1714.4	1834.3	1954.1	2074.0
40	Thullur	950.9	746.4	931.8	857.3	847.7	838.2	828.6	819.1	809.5	800.0	790.4
41	Tadepalli	1177.7	1009.0	1272.5	1247.9	1295.3	1342.7	1390.1	1437.5	1484.9	1532.3	1579.7
42	Mangalagiri	1086.1	944.7	1031.9	966.7	939.6	912.5	885.4	858.3	831.2	804.1	777.0
43	Tadikonda	955.4	546.7	985.6	859.5	874.6	889.8	904.9	920.0	935.2	950.3	965.4
44	Pedakurapadu	953.3	513.9	981.5	844.5	858.6	872.7	886.8	900.9	915.0	929.1	943.2

S. No	Mandals	Daily rainfall data (mm)											
		1993	1994	1995	1996	1997	1998	1999	2000	2001	2002	2003	2004
45	Sattenapalli	894.9	1861.2	1506.2	799.5	188.4	308.6	230.0	703.0	727.5	370.6	351.2	331.8
46	Rajupalem	971.8	2006.5	1533.7	897.1	247.4	372.1	277.2	792.0	803.6	435.4	415.1	394.8
47	Nekarikallu	682.0	910.0	923.0	827.0	1041.8	779.3	661.4	831.8	709.8	485.9	1143.5	639.9
48	Piduguralla	756.1	937.0	851.5	695.8	861.2	919.8	719.3	855.2	875.9	621.2	895.8	660.0
49	Karampudi	770.9	953.8	892.0	901.0	711.9	859.0	451.5	810.8	671.0	548.9	873.2	615.2
50	Durgi	626.8	937.3	823.0	1106.3	1031.9	854.2	565.2	778.0	803.8	491.4	853.8	642.8
51	Veldurthy	778.2	791.4	756.2	723.8	822.7	800.9	139.9	868.3	861.1	511.8	576.2	907.4
52	Bollapalli	657.3	797.4	891.5	927.0	928.7	686.1	554.2	993.2	899.8	615.8	861.6	742.1
53	Medikondur	730.0	914.0	823.0	825.0	850.0	1174.6	620.4	1033.2	940.6	526.4	981.1	751.6
54	Guntur	804.0	1032.0	1220.2	1157.8	708.6	921.8	691.5	1138.4	858.0	610.3	1149.1	1051.2
55	Pedakakani	923.0	1085.0	1123.0	1123.0	863.0	1051.5	556.3	1230.6	848.3	550.7	1210.3	961.4
56	Duggirala	1322.6	1851.2	838.9	1587.0	1148.6	1358.9	788.9	1640.0	1382.8	861.3	1427.8	1279.1
57	Kollipara	1469.4	2091.8	806.8	1751.6	1228.2	1473.8	852.9	1806.7	1523.3	941.9	1547.9	1397.6
58	Kolluru	1616.2	2332.3	774.8	1916.2	1307.7	1588.7	916.9	1973.3	1663.8	1022.4	1668.0	1516.2
59	Vemuru	1763.0	2572.8	742.7	2080.9	1387.3	1703.5	980.9	2139.9	1804.3	1103.0	1788.1	1634.8
60	Tenali	1909.8	2813.3	710.7	2245.6	1466.9	1818.4	1044.9	2306.5	1944.8	1183.6	1908.2	1753.3
61	Bhattiprolu	2056.6	3053.8	678.6	2410.2	1546.4	1933.3	1108.9	2473.1	2085.3	1264.1	2028.3	1871.9
62	Repalle	2203.4	3294.3	646.6	2574.9	1626.0	2048.2	1172.9	2639.7	2225.8	1344.7	2148.4	1990.4
63	Nagaram	2350.2	3534.8	614.5	2739.5	1705.6	2163.1	1236.9	2806.3	2366.3	1425.3	2268.5	2109.0
64	Nizampatnam	2496.9	3775.3	582.5	2904.2	1785.1	2277.9	1301.0	2973.0	2506.8	1505.9	2388.6	2227.6
65	Edlapadu	2643.7	4015.8	550.4	3068.8	1864.7	2392.8	1365.0	3139.6	2647.3	1586.4	2508.7	2346.1
66	Rompicherla	2790.5	4256.3	518.4	3233.5	1944.2	2507.7	1429.0	3306.2	2787.8	1667.0	2628.8	2464.7
67	Nadendla	2937.3	4496.9	486.3	3398.1	2023.8	2622.6	1493.0	3472.8	2928.4	1747.6	2748.9	2583.2
68	Cherukupalli	3084.1	4737.4	454.3	3562.8	2103.4	2737.5	1557.0	3639.4	3068.9	1828.2	2869.0	2701.8
69	Phirangipuram	3230.9	4977.9	422.2	3727.4	2182.9	2852.3	1621.0	3806.0	3209.4	1908.7	2989.1	2820.3

S. No.	Mandals	Daily rainfall data (mm)										
		2005	**2006**	**2007**	**2008**	**2009**	**2010**	**2011**	**2012**	**2013**	**2014**	**2015**
45	Sattenapalli	822.6	758.2	832.5	900.8	252.0	523.4	482.3	392.6	396.8	1046.0	215.2
46	Rajupalem	926.3	718.6	922.6	946.3	494.6	611.0	547.4	483.8	420.3	356.7	293.1
47	Nekarikallu	936.9	822.3	965.2	935.0	410.3	531.8	437.7	343.7	249.6	155.6	61.5
48	Piduguralla	891.0	593.9	873.7	720.0	298.4	357.7	251.8	145.9	39.9	66.0	171.9
49	Karampudi	895.3	658.6	816.0	680.1	346.6	356.6	249.0	141.4	33.8	73.8	181.4
50	Durgi	502.0	431.2	821.6	836.6	403.8	661.7	682.6	703.5	724.4	745.3	766.2
51	Veldurthy	679.6	378.1	581.6	675.1	289.4	375.7	327.4	279.1	230.7	182.4	134.0
52	Bollapalli	759.0	563.3	704.4	805.8	463.4	554.6	519.7	484.8	450.0	415.1	380.2
53	Medikondur	776.4	766.8	1182.4	1007.2	426.9	694.4	648.5	602.6	556.8	510.9	465.1
54	Guntur	1071.9	879.5	1018.8	1098.5	397.0	553.9	440.8	327.7	214.7	101.6	11.5
55	Pedakakani	1077.3	1091.8	935.6	1043.1	402.8	490.8	351.0	211.3	71.5	68.3	208.0
56	Duggirala	1211.6	1132.3	889.6	1050.6	310.2	353.5	165.1	23.4	211.8	400.3	588.7
57	Kollipara	1111.1	1124.9	853.8	982.6	244.8	301.0	113.5	74.0	261.5	449.0	636.5
58	Kolluru	1706.6	1487.6	929.2	1127.8	356.1	203.2	102.9	408.9	715.0	1021.0	1327.2
59	Vemuru	1163.5	1182.2	1049.1	1020.4	231.4	321.5	118.9	83.7	286.3	488.9	691.5
60	Tenali	1248.4	1156.2	1081.7	1128.4	251.2	366.5	164.3	37.9	240.1	442.4	644.6
61	Bhattiprolu	1149.6	1215.6	964.4	1056.6	416.6	473.1	310.6	148.1	14.4	176.9	339.4
62	Repalle	1058.7	1405.6	1097.2	1371.0	494.0	736.1	619.7	503.3	386.9	270.5	154.1
63	Nagaram	979.3	1253.6	1172.3	1371.0	425.6	743.4	644.4	545.4	446.4	347.4	248.4
64	Nizampatnam	976.3	1113.5	1205.8	1357.5	344.2	693.4	591.4	489.4	387.3	285.3	183.3
65	Edlapadu	888.2	670.7	843.4	844.1	367.3	462.2	375.4	288.5	201.7	114.9	28.0
66	Rompicherla	1046.2	623.0	725.9	844.6	361.6	376.0	261.2	146.5	31.7	83.1	197.8
67	Nadendla	970.2	771.0	901.2	813.6	255.1	325.9	187.2	48.4	90.3	229.1	367.9
68	Cherukupalli	747.0	1062.0	890.7	1104.5	268.0	539.8	448.2	356.7	265.1	173.6	82.0
69	Phirangipuram	1200.7	968.6	1049.9	1106.0	397.1	503.5	356.5	209.6	62.6	84.4	231.4

APPENDIX – II

S. No	Mandals	Latitude	Longitude
1	Veerullapadu	16.82	80.4
2	G Konduru	16.68	80.57
3	Mylavaram	16.76	80.64
4	A Konduru	16.96	80.65
5	Gampalagudem	16.99	80.53
6	Vissannapet	16.94	80.78
7	Reddigudem	16.86	80.74
8	Vijawada(R)	15.90	80.48
9	Vijawada (U)	16.50	80.65
10	Kankipadu	16.43	80.77
11	Chatrai	16.99	80.86
12	Pamidimukkala	16.28	80.86
13	Jaggayyapeta	16.90	80.1
14	Vatsavai	16.98	80.24
15	Penuganchiprolu	16.90	80.25
16	Nandigama	16.77	80.28
17	Ghantasala	16.16	80.94
18	Challapalle	16.12	80.93
19	Mopidevi	16.06	80.93
20	Movva	16.22	80.92
21	Koduru	13.95	79.35
22	Avanigadda	16.02	80.92
23	Nagayalanka	15.94	80.91
24	Machilipatnam	16.19	81.14
25	Kanchikacherla	16.68	80.39
26	Chandarlapadu	16.72	80.24
27	Tiruvuru	17.10	80.60
28	Penamaluru	16.46	80.71
29	Thotlavalluru	16.34	80.78
30	Ibrahimpatnam	16.59	80.52
31	Macherla	16.47	79.43
32	Rentachintala	16.55	79.55
33	Gurazala	16.55	79.64
34	Dachepalli	16.59	79.73
35	Machavaram	16.02	80.54
36	Bellamkonda	16.48	80.00
37	Atchempet	15.91	79.74
38	Krosur	16.54	80.14
39	Amaravathi	16.57	80.35
40	Thullur	16.52	80.47
41	Tadepalli	16.84	81.48

42	Mangalagiri	16.43	80.57
43	Tadikonda	16.42	80.45
44	Pedakurapadu	16.47	80.25
45	Sattenapalli	16.39	80.15
46	Rajupalem	14.05	79.85
47	Nekarikallu	16.37	79.94
48	Piduguralla	16.48	79.89
49	Karampudi	16.4	79.72
50	Durgi	16.42	79.54
51	Veldurthy	15.55	77.93
52	Bollapalli	16.18	79.68
53	Medikondur	16.34	80.30
54	Guntur	16.30	80.44
55	Pedakakani	16.34	80.49
56	Duggirala	16.32	80.63
57	Kollipara	16.28	80.75
58	Kolluru	16.18	80.8
59	Vemuru	16.17	80.74
60	Tenali	16.24	80.64
61	Bhattiprolu	16.10	80.78
62	Repalle	16.01	80.83
63	Nagaram	16.00	80.73
64	Nizampatnam	15.90	80.67
65	Edlapadu	16.16	80.22
66	Rompicherla	15.91	79.74
67	Nadendla	16.17	80.18
68	Cherukupalli	16.04	80.68
69	Phirangipuram	16.28	80.26